2019

Characterisation of Cholesterolcontaining Microparticles in Autoimmunity

Shuai Shuai Hu
Technological University Dublin

Characterisation of Cholesterol-containing Microparticles in Autoimmunity

Shuai Shuai Hu

Thesis submitted for the award of PhD
Technological University Dublin

2019

Characterisation of Cholesterol-containing Microparticles in Autoimmunity

Shuai Shuai Hu MD, MSc

Thesis submitted for the award of PhD
Technological University Dublin

Supervisor: Dr. Claire Wynne,
Co-supervisor: Dr. Steve Meaney,

School of Biological and Health Sciences

July 2019

Abstract

In recent years, it has become apparent that sub-micron scale remnants of cells, called microparticles (MPs), are present in human circulation. MPs contain DNA, RNA, protein and lipids (such as cholesterol). Increased numbers of MPs are observed in autoimmune conditions such as Systemic Lupus Erythematosus (SLE) and Rheumatoid Arthritis (RA). This work aims to address the deficiency in the literature concerning MP cholesterol (MPC) by establishing reference values for MPC in a representative healthy population group, and by investigating the potential of MP cholesterol as a biomarker in autoimmunity.

This study has optimised a reproducible and feasible method (centrifugation followed by size exclusion chromatography) to isolate apolipoprotein-deficient, cholesterol containing MPs from plasma, allowing the study of cholesterol without lipoprotein contamination in a disease model. A reference range for MPC was established in a representative healthy population. Studies in autoimmune patients suggest that MPC holds potential as a novel biomarker for SLE and RA patient diagnosis and stratification. RA patients have significantly more MPC than SLE patients and healthy controls. The study also confirmed the potential of 3-hexanoyl-7-nitrobenz-2-oxa-1,3-diazol-4-yl-cholesterol (3NBDC) as a versatile cholesterol tracer in different cell models and extracellular vesicles.

To the best of our knowledge, this thesis reports the first studies of lipoprotein deficient MPs in autoimmune disease. The methods used in this study could be applied to the investigation of this MP subset in other diseases. The work involving 3NBDC has shed new light on the multiple application of 3NBDC as a cholesterol tracer. In addition, the application of 3NBDC contributes to a better understanding of the dynamics of cholesterol and extracellular vesicles.

Declaration

I certify that this thesis which I now submit for examination for the award of PhD, is entirely my own work and has not been taken from the work of others, save and to the extent that such work has been cited and acknowledged within the text of my work. This thesis was prepared according to the regulations for graduate study by research of Technological University Dublin and has not been submitted in whole or in part for another award in any other third level institution. The work reported on in this thesis conforms to the principles and requirements of TU Dublin's guidelines for ethics in research.

Signature _____ Date _____

Acknowledgements

I would like to express my sincere appreciation to everyone who has helped me with this project.

Firstly, I would like to express my sincere gratitude to my main supervisor Dr Claire Wynne for her continuous support of my PhD study and related research and for her patience, motivation and immense knowledge. I am thankful to her for giving me the opportunity to undertake this PhD project and appreciated all her input and guidance. Her careful editing contributed enormously to the production of this thesis. I could not have imagined having a better supervisor for my PhD study. I am also thankful for the excellent role model that she has provided as a successful female scientist and supervisor.

Also, I would like to thank my co-supervisor Dr Steve Meaney for his great support and invaluable advice. At many stages in the research project, I benefited from his expertise, particularly when exploring new ideas and developing new projects. His positive and energetic outlook and confidence in my research inspired and motivated me. Many thanks to him for giving me the opportunity to become familiar with the field of cholesterol.

I would like to acknowledge the patients and healthy volunteers who donated samples for my studies. This project could not have been possible without their consent.

I much appreciated the support received from our collaborative work undertaken with the Cedars-Sinai Hospital, California, US. Thanks to Prof Caroline Jefferies for her encouragement and supervisory role. I appreciated all her time, funding and advice. I really enjoyed the time we spent together. Thanks to the team in her lab, I had a good time with them (Erica, Jane, Luisa, Gantsetseg and Duygu).

Many thanks also for the support I received from all the technicians in TU Dublin. Especially thanks to Paul, Beth, Dolores, Patrick, Conor, and Karen for their help during my PhD research.

I would also like to thank the FOCAS research institute for the resources and support provided.

It is a pleasure to thank all the other PhD students in our group, for the beautiful times we shared and spent together, who also made my stay in Ireland memorable.

Last but not least, I am grateful to my family for their continuous and unparalleled help and support. I am thankful to my parents for giving me the opportunities to study abroad. They selflessly encourage me to realise my dreams and explore my own life. I am grateful to my husband for always being there to support me. This PhD journey would not have been possible without them.

Abbreviations List

3NBD Cholesterol: 6-[(NBD)amino]-cholest-5-en-3-ol

3NBDC: 3NBD Cholesterol

22NBD Cholesterol: 22-(*N*-(NBD)amino)-23,24-bisnor-5-cholen-3β-ol

22NBDC: 22NBD Cholesterol

25NBD Cholesterol: 25-(*N*-(NBD)methylamino27-norcholesterol

25NBDC:25 NBD Cholesterol

ACPA: Anti-citrullinated protein antibody

ANA: Antinuclear antibody

APA: Antiphospholipid antibody

APC: Allophycocyanin

APCs: Antigen presenting cells

APO: Apolipoprotein

AUC: Area under the curve

BSA: Bovine serum albumin

CCP: Cyclic citrullinated peptides

CI: Confidence interval

CRP: C-reactive protein

CSF: Cerebrospinal fluid

CVD: Cardiovascular disease

DAMPs: Damage-associated molecular patterns

DAS 28 CRP: Disease activity score-28 for rheumatoid arthritis with CRP

DCs: Dendritic cells

DMARDs: Disease-modifying anti-rheumatic drugs

DMEM: Dulbecco's modified essential medium

DLS: Dynamic light scattering

dsDNA: double stranded DNA

ELISA: Enzyme-linked immunosorbent assay

ESR: Erythrocyte sedimentation rate

EV: Extracellular vesicle

FBS: Foetal bovine serum

FITC: Fluorescein isothiocyanate

HCQ: Hydroxychloroquine

HDL: High density lipoprotein

HMDM: Human monocyte derived macrophage

HRP: Horseradish peroxidase

IDL: Intermediate-density lipoprotein

IFN: Interferon

IL-6: Interleukin-6

IRFs: Interferon regulated factors

LDL: Low-density lipoprotein

LN: Lupus nephritis

LPS: Lipopolysaccharides

miR: MicroRNA

MPC: Microparticle cholesterol

MP: Microparticle

MS: Multiple sclerosis

MTX: Methotrexate

N/A: Not applicable

NBD: 7-nitrobenz-2-oxa-1,3-diazol-4-yl

NK: Natural killer

NLRs: Nucleotide-binding oligomerisation domain-like receptors

NOD: Nucleotide-binding oligomerisation domain

NTA: Nanoparticle tracking analysis

PAMPs: Pathogen-associated molecular patterns

PC: Phosphatidylcholine

PE: Phosphatidylethanolamine

PE: Phycoerythrin

PFP: Platelet-free plasma

PFS: Platelet-free supernatant

PMA: Phorbol 12-myristate 13-acetate

PMN: Polymorphonuclear leucocyte

PPP: Platelet poor plasma

PRRs: Pattern-recognition receptors

PS: Phosphatidylserine

RA: Rheumatoid arthritis

RF: Rheumatoid factor

RLR: RIG-I-like receptor

ROC: Receiver operating characteristic

SEC: Size-exclusion chromatography

SLAM: Systemic lupus activity measure

SLE: Systemic lupus erythematosus

SLEDAI: Systemic lupus erythematosus disease activity index

SLICC: Systemic lupus international collaborating clinics

SM: Sphingomyelin

SS: Sjögren's syndrome

SSc: Systemic sclerosis

SSZ: Sulfasalazine

TAG: Triacylglycerol

TBS-T: Tris buffered saline with tween

TCR: T-cell receptor

TIR: Toll/IL-1receptor

TLR: Toll-like receptor

TNFα: Tumour necrosis factor alpha

VLDL: Very low-density lipoprotein

Table of Contents

List of Tables

List of Figures

1.0 General Introduction

1.1 Extracellular Vesicles

The first study of extracellular vesicles (EVs) as procoagulant platelet-derived particles in normal plasma was described by Chargaff and West in 1946. In 1967, Peter Wolf referred to EVs as "platelet dust" to describe this subcellular coagulant material (1, 2). Over the past few decades, accumulating data, indicates that EVs are a heterogeneous group based on their contents, size and cellular source. At present, EVs are generally classified into three main types that exist in circulation: microparticles (MPs)/microvesicles, exosomes and apoptotic bodies (Figure 1.1). Exosomes are derived from endosomal compartments within the cell, with their size ranging from 0.04-0.1μm. Apoptotic bodies are derived from cells undergoing apoptotic processes and contain remnants of apoptotic cells including cytoplasm, organelles and nuclear contents (3). Their size is around 0.8-5μm, making them much larger than exosomes and MPs (4, 5). MPs are small vesicles (with a diameter of 0.1-1μm) derived from almost all cell types in response to activation, apoptosis and injury (4, 5). There are some key differences between these three subtypes of EVs, specifically in their physical characteristics and the methods used to isolate and detect them (Table 1.1).

The main focus of this study is around the characterisation and role of plasma derived MPs. MPs, present in the circulation, are predominately derived from platelets, erythrocytes, leucocytes and endothelial cells (6, 7). Many different antigens may be used to detect their cellular origin, usually by flow cytometry. In recent years it has been shown that MPs are involved in pathophysiological processes in autoimmune disease, cardiovascular disease (CVD) and many other diseases (8). The exact details around MP biogenesis, secretion and their fate in different diseases still remains to be elucidated.

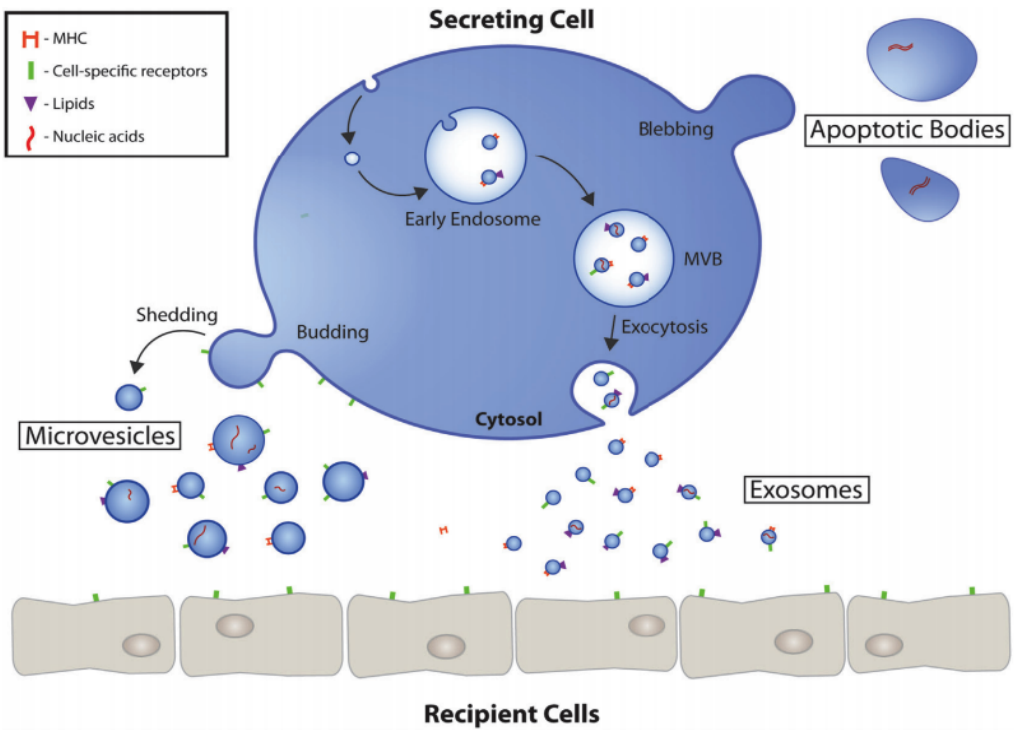

Figure 1.1 Different types of extracellular vesicles. Exosomes are secreted from endosomes. Microvesicles (microparticles) are derived from cell membranes by budding and shedding processes. Apoptotic bodies are formed in the late phase of apoptosis when the cell's cytoskeleton breaks down and causes the membrane to bulge outward. Extracellular vesicles express numerous markers such as MHC, cell specific receptors, lipids and nucleic acids (9).

Table1.1: Comparison of the Common Characteristics of Exosomes, Microparticles and Apoptotic Bodies

Characteristics	Exosomes	Microparticles	Apoptotic bodies
Size (diameter)	0.04-0.1µm	0.1-1µm	0.8-5µm
Origin	Multivesicular bodies (endosomes/ lysosomes)	Different cells membrane	Different apoptotic cells
Mechanism of release	Cell activation	Cell apoptosis, activation or injury	Late phase of apoptosis
Composition	Protein, nucleic acid, lipid	Protein, nucleic acid, lipid	Cytoplasm, organelles, Nuclear contents
Centrifugation force	100,000 - 200,000g	~20,000g	10,000 - 16,000g
Isolation methods	1. Differential ultra-centrifugation 2. Density gradient ultra-centrifugation 3. Size-exclusion chromatography 4. Kit based precipitation	1. Differential ultra-centrifugation 2. Density gradient ultra-centrifugation 3. Size-exclusion chromatography 4. Kit based precipitation	1. Differential centrifugation
Methods for detection	1. Electron microscopy 2. Flow cytometry 3. Dynamic light scattering 4. Tunable resistive pulse sensing 5. Nanoparticle tracking analysis	1. Electron microscopy 2. Flow cytometry 3. Dynamic light scattering 4. Tunable resistive pulse sensing 5. Nanoparticle tracking analysis	1. Flow cytometry
Markers used to detect the particles	CD63, CD9,CD81	Variable, depends on cell of origin (see Table 1.2)	Annexin-V
References	(4) (5) (10)	(10) (11)	(5) (12)

1.2 Microparticles

All cell types appear to be able produce MPs in response to stimuli and are typically detected by flow cytometry utilising the expression of different cell surface markers (Table 1.2). MPs are present in biological fluids such as plasma and are involved in various physiological and pathological processes (1). They are composed of protein, nucleic acid and lipid (7).

Table 1.2: Common Antigens Used to Identify Microparticle Cellular Origin

Microparticle Cell of Origin	Antigen	References
Erythrocyte	CD235a	(13)
Platelet	CD41, CD42a, CD42b, CD61,CD62P CD31+/CD42+, CD63	(14) (15)
Endothelial cell	$CD31^{+}$/CD42, CD146, CD106, CD51, CD144, CD62E, CD105, CD54	(14) (15)
Leucocyte	CD45	(13)
Granulocyte	CD66b	(13)
Monocyte	CD14	(13)
Lymphocyte	CD4, CD8, CD20,CD3	(13) (14) (16)

1.2.1 Structure of microparticles

Lipid content and membrane features

Under resting conditions, phospholipids are asymmetrically distributed in the inner and outer leaflets of the plasma membrane, with phosphatidylcholine (PC) and sphingomyelin (SM) enriched in the outer leaflets and phosphatidylserine (PS) and phosphatidylethanolamine (PE) enriched in the inner leaflets (17). It is generally accepted that when a cell membrane loses the asymmetrical distribution of these lipids, this results in the release of MPs (18). During apoptosis or cellular activation, the cytoskeleton is reorganised, leading to PS exposure on the outer cell membrane and shedding of MPs (18). PS externalisation is a widely accepted hallmark of MPs. This PS may be detected via a variety of PS-specific proteins coupled to fluorophores such as annexin-V and lactadherin, which are the most commonly used probes (19). Annexin-V binds to PS to identify apoptotic cells in the presence of calcium, while lactadherin is also a PS binding

protein, but independent of calcium (20). However, several studies have shown that PS-negative MPs also exist in circulation (21, 22, 23). Furthermore, a number of studies have detected that MPs contain three other phospholipids, PC, SM and PE (24, 25, 26). Nieuwland *et al* report that MPs contain 59% PC, 20.6% SM and 9.4% PE (27). A lipidomic study further reported that MPs contain other lipid species, such as phosphatidylinositol, phosphatidic acid and phosphatidylglycerol (28). Biró *et al* demonstrated that platelet-derived MPs also contain cholesterol and phospholipids (29). However, it should be noted that most of these studies have in fact analysed the lipidomes of exosomes rather than MPs (30, 31). There is, therefore, a lack of information around the lipid content of MPs within the field, with further studies being needed to elucidate both the lipid composition and biological function of these particles.

Protein Composition

Proteins are critical bioactive contents of MP, with proteomic methods commonly used approach to study MP-derived protein. Multiple studies have identified different proteins present in plasma MPs, with the overall MP proteome influenced by different isolation strategies and biological sources (32, 33). Recently, Tamar *et al* have identified 5374 proteins to be present in plasma MPs which is the largest proteome reported so far (34). According to Vesiclepedia (35) there are 100 proteins regularly identified in EVs. Among these 100 proteins, PDCD61P, GAPDH and HSPA8 are the most frequently identified in EVs including MPs.

Nucleic Acid Cargo

Numerous studies have reported that MPs contain different nucleic acids including DNA, microRNAs (miRs) and messenger RNA (mRNA) (36, 37, 38). During cell death, either apoptosis or necrosis, DNA can exit the cell and enter into the extracellular space (39). Pisetsky *et al* have reported that MPs are a source of extracellular DNA (39). It is also generally accepted that MPs act as transport vesicles for miRs (38) and MPs may act as protective transport vesicles for miRs in the circulation (38). This activity is attributed to exclusion of circulating RNases from the MP cargo. Several studies have demonstrated that MPs can transport mRNA or miRs to recipient cells

(40, 41), and can transfer this mRNA or miRNA into recipient cells (such as macrophages, leucocytes and endothelial cells) by internalisation to regulate cell function and gene expression (42).

1.2.2 Biological activities of microparticle content and disease association

The biological activities of MPs are closely related to their contents. Phospholipids are known play a key role in the pro-coagulant process (43,44,45). Wolberg *et al* have reported that PS^+ positive MPs contribute to the formation of coagulation complexes and increase tissue factor activity (46). One study further suggested that PS^+ positive MPs are more pro-coagulant than PS-negative MPs, due to PS binding coagulation proteins called "vitamin K-dependent carboxylation/γ-carboxyglutamic acid-rich (GLA)" domains (47), which are involved in coagulation. These PS exposed MPs are associated with thrombotic diseases (47).

Some studies have analysed the proteome of MPs and discovered MPs derived protein as biomarkers in different diseases (48, 49). For example, in type 2 diabetes, a total of 496 proteins have been identified in plasma MPs, with 20 MP proteins having a higher expression in the patient group when compared to healthy controls (50). Wattes *et al* identified a total of 160 proteins in plasma MPs in a pulmonary embolism group and healthy control group, with 23 unique proteins being found in the pulmonary embolism group alone (51). These studies suggest MP-derived proteins may hold promise as novel biomarkers in multiple diseases.

Furthermore, various studies have reported that MPs contain different miRs in different disease situations. Jansen *et al* report that the level of miR-126 and miR-26a is significantly reduced in diabetes compared to non-diabetes (52). They suggest that endothelial cell MPs are the main source of miR-126 and miR-26a and these miRs are related to appropriate vascular performance. Endothelial MPs can deliver functional miR-126 which contributes to endothelial cell repair. This study also identified ten miRs (miR-126, miR-222, miR-let7d, miR-21, miR-20a, miR-27a, miR-92a, miR-17, miR-130, and miR-199a) present in circulating MPs in stable coronary artery disease which were related to vascular performance. Endothelial cells and platelets

are believed to be the main sources of MPs containing miR-126 and miR-199a (52, 53). A more recent study demonstrated that miR-9 and miR-451 were differentially expressed in cerebrospinal fluid (CSF), with more MPs being derived from brain injured patients compared to non-injured subjects, suggesting MPs containing miR may play a role in the adaptive response to injury (54). Additionally, CSF MPs have been shown to contain mRNA (54). Charles *et al* also reported that MPs contain DNA and RNA after studying apoptotic Jurkat and HL-60 cell models (55). Taken together, these studies demonstrate that MP contents contribute to MPs acting as a messenger and transmitter of biological information.

1.2.3 Isolation and purification of microparticles

The options available for isolation and purification of pure MPs are limited. Currently, there are four main methods used to isolate MPs derived from body fluids and conditioned media. These are differential ultra-centrifugation, density gradient ultracentrifugation, size-exclusion chromatography (SEC) and precipitation (Table 1.3). The most commonly used method for MP isolation from body fluids or cell culture media is differential centrifugation/ultra-centrifugation. This method involves a series of centrifugation steps, which is time-consuming. Another drawback to this method is that the isolated MPs potentially contain soluble plasma proteins and lipoproteins (56). It is thought that certain purification methods can influence the function of MPs, for example, it has been shown EVs isolated by a protein organic solvent precipitation method and treated cells resulted in reduced cell viability *in vitro* (57). Other methods like immunoaffinity isolation methods (microbeads coated with certain EV surface markers) can lead to substantial populations of EVs being lost due to beads only binding a certain subset of EVs (58). Furthermore, other studies suggest that the use of a density gradient ultracentrifugation method may in fact influence the biological functions of MPs (59). In general, it is challenging to directly compare results for any MP isolation method used across different laboratories due to the variation in protocols and equipment. MPs also share biophysical properties with other small vesicles (such as lipoproteins and virions) and these factors can significantly complicate their isolation from the circulation (10,

60). As a result, careful selection of the preferred isolation method is required in MP studies. As our research question was focused on the biological role of MP-derived cholesterol, separation of MPs from lipoprotein was a key requirement. A comparison of the four main methods used for MP purification is outlined in table 1.3 overleaf. Differential ultra-centrifugation and density gradient ultra-centrifugation methods are insufficient in separating MPs from lipoprotein and precipitation methods may influence the biological functions of the purified MPs. For those reasons, the method chosen to separate MPs from lipoproteins in this study was SEC. SEC is a chromatographic method and molecules are separated by their size.

Table 1.3: A Comparison of Methods Used to Isolate Microparticles

	Differential ultracentrifugation	Density gradient Ultra-centrifugation	Size-exclusion Chromatography	Precipitation
Method	Low speed spin of 1200-2000g for 15-20 min then a high speed spin of 20,000g for 20-30 min.	Centrifugation at 1550g for 20 min to remove cells followed by potassium bromide density gradient or Sucrose gradient/ Iodixanol gradient.	Centrifugation at 1550g for 20 min to remove cells followed by a sepharose CL-2B column.	Protein organic solvent precipitation, acetate buffer.
Microparticle isolation site	MPs derived from body fluids (plasma) or cell culture medium.	Plasma, human salivary. Conditioned medium.	Platelet, plasma.	Plasma, tissue derived from central nervous system.
Advantage	It is the most common and standard method and serves as the backbone for other methods.	Separates low-density lipoproteins and very low-density lipoproteins from MP based on density.	Less protein and lipoprotein contamination.	Quick, removes soluble protein, inexpensive.
Disadvantage	Contamination from proteins and lipoproteins can be an issue.	Takes a long time (> 10 hours). Co-isolation of MPs and high-density lipoproteins, loss of biological function by sucrose gradient density.	Sepharose CL-2B is expensive.	The organic solvent used may influence the MPs biological functions.
References	(61)	(62)	(63) (18)	(57) (64)

MP: Microparticle

1.3 Cholesterol

1.3.1 Cholesterol structure

Cholesterol has a molecular formula of $C_{27}H_{45}OH$ and is composed of three features (65): a hydrocarbon tail, a ring structure region with four hydrocarbon rings, and a C3 hydroxyl (OH) group (Figure 1.2). The four-ring regions present in cholesterol is the signature of all steroid hormones (such as testosterone and estrogen). The combination of the steroid ring structure and the hydroxyl (alcohol) group classifies cholesterol as a 'sterol'. The final region is the hydrocarbon tail. Like the steroid ring region, this region is composed of carbon and hydrogen atoms. Both the ring region and tail region are non-polar.

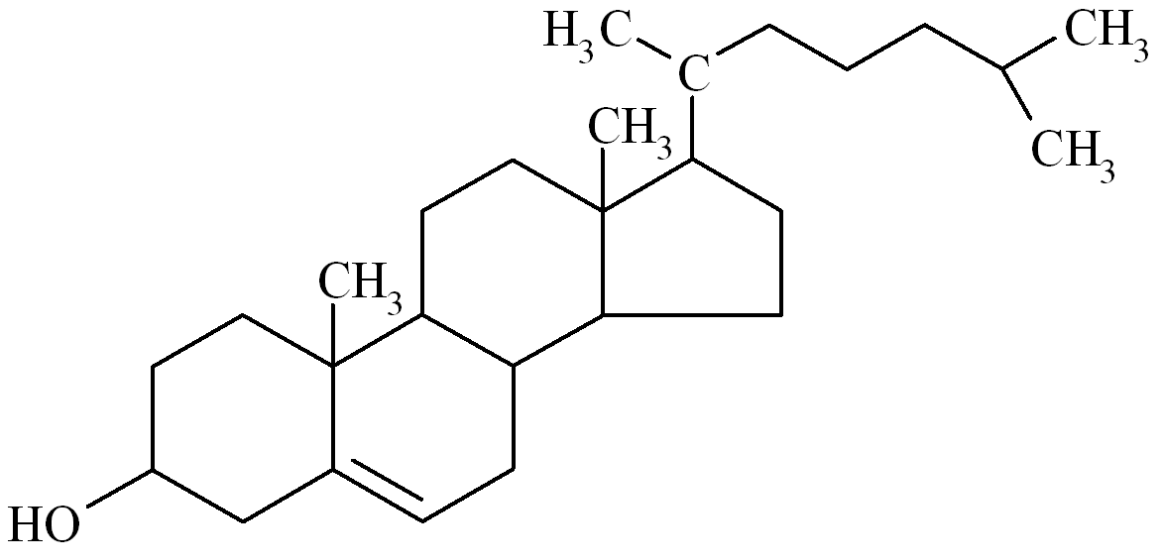

Figure 1.2 Chemical structure of cholesterol. Cholesterol is composed of three regions; a hydrocarbon tail, a ring structure region with 4 hydrocarbon rings and a hydroxyl group on C-3 (65).

1.3.2 Cholesterol production and regulation

Cholesterol is a waxy, whitish-yellow fat, which is a crucial building block of cell membranes and is also used to make hormones and bile acids (66). It is about 20% of cholesterol in the bloodstream comes from food items such as meat, poultry, fish, eggs, milk products, and other animal foods. The remainder of our cholesterol in circulation is made by the liver and intestines (67). Biosynthesis of cholesterol starts at acetyl coenzyme A and may be divided into three main synthesis stages (Figure1.3). Stage one is the synthesis of isopentenyl pyrophosphate, stage two is

the synthesis of squalene from six molecules of isopentenyl pyrophosphate and stage three is where squalene is converted to form cholesterol. Biosynthesis of cholesterol is regulated by cholesterol levels. Intracellular cholesterol is mainly regulated by the protein sterol regulatory element-binding protein pathways (68, 69).

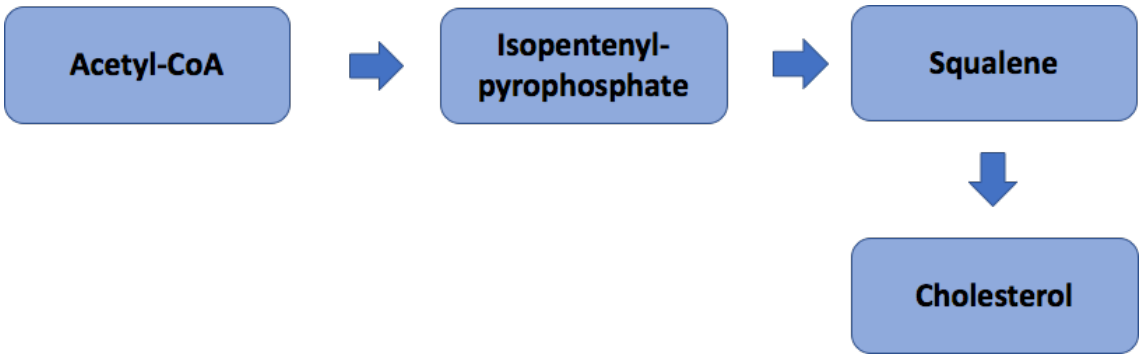

Figure 1.3 Overview of cholesterol biosynthesis. Cholesterol synthesis starts with acetyl-coenzyme A (Aceetyl-CoA). Three stages include isopentenyl-pyrophosphate, squalene and cholesterol synthesis.

1.3.3 Transport of cholesterol in the plasma

Lipoproteins are present in the plasma and are essential for the transport of cholesterol around the body (70). Specifically, lipoproteins contain triacylglycerol (TAG), cholesterol, phospholipids and apolipoproteins (APOs) (Figure 1.4A). There are five main types of lipoproteins isolated and characterised in the blood by centrifugation methods: chylomicrons, very low-density lipoprotein (VLDL), intermediate-density lipoprotein (IDL), low-density lipoprotein (LDL) and high-density lipoproteins (HDL). These vary in size (5–1000nm), protein/lipid composition function and in biological role (Figure 1.4). The APOB containing chylomicrons and VLDL deliver TAG to cells in the body, while IDL delivers triglyceride and cholesterol. In contrast, LDL only delivers cholesterol, and HDL removes excess cholesterol. A lipid profile therefore includes total cholesterol, HDL cholesterol, LDL cholesterol and triglycerides (71), with each parameter having a normal range (Table 1.4). The protein moiety of lipoprotein is known as APO, e.g. APOA1, APOB, APOE. Chylomicrons contain $APOB_{48}$, APOC, and APOE. VLDL molecules contain $APOB_{100}$ and APOE. IDL molecules contain $APOB_{100}$. LDL molecules mainly contain APO_{B100} whereas HDL mainly contain APOA1. Generally, each LDL particle contains one APOB

molecule (72). HDL contains variable amounts of APOA1 with the median content considered between one and two per particle (73, 74). The main function of APOA1 is in reverse cholesterol transport (75).

APOB contains two main isoforms in the plasma: $APOB_{48}$ and $APOB_{100}$. $APOB_{100}$ is composed of 4563 amino acids while $APOB_{48}$ consists of 2152 amino acids. They both share a common N-terminal sequence and $APOB_{48}$ does not have a C-terminal LDL receptor binding region (76). APOB plays an important role in lipoprotein transport. APOE contains 299 amino acids and multiple amphipathic α-helices. The N-terminal region forms an anti-parallel four-helix bundle and the C-terminal domain contains three α-helices and a LDL receptor-binding site. The main function of APOE is transporting lipids, fat-soluble vitamins and cholesterol into the blood through the lymph system (77). It is well understood that APOA1, APOB and APOE are the three major APOs that are involved in lipids transportation and metabolism compared to other APOs (APOD, APOH, APOM, APOJ).

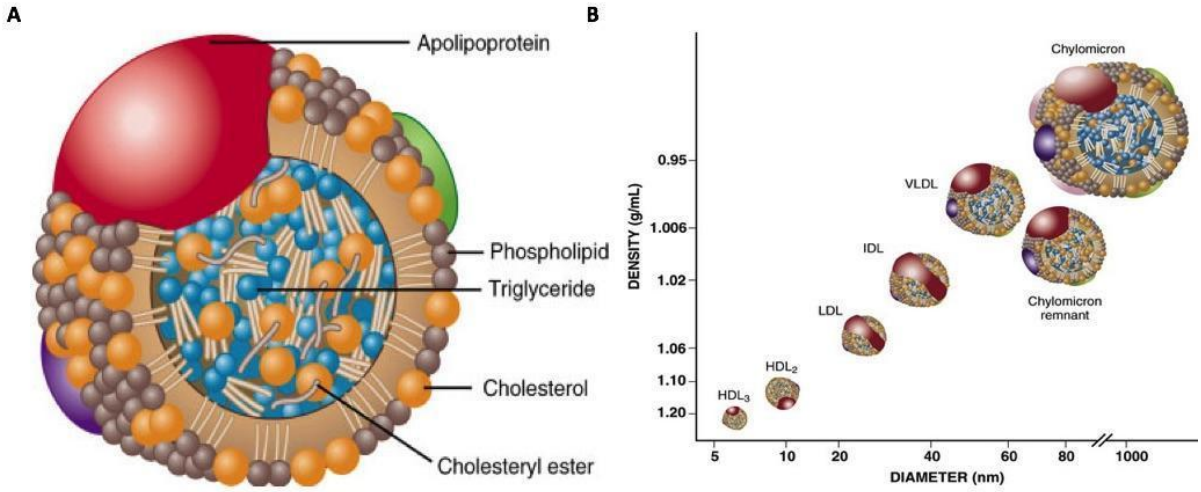

Figure 1.4 Structure and size of lipoprotein. (A) The structure of lipoprotein: The general structure of lipoprotein consists of cholesteryl esters, cholesterol, triglycerides and phospholipids. The protein moiety of lipoprotein is known as apolipoprotein (APO) such as APOB and APOA1 (78). (B) The size and density of different types of lipoproteins (79).

Table 1.4: Normal Ranges for Tests Which Make Up a Lipid Profile (71)

	Normal	Borderline	High
Total cholesterol (mmol/L)	< 5.2	5.2 - 6.2	> 6.2
LDL cholesterol (mmol/L)	< 3.3	3.4 - 4.1	> 4.1
Triglycerides (mmol/L)	< 1.7	1.7 - 2.2	> 2.3
	Poor	**Better**	**Best**
HDL cholesterol (mmol/L)	< 1	1 - 1.5	> 1.5

LDL: Low-density lipoprotein; HDL: High density lipoprotein

1.3.4 Role of cholesterol

There are three types of lipids present in plasma membranes; phospholipids, glycolipids and cholesterol (Figure 1.5). The plasma membrane contains more than 90% of cellular cholesterol (80). Properties of membrane cholesterol include maintaining cell membrane stability, keeping membrane fluid inside the cell and interacting with other biomolecules. Membrane cholesterol is widely reported to be involved in multiple diseases (81-82), for example it is known to affect Alzheimer's Disease by influencing $A\beta P_{1-40}$ and $A\beta P_{1-42}$ peptides cytotoxicity (83). Cholesterol is an obligate precursor for many steroid hormones. In addition, cholesterol helps the liver to create bile acid that, in turn, aids in the absorption of the fat soluble vitamins A, D, E, and K.

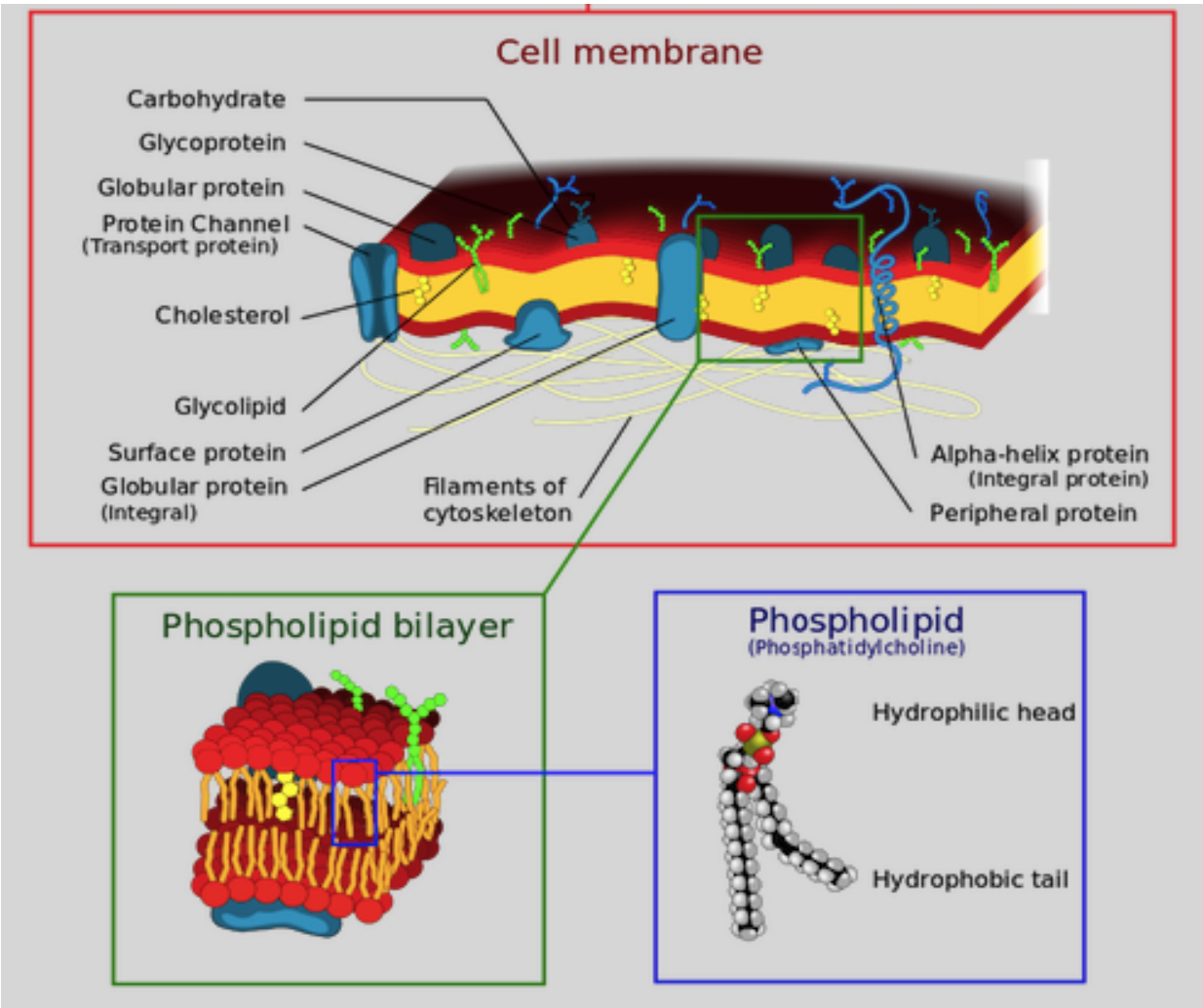

Figure 1.5 Cell membrane structure. The cell membrane is a semipermeable phospholipid bilayer which contains a variety of biological molecules, primarily proteins (glycoprotein, globular protein, surface protein, alpha-helix protein and peripheral protein) and lipids (cholesterol, glycolipid and phospholipid) (84).

1.3.5 Cholesterol in cardiovascular disease

Generally, total cholesterol, HDL cholesterol and LDL cholesterol are measured to assess the risk of CVD (85, 86, 87, 88). It is well known that LDL cholesterol is the "bad" cholesterol that contributes to the progression of CVD, whereas HDL cholesterol on the other hand is often called "good" cholesterol because of its' anti-inflammatory, anti-apoptotic, anti-oxidative (including prevention of LDL oxidation), anti-thrombotic and endothelial protective qualities (89). Most work has been done around the increased risk of CVD associated with LDL cholesterol, with small dense LDL particles being associated with an increased risk of CVD rather than large LDL particles (90). Furthermore, small LDL particles can easily penetrate the intimal vessel wall and become exposed

to oxidation. Macrophages can then take up oxidised LDL to be a part of atherosclerotic plaque (91). Small dense LDL particles have also been associated with endothelial dysfunction (92).

HDL cholesterol is known as "good" cholesterol because HDL cholesterol helps remove cholesterol from the bloodstream. Additionally, HDL cholesterol may have antioxidant, antithrombotic/profibrinolytic and anti-inflammatory properties (93). HDL exerts anti-inflammatory effects by promoting cholesterol efflux via ABCA1 and ABCG1 (94). Yvan-Charvet *et al* have reported ABCG1 transporter deficient macrophages can increase inflammatory gene expression (94). Clinically, statins are used to reduce LDL cholesterol and increase HDL cholesterol (95). Interestingly, the development of CETP (cholesteryl ester transfer protein) inhibitors which was designed to raise HDL levels failed in phase III of a clinical trial (96). HDL cholesterol can, however, turn into "bad" cholesterol according to several studies which showed that HDL becomes dysfunctional, even pro-atherogenic in CVD (97, 98, 99). Pan *et al* report that in particular, oxidised HDL reduces the proliferation and migration of endothelial cells which greatly contributes to the pathology associated with CVD (100). More recently, Bae *et al* reported low serum total cholesterol (< 4.14mmol/L) or high serum total cholesterol (≥6.21mmol/L) to be strongly associated with CVD mortality (101). A recent large Korean study has shown that it is unclear whether the association between total cholesterol levels and all-cause mortality varied with sex and age (102).

Regarding the role of membrane cholesterol in causing cardiovascular dysfunction, the following four points should be considered - 1) High levels of cholesterol cause changes to cell membrane structure and function; 2) Myocardial contractility, excitability and conduction properties have been affected by alterations of membrane cholesterol content; 3) Endothelial dysfunction and smooth muscle abnormalities are seen in high cholesterol situations.; 4) High cholesterol is associated with the oxidation products of cholesterol. It has also been shown that the total cholesterol content of the erythrocyte membrane is positively associated with severe coronary artery diseases (103). Furthermore, HDL efflux capacity is also impaired during acute

inflammation which may contribute to cholesterol retention in the cell membrane in inflammatory disorders (104). Therefore, considering the results of all of these studies, both lipoprotein cholesterol and membrane cholesterol have been shown to be involved in the pathophysiological processes of CVD.

1.4 Cholesterol Tracers

As noted above cholesterol is a crucial component of cellular membranes and plays an important role in multiple biological functions including cellular signalling and cell metabolism. However, the knowledge of cholesterol intracellular dynamics is limited due to the limited availability of cholesterol tracers. Cholesterol transport into cells can be studied using radiolabelled cholesterol such as ^{3}H-cholesterol (105, 106). Radiolabelled cholesterol methods are not feasible in every laboratory and are also very time-consuming. In addition, contamination with a small fraction of membranes with high cholesterol content can result in significant errors in cholesterol content measurement, therefore, various fluorescent probes of cholesterol have been developed and are widely used (106). Various studies make use of filipin, intrinsically fluorescent mimics of cholesterol (cholestatrienol and dehydroergosterol), or organic dye-labelled cholesterol analogs (NBD-cholesterol, BIODPY-cholesterol) (107). There are drawbacks to each of these methods as none truly reflect the physiological function of cholesterol. For example, cells labelled with filipin require fixation, so it is not practical to study time-lapse with living cells using this method. In addition, filipin labels all cellular cholesterol pools equally, and it is thus difficult to distinguish between lipoprotein-derived cholesterol and endogenous-derived cholesterol (107). The high photobleaching propensities of cholestatrienol and dehydroergosterol make it a challenging prospect to repeat imaging of the samples. For these reasons, organic dye-labelled cholesterol analogs have drawn a lot of attention recently, with 22-(*N*-(7-nitrobenz-2-oxa-1,3-diazol-4-yl)amino)-23,24-bisnor-5-cholen-3β-ol (22NBDC) and 25-(*N*-(7-nitro-2-1,3-benzoxadiazol-4-yl) methylamino27-norcholesterol (25NBDC) being widely used to study membrane cholesterol (108,

109). However, based on 22NBDC and 25NBDC chemistry and cell membrane structure, these two sensors are inserted in the membrane in a way that could potentially change the ability of cholesterol to move in a normal fashion within the cell (110). For example, the rate of 22NBDC and 25NBDC exchange between the cell and an acceptor has been shown to be much faster when compared to a normal cholesterol exchange rate (110, 111). As an alternative, 3-hexanoyl -7-Nitrobenz-2- oxa-1,3-diazol-4-yl-cholesterol (3NBDC) is attached to carbon 3 via a C6 spacer, at the hydrophilic end of cholesterol (Figure 1.6). The basic chemistry of this molecule means it is expected to more appropriately mirror the normal orientation of cholesterol in the membrane and recapitulate the interactions with other membrane components such as phospholipids. As part of our study is to identify an MP-compatible cholesterol tracer, we explored the use of 3NBDC to recapitulate cholesterol movement in various cell systems (THP-1 cells, HMDM cells, HeLa cells and HEK 293T cells).

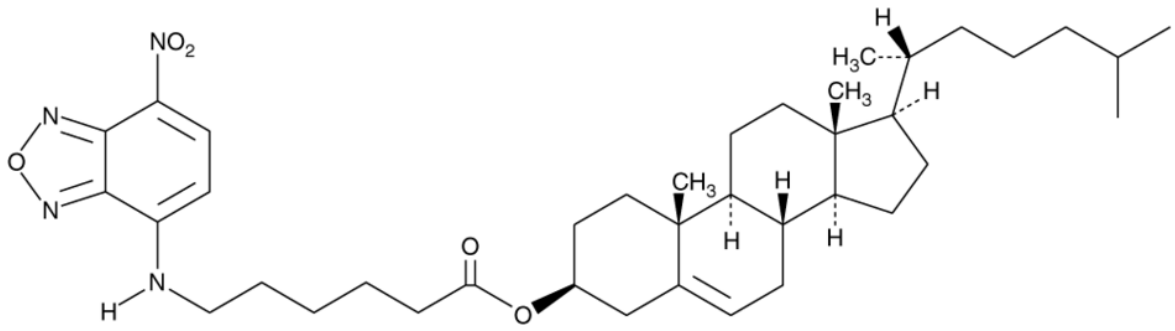

Figure 1.6 The structure of 3-NBD-Cholesterol. The fluorescence tag of 3-hexanoyl- 7-Nitrobenz-2-oxa-1,3-diazol-4-yl-cholesterol (3NBDC) is attached to carbon 3 via a C6 spacer, at the hydrophilic end of cholesterol (112).

1.5 The Immune System

The immune system has evolved in vertebrates to protect the body against invading micro-organisms and the diseases they cause. The foundation of the immune system consists of two separate branches: one is specific or adaptive immunity, which is characterised by slow response

kinetics and memory, and the other is non-specific or innate immunity which displays rapid response kinetics but lacks memory (113). It used to be thought that both these systems acted relatively independently although research into innate immune recognition systems has long established that there is crosstalk between the two systems which coordinates their action (114, 115), the links between both systems often impinging on the course that autoimmune diseases take. An example of a link between the innate and adaptive immune system was very nicely shown during the development of the granulomas which are involves both Toll-like receptor (TLR) and Notch activation (116). Interplay between both the innate and adaptive response is crucial in mounting an appropriate combined response to invading pathogens. The innate response to infection can stimulate the adaptive immune response through the release of cytokines and chemokines, which subsequently attract additional cells to the site of infection or induce the migration of APCs from the tissues to lymph nodes where naïve T cells can be activated (117). Adaptive immune responses contribute to innate immunity by enhancing the antimicrobial activities and defence mechanisms of this system (117).

The early concept of innate immunity was that it non-specifically recognised microbes. However the discovery of TLRs in the mid 1990s demonstrated that pathogen recognition by the innate immune system is actually reasonably specific, relying on germline-encoded pattern-recognition receptors (PRRs) that have evolved to detect components of foreign pathogens, referred to as pathogen-associated molecular patterns (PAMPs) (118, 119). The main cell types involved in innate immunity are natural killer (NK) cells, mast cells, eosinophils, basophils and the phagocytic cells such as macrophages, neutrophils and dendritic cells (DCs) (120, 121). Two major functions of this system are recruitment of immune cells to sites of infection through the production of cytokines and activation of the complement cascade to identify bacteria and promote their clearance. Macrophages and DCs routinely take up and present self-antigens, however these cells themselves can also become activated by self-antigens such as cell debris as a result of cell damage caused by the infection (121,122,123).

Rapid induction of type I and II interferon (IFN) expression is a central event in the establishment of the innate immune response against viral infection. To trigger IFN expression, host cells recognise infection through several families of PRRs, including TLRs, RIG-I-like receptors (RLRs), nucleotide-binding oligomerisation domain (NOD)-like receptors (NLRs), as well as the cytoplasmic sensors of DNA virus infection (124). Following engagement of viral sensors by their cognate PAMPs, the host cell activates multiple signalling cascades that stimulate an antiviral state, the induction of host restriction factors and the mobilisation of the adaptive arm of the immune system (125). The resulting coordinated response disrupts viral replication at multiple levels, including the recruitment of NK cells, which provide rapid responses to virally infected cells (126). In autoimmunity, these processes may happen in response to self-antigens in addition to external antigens (127).

1.5.1 Toll-like receptors

TLRs are a class of protein that are critical for both innate and adaptive immune responses to recognise specific molecular patterns that are derived from different pathogens (128). TLRs include TLR1-13 in mammals, with TLR1-10 being found in humans while TLR1-9 and TLR11-13 are found in mice (129). TLRs are generally located on the plasma membrane with the exception of TLR3, TLR7, TLR8 and TLR 9, which are located in the endosomal compartment (Figure 1.7). TLR expression has been found on many different immune cells, including T cells, B cells, monocytes and macrophages (Table 1.5) (129,130). As described in Table 1.5, TLR4 is widely expressed on macrophages and monocytes (130), therefore, THP-1 cells (a human monocytic cell line) and human monocytes derived macrophages (primary macrophages) were used as cell models in this study. Data from human patients and animal models of autoimmune diseases indicate that inappropriate triggering of TLR pathways might cause an autoimmune reaction and tissue damage by releasing inflammatory cytokines, chemokines and other biomolecules (131). Aberrant TLR signalling has been implicated in a variety of autoimmune diseases such as Sjögrens Syndrome (SS), Systemic Lupus Erythematosus (SLE), Rheumatoid Arthritis (RA) and Multiple Sclerosis

(MS) (132). Therefore, the influence of autoimmune diseases (SLE/RA) derived MPs on TLR4 expression *in vitro* and *ex vivo* cell models was one part of this study.

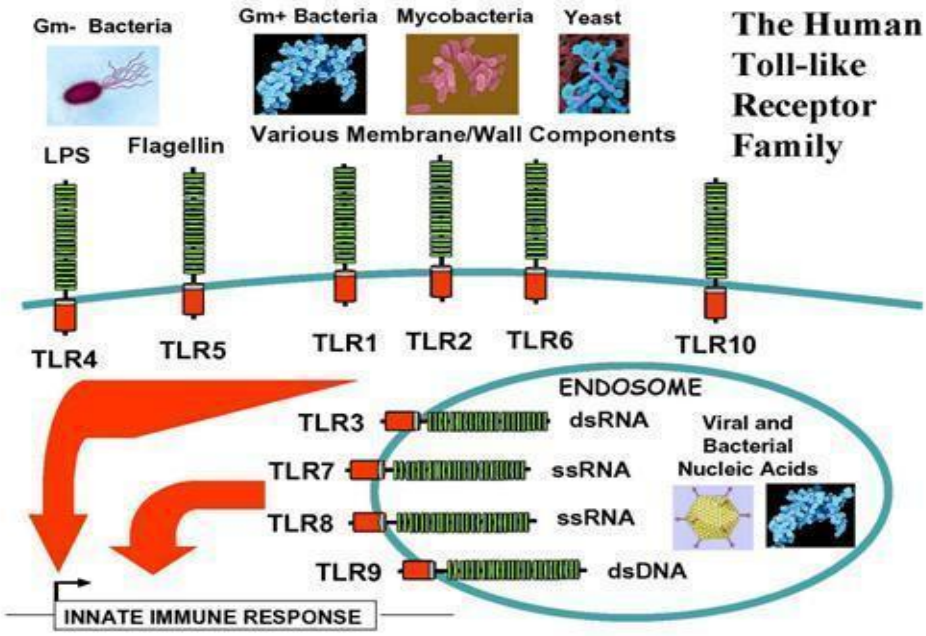

Figure 1.7 Locations of human toll-like receptors. TLR1, 2, 4, 5, 6 and 10 are located on the plasma membrane. TLR 3, 7, 8 and 9 are located within the endosomal compartment (133).

Table 1.5 The Expression Pattern of Human Toll-like Receptors on Immune Cells (130)

TLR	Expression on immune cells
1	Monocytes, macrophages, Bcells, Tcells, DCs, PMN, NK cells
2	PMN, DCs, monocytes, macrophages
3	DCs, NK cells, macrophages, mast cells
4	Macrophages, DCs, Monocytes, PMN
5	Monocytes, DCs, T cells, PMN, macrophages
6	Monocytes, macrophages, B cells, T cells, DCs, PMN, NK cells
7	B cells, plasmacytoid DCs
8	Monocytes, myeloid DCs
9	B cells, plasmacytoid DCs,
10	B cells; plasmacytoid DCs

TLRs: Toll-like receptors; DCs: Dendritic cells; PMN: Polymorphonuclear leucocyte; NK: Natural Killer;

TLRs are a class of PRRs that are activated subsequent to the recognition of PAMPs and damage-associated molecular patterns (DAMPs) (134). A series of processes not only trigger host innate immune responses but also host adaptive immune responses (135). TLRs interact with their respective PAMPs and DAMPs and combine with co-receptors or molecules to form a homo- or heterodimer to initiate downstream signalling pathways (135). TLRs are composed of an ectodomain which recognises PAMPs and DAMPs, a transmembrane domain and a cytoplasmic Toll/IL-1 receptor (TIR) domain which binds MyD88 and TRIF, two adaptor proteins (136). When TLRs recognise PAMPs and DAMPs, MyD88 or TRIF is activated which results in downstream phosphorylation events culminating in the activation of NF-κB or interferon regulated factors (IRFs) and production of pro-inflammatory cytokines and type I IFN which protect the host from microbial infection (Figure 1.8) (136, 137).

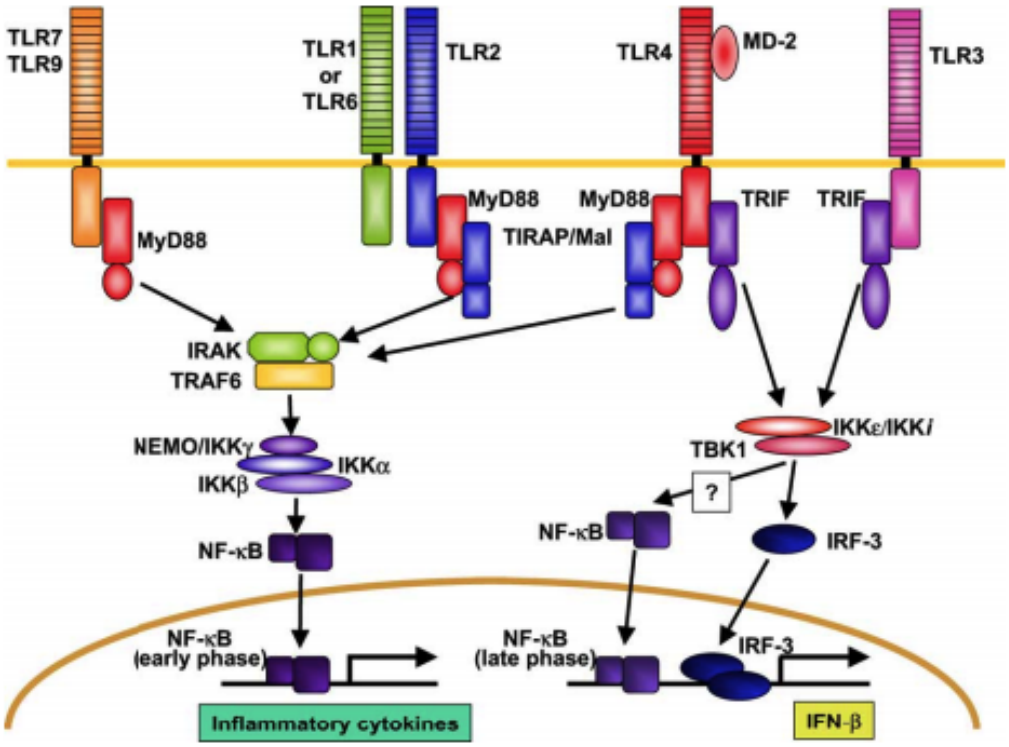

Figure 1.8 Toll-like receptor signalling pathways. Activation of the MyD88 or TRIF signalling pathways downstream of Toll-like receptors (TLRs) results in pro-inflammatory cytokine production or type I interferon production respectively (137).

1.6 Autoimmune Disorders

Autoimmune disorders are multifactorial diseases characterised by an abnormal immune response to reactive self-antigens by T and B cells, resulting in chronic inflammation (138). Inflammation in autoimmune disorders can involve multiple organs, leading to systemic autoimmune diseases, such as SS, RA, SLE, systemic sclerosis (SSc) and primary biliary cirrhosis to name but a few (139).

1.6.1 Systemic Lupus Erythematosus

SLE is a multi-organ autoimmune disease that often results in end-organ failure (140). Redundant autoantibodies are produced against self-antigens that are located in the nucleus of cells, with genetic, environmental and hormonal factors contributing to the occurrence of SLE (141). SLE occurs worldwide, with most cases seen in women of childbearing age. The pathogenesis of SLE is complex, with key events resulting in the increased presence of apoptosis-related endogenous nucleic acids which subsequently stimulate IFNα production and promote autoimmunity by breaking self-tolerance through the activation of APCs (Dendritic cells, B cells), following the amplification of immune complexes and inflammation (142) (Figure 1.9). Aberrant innate immune responses play a key role in the pathogenesis of SLE, which contributes to tissue injury and aberrant activation of autoreactive T and B cells (143). Autoreactive T and B cells activation leads to autoantibody production and end-organ injury (143).

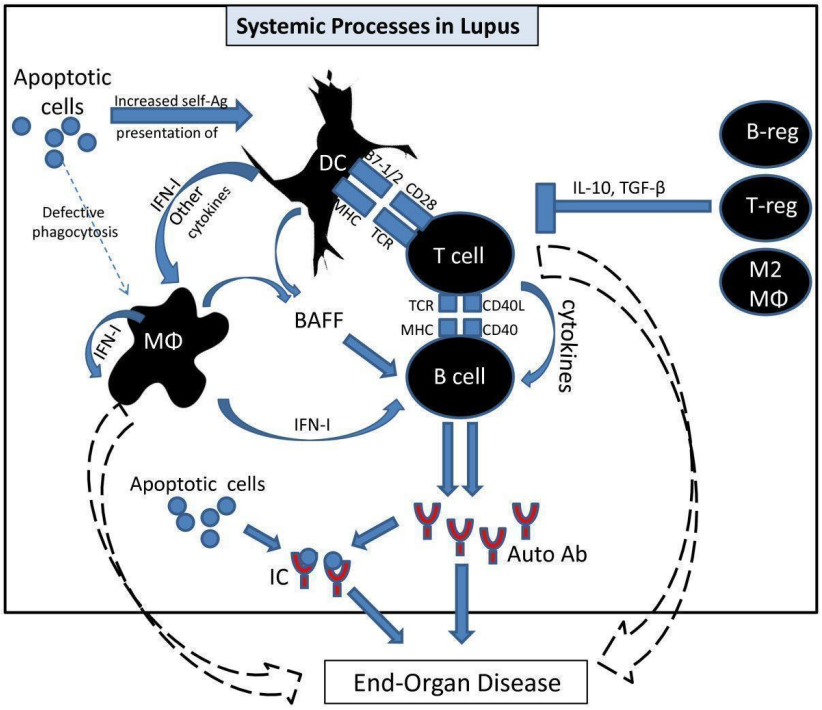

Figure 1.9 Pathogenic mechanisms of Systemic Lupus Erythematosus. Different subpopulations of immune cells, immune complex and cytokine interplay contributes to disease progression and leads to end organ failure (kidneys and heart). Ab, antibody; BAFF, B-cell activation factor; DC, dendritic cell; IC, immune complex; IFN-I, interferon-I; IL-10, interleukin-10; MΦ, macrophage; MHC, major histocompatibility complex; self-Ag, self-antigen; TCR, T-cell receptor; TGF-β, transforming growth factor-beta (142).

The diagnosis of SLE is based on a combination of clinical symptoms and positive serologies. SLE has heterogenous clinical manifestations, resulting in the development of several classification criteria such as the Systemic Lupus International Collaborating Clinics (SLICC) criteria (144) (Table 1.6). Assessing SLE disease activity is an integral part of diagnosis, with many patients continuing to suffer from disease effects even after being provided with appropriate treatment (144). Several sets of indices have been developed and used as a clinical index for the measurement of SLE, such as the Systemic Lupus Activity Measure (SLAM) and Systemic Lupus Activity Index (SLEDAI). SLEDAI is used as a global index due to its validity, reliability and sensitivity, consisting of 24 weighted clinical and laboratory variables of nine organ systems. Manifestation items are weighted with scores ranging from 1 to 8 (145) (Table 1.7). SLE patients with a SLEDAI score ≥ 6 are considered to have "active" disease. For the clinical management of SLE, there is no effective medicine that is conducive to treatment; rather the approach combines immunomodulators, facilitates immunosuppression and prevents organ damage.

Table 1.6: Systemic Lupus International Collaborating Clinics Criteria (144)

Clinical Features	Immunologic Features
Acute cutaneous lupus (maculopapular lupus rash, malar rash, photosensitive lupus rash, etc)	High ANA concentration
Chronic cutaneous lupus (discoid rash, mucosal lupus, etc.)	High anti-dsDNA antibody concentration
Oral or nasal ulcers	Presence of anti-Sm
Non-scarring alopecia	Positive APA
Synovitis in 2 joints	Low complement (C3,C4,CH50)
Serositis	Direct Coombs test
Renal (urine protein or RBC casts)	Must have a total of 4 features with 1 clinical feature and 1 immunologic feature or biopsy-proven LN with anti-dsDNA antibodies or ANA
Neurologic (seizures, psychosis, other)	
Haemolytic anaemia	
Leucopoenia or lymphopenia (without an identifiable cause)	
Thrombocytopenia) without an identifiable cause)	

ANA: antinuclear antibody; APA:antiphospholipid antibody; dsDNA:double-stranded DNA; LN:Lupus nephritis; SLICC:Systemic Lupus International Collaborating Clinics; Sm:Smith.

Table 1.7: Systemic Lupus activity index scores (145)

SLEDAI	Yes	No	Descriptor	Definition
8	1	0	Seizure	Recent onset. Exclude metabolic, infectious or drugs causes.
8	1	0	Psychosis	Altered ability to function in normal activity. Include hallucinations, incoherence, marked loose associations, marked illogical thinking, bizarre, disorganised, or catatonic behaviour.
8	1	0	Organic brain syndrome	Altered mental function, impaired orientation, memory or other intellectual function, rapid onset and fluctuating clinical features.
8	1	0	Visual disturbance	Retinal changes of SLE. Include cytoid bodies, retinal haemorrhages, serous exudate or haemorrhages in the choroid or optic neuritis.
8	1	0	Cranial nerve disorder	New onset of sensory or motor neuropathy involving cranial nerves.
8	1	0	Lupus headache	Severe, persistent headache; may be migranious, but must nonresponsive to narcotic analgesia.
8	1	0	CVA	New onset of cerebrovascular accident(s). Exclude arteriosclerosis
8	1	0	Vasculitis	Ulceration, gangrene, tender finger nodules, periungual infarctions, splinter haemorrhages, or biopsy or angiogram proof of vasculitis.
4	1	0	Arthritis	More than 2 joints with pain and signs of inflammation
4	1	0	Myositis	Proximal muscle aching/weakness, associated with elevated CPK/aldolase/EMG changes/biopsy showing myositis
4	1	0	Urinary casts	Leme-granular or red blood cell casts
4	1	0	Haematuria	>5 red blood cells/high power field. Exclude stones, infection, other.
4	1	0	Proteinuria	>0.5mg/24hours.
4	1	0	pyuria	>5 white blood cells/high power field. Exclude infection.
2	1	0	Rash	Inflammatory type rash.
2	1	0	Alopecla	Abnormal patchy or diffuse loss of hair.
2	1	0	Mucosal ulcers	Oral or nasal ulcerations.
2	1	0	Pleurisy	Pleuritic chest pain with pleural rub or effusion,or pleural thickening.
2	1	0	Pericarditis	Pericardial pain with at least 1 of the following: rub, effusion, or positive ECG or echo
2	1	0	Low complement	Decrease in CH50. C3 or C4 below the lower limit of normal for testing.
2	1	0	Increased DNA binding	Increase DNA binding above normal range for testing laboratory.
1	1	0	Fever	>38 degrees C, exclude infectious cause.
1	1	0	Thrombocytopenia	$<100 \times 10^9$ platelets/L, exclude drug causes.
1	1	0	Leucopenia	$<3 \times 10^9$ WBC/L, exclude drug causes.

1.6.2 Rheumatoid Arthritis

RA is a systemic, autoimmune inflammatory disease which is characterised by damaged synovial joints which leads to deformity and disability (146). The disease is caused by the immune system

attacking healthy body tissue, but what triggers it remains unclear. Some risk factors may contribute to the occurrence of RA such as family history, obesity, age, and smoking (147). There are two major subtypes of RA based on the presence or absence of anti-citrullinated protein antibodies (148). The pathological processes of RA involves T cells, B cells, DCs, macrophages, cellular cytokines and cell surface molecules. The complex pathogenesis of RA is summarised in figure 1.10 (148). Genetic and environmental factors disturb peptide citrullination, followed by APCs (macrophages and DCs) and fibroblast-like synoviocytes being activated which results in local inflammation and antigen presentation. This ultimately leads to activation of the innate immune system and severe organ damage (148). Aberrant intracellular signalling pathways may contribute to the development of RA. Cytokines, chemokines, antibodies and antigens that contribute to inflammation bind to receptors on the cell surface of immune cells. Once receptors are bound, a cascade of intracellular signalling is initiated which ultimately results in pro-inflammatory gene expression (149). Overall, immune activation and RA disease progression is a complex process that involves both adaptive and innate immune systems (149).

Criteria for RA diagnosis include patients having at least one joint with swelling and/or a number of small joints involved, in which case the joint swelling cannot be explained by another disease (146). Patients with diagnosis of inflammatory arthritis with the presence of rheumatoid factor, anti-citrullinated protein antibodies, elevated C-reactive protein (CRP) levels, or an erythrocyte sedimentation rate (ESR) (150), also suggest the patient has RA. Diagnostic criteria are shown in Table 1.8, according to the American College of Rheumatology/European League against Rheumatism. Treatment of RA aims to control the inflammation of synovitis and prevent joint injury. Medicine-based therapies include nonsteroidal anti-inflammatory drugs, anti-rheumatic drugs, immunosuppressants and corticosteroids, depending on disease activity and the sensitivity of patients to certain drugs.

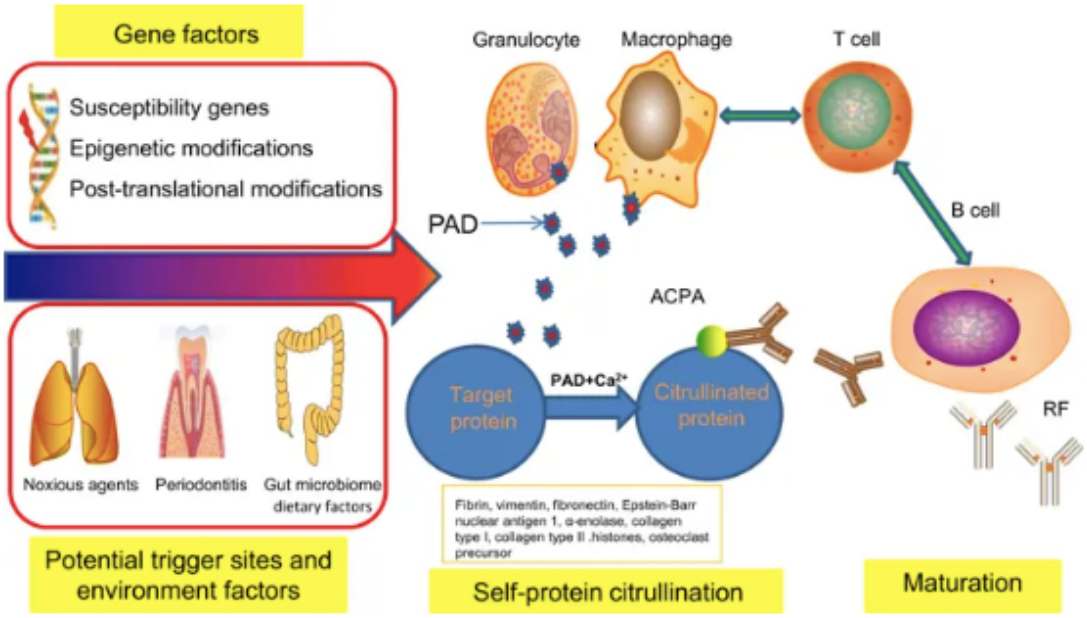

Figure 1.10 Disease mechanisms in Rheumatoid Arthritis. Genetic and environmental factors disturb peptide citrullination to produce anticitruline antibodies, followed by immune cells activation (T cells, B cells, macrophages and dendritic cells) leading to organ damage (148).

Table 1.8: Rheumatoid Arthritis Diagnostic Criteria (151)

CRITERIA	SCORE
Target population (who should be tested?): patients who: 1) have at least one joint with definite clinical synovitis (swelling) 2) with the synovitis not better explained by another disease	
Classification criteria for RA (score-based algorithm: add score of categories A through D; a score of ≥ 6 out of 10 is needed for classification of a patient as having definite RA):	
A. Joint involvement	
One large joint	0
2-10 large joints	1
1-3 small joints (with or without involvement of large joints)	2
4-10 small joints (with or without involvement of large joints)	3
> 10 joints (at least one small joint)	5
B. Serology (at least one test result needed for classification)	
Negative RF *and* negative ACPA	0
Low positive RF *or* low positive ACPA	2
High positive RF *or* high positive ACPA	3
C. Acute phase reactants (at least one test result needed for classification)	
Normal CRP *and* normal ESR	0
Abnormal CRP *or* normal ESR	1
D. Duration of symptoms	
< six weeks	0
≥ six weeks	1

ACPA = anti-citrullinated protein antibody; CRP = C-reactive protein; ESR = erythrocyte sedimentation rate; RA = Rheumatoid Arthritis.

1.6.3 Cytokine production in autoimmunity

Inflammation is caused by the interplay of pro-inflammatory and anti-inflammatory cytokines (152). Understanding the exact physiological role of these cytokines in inflammation and their pathogenic role in disease status is essential for the foundation of new therapies in autoimmune conditions. Generally, the pro-inflammatory factors include interleukin- 6 (IL-6), IL-8, tumour necrosis factor alpha (TNFα), IFN, IL-13/17 and B-cell activation factor. Anti-inflammatory cytokines include IL-1 receptor antagonist, IL-4, IL-6, IL-10, IL-11 and IL-13. These cytokines are produced by macrophages and other immune cells. Human TNFα is a non-glycosylated protein, and the TNFα gene is located on chromosome 6p23-6q12. TNFα exists both in soluble and membrane bound forms (153). TNFα is not only a powerful regulator of pro-inflammatory

cytokines but also increases lipid transduction mediators (154). TNFα signals through two transmembrane receptors, TNFR1 and TNFR2, and regulates a number of critical cell functions including cell proliferation, survival, differentiation, and apoptosis (155). Macrophages are the major producers of TNFα and interestingly are also highly responsive to TNFα (155). Aberrant TNFα production and TNF receptor signalling have been associated with the pathogenesis of several diseases, including RA, Crohn's disease, atherosclerosis, psoriasis, sepsis, diabetes, and obesity (155). TNFα has been shown to play a pivotal role in orchestrating the cytokine cascade in many inflammatory diseases and because of this role as a "master-regulator" of inflammatory cytokine production, it has been proposed as a therapeutic target for a number of diseases. Indeed anti-TNFα drugs are now licensed for treating certain inflammatory diseases including RA and inflammatory bowel disease (156). Studies have shown that TNFα blockers reduce the number of infiltrating synovial granulocytes and macrophages and reduce chemokine IL-8 and monocyte chemotactic protein-1 in RA (157). This type of treatment however is not advised in all autoimmune conditions as TNFα blockers can also block the immunoregulatory and anti-apoptotic effects of TNFα in conditions such as SLE and so is ill-advised in this case (158).

1.7 Microparticles in Autoimmune Disorders

It is well known that TNFα stimulates the release of MPs, with recent studies showing MPs as substrates for inflammation (159). Furthermore, other studies have also shown MPs induce, amplify and maintain the process of inflammation by combining with other inflammatory factors (159, 160, 161, 162). Due to the diversity of MP content and biological function, specific parts of MPs have also been shown to have anti-inflammatory functions (163). Whether the MP produced has pro-inflammatory or anti-inflammatory properties appears to be dependent on the stage of the disease.

Increased levels of pro-inflammatory cytokines (IFN and TNFα) are observed in SS patients (164, 165), suggesting inflammation plays an important role in SS pathology. Although there are few

studies reporting the role of MPs in SS, Sellam *et al* report that both platelet and leucocyte-derived MPs are increased in SS patients, implying that MPs may play a role in the process of inflammation in SS (166). More recently, a study reported that endothelial MPs are directly correlated with SS duration, explicitly suggesting that endothelial MPs are involved in the pathogenesis by participating in the processes of inflammation and endothelial dysfunction (167). Further studies are needed to highlight the precise mechanisms which MPs play in SS and to assess if MPs can act as an inflammatory indicator in this disorder.

Psoriasis is a chronic inflammatory disorder leading to skin and joint injury (168). Several studies report that the levels of both endothelial- and platelet-derived MPs are increased in psoriasis patients (169, 170). Reports imply that MPs are involved in the activation of inflammation and endothelial dysfunction which leads to increased CVD risk in these patients (170). Furthermore, another study supports previous studies and reports that the level of MPs from endothelial cells, platelets and monocytes is increased (171), further suggesting that MPs aggravate the development of psoriasis by leading to the activation of inflammation and endothelial dysfunction. More recently, Pirro *et al* have demonstrated that endothelial MPs are correlated with systemic inflammation (172). Another study suggests platelet MPs and endothelial MPs are significantly reduced when TNFα is blocked in psoriasis patients (173), and suggests TNFα may induce MP release to initiate inflammatory activation and increase CVD risk in psoriasis. Further studies are needed to illuminate how MPs, derived from different cell types, do in fact regulate the inflammatory process in psoriasis.

1.7.1 Microparticles and Systemic Lupus Erythematosus

SLE is a chronic inflammatory autoimmune disease which affects almost all organs in the body. As a result of this, the pathophysiology of SLE is complex and involves a multifactorial response with studies confirming inflammation plays a vital role during the process (174). There is, therefore, a rationale in finding an inflammatory indicator which could be used to monitor disease progression or which could function as a druggable target. Recently MPs have been implicated in

many diseases involving inflammatory processes, however, there are still limited studies directly reporting MPs as an inflammatory indicator in SLE, with the role that MPs play in SLE patients still being argued (175). One study reports endothelial MPs do not show any significant difference between SLE patients and healthy people (176). On the other hand, Parker *et al* report that suppressing inflammation can in fact reduce the levels of endothelial derived MPs in SLE suggesting there is a clear link between MPs and the inflammatory process in this condition (177). The heterogeneous nature of SLE in addition to patients entering disease flares versus being quite well may be the reason why studies yield different results regarding the role which MPs play in the disease process. Some authors find similar endothelial MPs levels between SLE patients and healthy controls, when disease activity is controlled, aligning with the idea that inflammation is one of the mechanisms of endothelial dysfunction (177). Another study reports that the levels of $CD54^{+}$ endothelial MPs in SLE patients is higher than in healthy controls (178). This study mentions several reasons why other papers did not find significant differences in other endothelial MP markers (CD62E, CD51, CD146) with reasons including the different techniques employed in MP isolation, in addition to endothelial activation or apoptosis (178). Overall these studies confirm the heterogeneous nature of MPs and suggest the need for further work to investigate the usefulness of MPs in monitoring inflammatory processes and endothelial dysfunctional in SLE.

More recently, one study has shown monocyte MP levels to be much higher in SLE active patients compared to inactive patients ($p<0.05$), however endothelial cell MPs, platelet MPs and B lymphocyte MPs showed no significant difference between both groups (179). It is well understood that IFNα is a major inflammatory factor in SLE, with Niessen *et al* reporting that IFNα and apoptotic-cell-derived MPs together can amplify and maintain inflammation (180). A more recent study further reports endothelial MPs and partial granulocyte MPs increase the expression of pro-inflammatory cytokines in SLE patients (181). Different results observed in the above studies discussed may be due to SLE disease activity in addition to the heterogeneous nature

of MPs and knock on diverse biological function, even relating to MPs derived from the same cell type. Further studies are required to evaluate the potential of MP inflammatory indicators in SLE.

1.7.2 Microparticles and Rheumatoid Arthritis

RA is a chronic progressive autoimmune disease with unknown aetiology, causing inflammation in the small joints which results in their deformity and immobility (182). Currently, there is limited research directly reporting MP involvement in RA associated inflammation, with studies generally involving MPs derived from the plasma and synovial fluid of RA patients. In 2002, pioneering research in the field reported that platelet MPs were increased and related to disease activity in RA (183). Although this study indirectly reports that MPs are involved in the inflammatory process in RA, the mechanism by how they do this is still poorly understood. The direct role which MPs play in the inflammatory response in RA was not reported until 2005 when a subsequent study suggested that MPs derived from synovial fluid increased the levels of inflammatory chemokines and cytokines such as IL-6 and IL-8 (184). A later study discovered one of the mechanisms of leukocytapheresis related to decreased platelet MPs and increased granulocyte-derived MPs, also indicating that MPs play a key role in the inflammatory response seen in RA (185). On the other hand, MPs derived from different cells types play different biological functions, with platelet MPs releasing inflammatory cytokines and granulocyte-derived MPs increasing anti-inflammatory cytokines, suggesting the complicated biological functions of MPs (185). More recently, an *in-vitro* study involving different cell-derived MPs from plasma and urine in RA patients reported that MPs are highly associated with disease activity and release of IL-1, IL-17 and TNFα (179). Considering the above studies, it appears that MPs play a key role in the inflammatory process in RA, but the precise mechanism of how they do this still remains elusive.

1.8 Cholesterol in Autoimmune Disorders

Cholesterol plays an important role in cellular and systemic metabolism involved in the regulation of immune cell activity (186,187). The major part of cellular cholesterol is located in the cellular

membrane in particular the lipid raft region is enriched with cholesterol (188). To date, previous studies have shown that the lipid raft plays an essential role as a signalling pathways. Several studies have demonstrated that TLR4 and T cell receptor (TCR)-mediated immune activation and pro-inflammatory responses are suppressed by cholesterol depletion from the lipid raft, while cholesterol loading has the opposite effect (186, 189). Furthermore, Tall *et al* reported that activation of TLR signalling results in reduced cholesterol efflux, which leads to cholesterol accumulation and amplification of the inflammation response (189). Yvan-Charvet *et al* have also shown free cholesterol accumulation and an increased in TLR signalling in ABCG1 transporter deficient macrophages (94). A number of studies have indicated that lipid abnormalities are observed in autoimmune diseases such as SLE and RA, with one study reporting that low HDL cholesterol is associated with a higher risk of autoimmune disease development (190, 191). Abdalla *et al* reported that there are significantly higher cholesterol and LDL cholesterol levels in SLE patients with lupus nephritis when compared to SLE patients without lupus nephritis (192). Although the exact mechanisms have not been elucidated, one study shows that the functional properties of HDL play a key role in inflammatory pathophysiology properties of HDL (193). Specifically, in an acute-phase response of inflammation, APOA1 (which is the major protein component of HDL) is replaced by other acute-phase proteins, like SAA protein. SAA protein can promote the pro-inflammatory properties of HDL (193). The pathogenesis associated with the dyslipidaemia in SLE is shown in figure 1.11. Multiple pathogenic mechanisms are suggested, including antibodies against lipoprotein lipase and the balance between pro-atherogenic lipoproteins and anti-atherogenic lipoproteins being affected by cytokines (194).

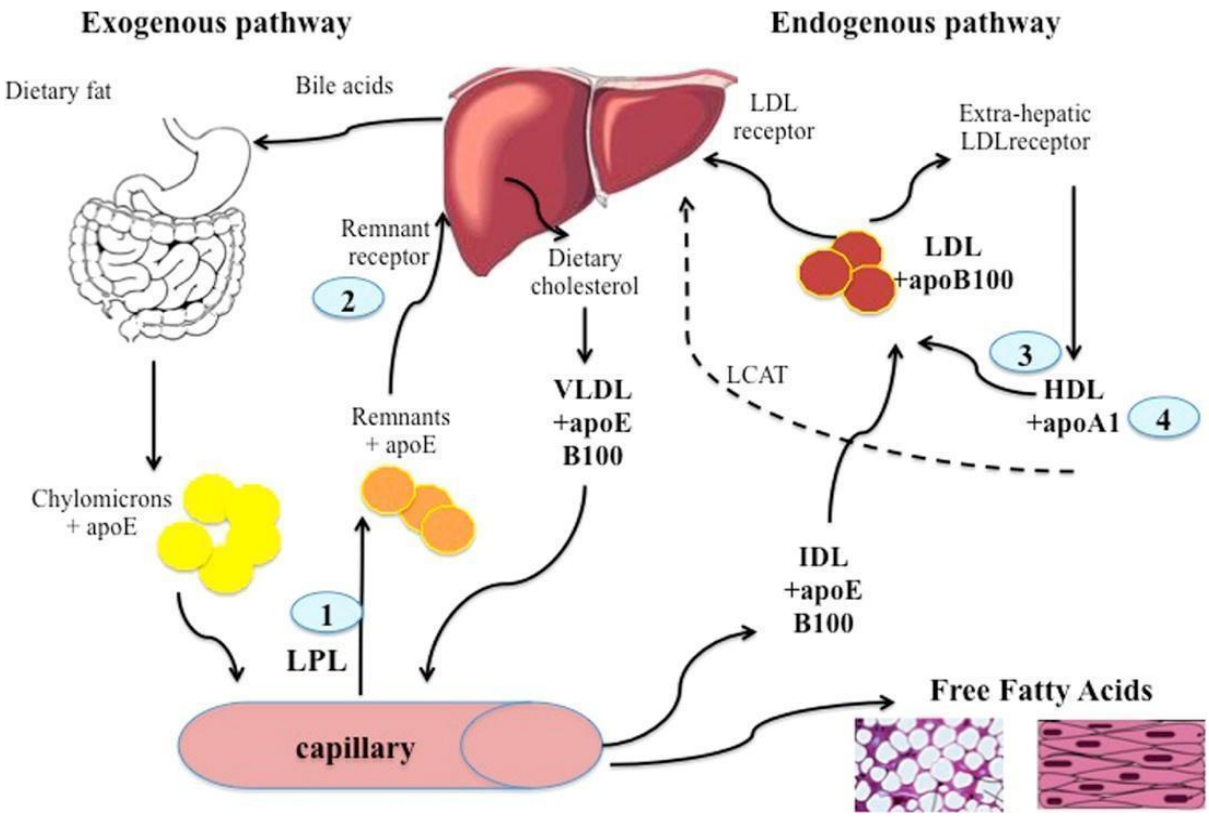

Figure 1.11 Lipid metabolism abnormalities have been shown in Systemic Lupus Erythematosus. 1): Antibodies against lipoprotein lipase (LPL) may decrease the ability to degrade chylomicrons. 2): Removal of chylomicrons is delayed. 3): & 4): HDL dysfunction (194).

It is well-known that autoimmune patients are at a higher risk of CVD (195). However, little is known of the underlying mechanism. Generally, it is accepted that high total cholesterol and high LDL-C increases risk of CVD. Interestingly, dyslipidaemia is sometimes present in RA, with patients often showing low total cholesterol and low HDL-C when compared to that of the general population (196). Elena *et al* have reported low LDL-C and low total cholesterol is associated with CVD risk (197). Although a mechanistic explanation is lacking. Studies have suggested that the reason for this lipid paradox is inflammatory effects influencing lipid ratio (196). A recent study by Huang *et al* has suggested that one of the principal causes of CVD in mice with psoriasis-like conditions was cholesterol trapped in inflexible vessels walls, which inevitably led to CVD (198). Taken together, these studies suggest that cholesterol may contribute to the disease processes observed in autoimmunity.

1.9 Overall Aims of the Study

- Optimise a method for the estimation of cholesterol in circulating MPs from platelet concentrates
- Establish a reference range for MP cholesterol (MPC) in a healthy representative population group
- Investigate the potential of MPC as a biomarker in autoimmune disorders (SLE and RA)
- Characterise inflammatory properties of MPs derived from autoimmune disease patients in *in vitro* and *ex vivo* models
- Develop 3NBDC as a versatile membrane cholesterol tracer

2.0 Materials and Methods

2.1 Sample Collection

2.1.1 Processing of platelet concentrates

Platelet concentrates were obtained from the Irish Blood Transfusion Service in St James Hospital. A 50ml aliquot of this concentrate was centrifuged at 879g for 10 minutes to remove platelets. This procedure was repeated three times before the supernatant was finally centrifuged at 879g for 5 minutes to remove residual platelets completely. The platelet-free supernatant (PFS) was aliquoted into 1.5ml sized fractions and stored at -80℃.

2.1.2 Processing of whole blood

Fasting (at least 12 hours) or non-fasting blood samples were collected from healthy volunteers from the student and staff population of TU Dublin. Patients with autoimmune conditions (SLE and RA) were recruited from clinics in Beaumont Hospital. Written informed consent was obtained from each donor under TU Dublin (DIT) REC-16-49 and Beaumont hospital reference REC-17-17. In all cases, venous blood samples were collected into 3.5ml sodium citrate tubes (vacutainer) using a 21 gauge needle. All blood samples were anonymised with a unique code according to the order of blood draws taken. All samples were processed by the same operator within 4-6 hours after blood collection. Briefly, samples were centrifuged at 1,500g for 10 minutes at room temperature to collect platelet poor plasma (PPP). PPP was then centrifuged at 13,000g for 10 minutes at 4℃ to remove any remaining platelets. This platelet free plasma (PFP) was aliquoted into 1.5ml eppendorf tubes and stored at -80℃.

2.2 Microparticle Preparation

2.2.1 Size-exclusion chromatography

A 10ml volume of Sepharose CL-2B 300 (Sigma) was washed three times with PBS containing 0.32% trisodiumcitrate (pH 7.4, 0.22 μm filtered). A 10ml syringe was then packed with washed Sepharose CL-2B to create a column as described previously in Boing *et al* (63). Each column was used only once (Figure 2.1).

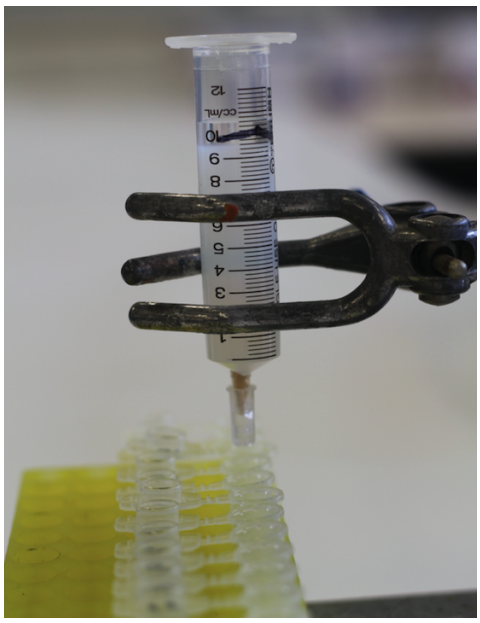

Figure 2.1 Sepharose column used to collect fractions. Up to 35 fractions were collected using this SEC method. Sample volume loaded onto the column was either 1.5ml or 0.5ml.

2.2.2 Collection of fractions

PFS (1.5ml) from the platelet concentrate or PFP (1.5ml/0.5ml) from donors was loaded onto the sepharose column, followed by elution with PBS/0.32% citrate (pH 7.4, 0.22µm filtered). In all cases, the elute was collected in 30-35 fractions of approximately 450µl in size. All fractions were stored at -80℃ for later batch analysis. Chapter 4 is mainly focused on characterising fractions 8-13 as these fractions are lipoprotein deficient.

2.3 Microparticle Size Analysis

2.3.1 Dynamic light scattering

MP size was determined using the Malvern Zetasizer ZS. The Malvern system determines the size of particles by measuring the speed of particles undergoing Brownian motion in a sample using Dynamic Light Scattering (DLS). A schematic figure of the DLS technique is shown in Figure 2.2. Briefly, 50µl samples from fractions 8-13 were diluted in 1ml of 0.32% PBS/citrate and were measured at 10℃. The number distribution or intensity distribution function was applied to analyse MP size. The intensity distribution function is naturally weighted based on the scattering intensity

of each fraction's particles. The intensity distribution is sensitive to the presence of large particles. The number distribution provides the relative distribution from the different size in terms of how many particles there are, which are derived from the intensity distribution using Mie theory (199).

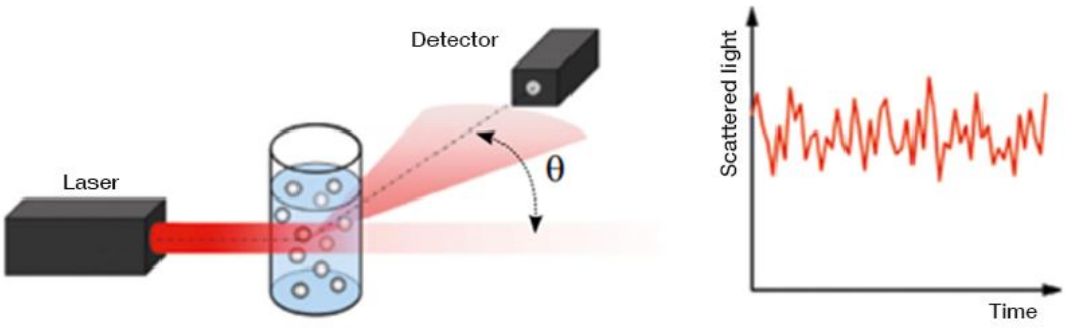

Figure 2.2 The Principle of Dynamic Light Scatter. The sample is contained in a cuvette and the scattered light of the incident laser can be detected at different angles. The scattered light is dected at a certain angle over time and the signal is used to determine the particles size by theStokes-Einstein equation (200).

2.3.2 Nanoparticle tracking analysis

Nanoparticle tracking analysis (NTA) is the method used to visualise and measure nanoparticles in suspension in the range from 10-1000nm and is again based on the analysis of Brownian motion. A schematic figure of the NTA technique is shown in Figure 2.3. Briefly, a representative fraction from the platelet concentrate and donor plasma was measured using NTA (Nanosight LM10). Fractions were diluted 5-100 fold in PBS to reduce the number of particles in the field. Camera level was set to 14 and the detection threshold was 32. The analysis was performed by the instrument software NTA. In some cases, NTA (NS300) was used to measure fractions 8-13 MP size. In those cases, the camera level was set to 9, threshold 9 and screen gain 4.0. At least three recordings were performed for each fraction.

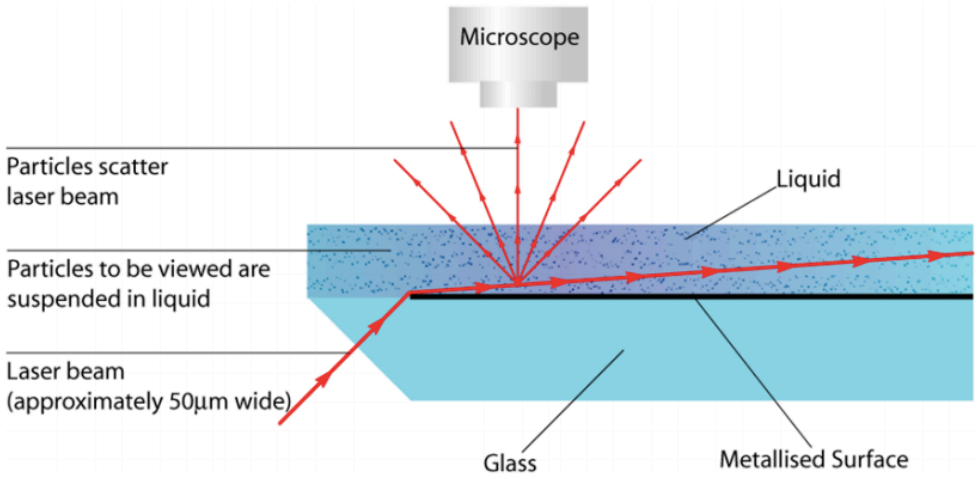

Figure 2.3 Schematic diagram of Nanoparticle Tracking Analysis. The particles are suspended in liquid and detected by a laser beam (201)

2.3.3 Transmission electron microscopy

To visualise MPs, 5µl of the sample from each fraction 8-13 was placed on a 200-mesh formvar and carbon coated copper grid (Ted Pella) and allowed to adhere for 10 minutes at room temperature. Excess sample was wicked away with filter paper and the grid was floated on a 20µl drop of EM Stain 336 (Uranyl Acetate Alternative) (Agar Scientific) diluted 1:4 with distilled water. Excess stain was wiped away with filter paper to leave a dry grid. Images were acquired using a Hitachi H7650 transmission electron microscope operating at 100 kV and side mounted camera.

2.4 Flow Cytometry

Flow cytometry is a technique used to detect and measure physical properties (size and internal complexity) and fluorescence characteristics of cells or particles. For conventional flow cytometry, the limit of detection is around 300nm. A schematic figure of the flow cytometry technique is shown in Figure 2.4. Briefly, cells or particles are suspended in a fluid and injected into the flow cytometry instrument. The detection of cells or particles is performed by passing them through a flow chamber with one or several laser beams. Cells or particles are often labelled with fluorescence markers so that fluorescent signal emissions can be detected. The data gathered are processed by a computer. The resulting information is usually displayed in dot-plots or histograms.

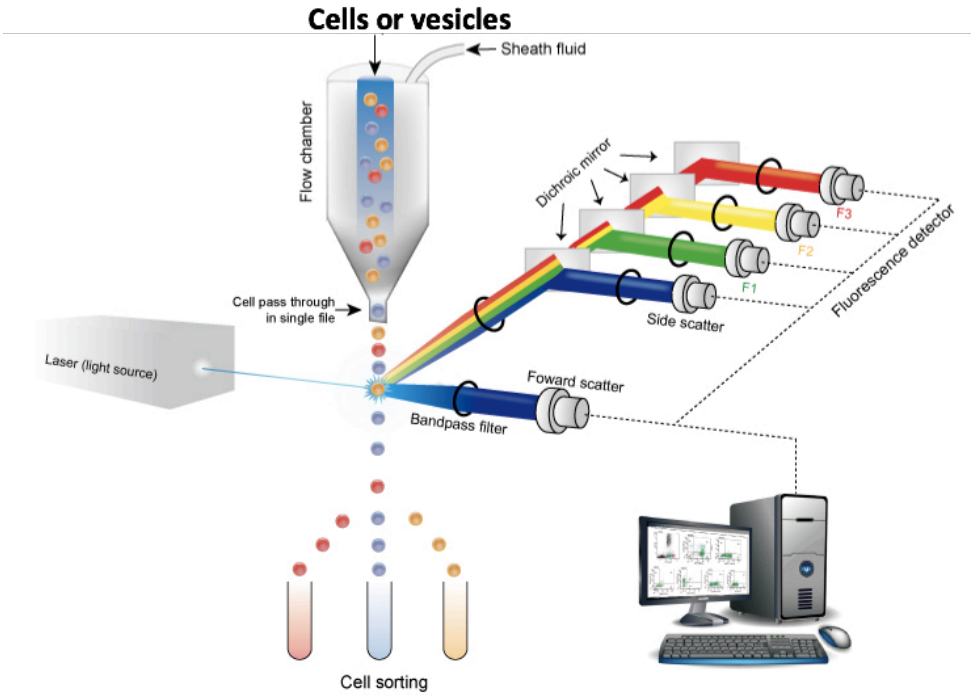

Figure 2.4 Schematic diagram of flow cytometry (202)

2.4.1 Microparticles

In the case of fractions from platelet concentrates, 20µl of each fraction 9-12 was incubated with 5µl phycoerythrin (PE)-labelled anti-CD61 (catalogue number 555754, BD Biosciences) for 45 mins on ice. In the case of fractions from donor plasma, 20µl of each fraction 8-13 was incubated with one of the following fluorescent monoclonal antibodies: 5µl phycoerythrin (PE)-labelled anti-CD61 (catalogue number 555754, BD Biosciences), 5µl phycoerythrin (PE)-labelled anti-CD45 (catalogue number 555483, BD Biosciences), 4µl Fluorescein isothiocyanate (FITC)-labelled anti-CD235a (catalogue number 559943, BD Biosciences), 5µl phycoerythrin (PE)-labelled anti-31 (catalogue number 555446, BD Bioscience) and 5µl Allophycocyanin (APC)-labelled anti-CD42b (catalogue number 551061, BD Bioscience) for 45 mins on ice. Thereafter, all samples were incubated at room temperature for 20 minutes, diluted with 300µl PBS/Citrate and analysed by flow cytometry on the Accuri C6 (Accuri Cytometers). For flow cytometry analysis of MPs, events calibrated by internal standard beads (0.8µm; Sigma) were identified in forward-scatter and side-scatter intensity dot representation, gated as the MPs, and plotted on one colour fluorescence histograms. For MP numeration, Accuri C6 automatically calculated counts per µl for gated

populations. The direct counts correlated highly (r^2=0.999), and are as precise as counts performed with counting beads. Unstained samples and isotype control antibodies were used as negative controls in all measurements. Additionally, fluorescence minus one (FMO) controls were used to identify $CD31^+$ or $CD42b^+$ MP in CD31/CD42b double staining analysis.

2.4.2 Cells

Post MP or LPS treatment, THP-1 cells or HMDMs were washed twice with PBS and re-suspended in 100µl of PBS containing 2% FBS, before staining with 5µl of APC-anti-human CD284 (TLR4) (BioLegend) for 45 minutes on ice. After being washed twice with PBS, cells were finally resuspended in 400µl of PBS containing 2% FBS. Unstained samples were used as a negative control. Flow cytometry was performed on the Accuri C6 (Accuri Cytometers).

2.5 Estimating Cholesterol Concentration

2.5.1 Donor plasma and microparticles isolated from platelet concentrate

For quantitative determination of total cholesterol in donor plasma and in MPs isolated from platelet concentrates, a manual colorimetric cholesterol assay was applied (Cholesterol assay, AUDIT Diagnostic, Randox). Total cholesterol levels in donor plasma and in MP fractions 9-12 were estimated. Briefly, 10µl of plasma or each fraction/standard was added to a 1ml cuvette followed by 1ml of cholesterol kit reagent. The samples were incubated for 10 minutes at 37℃ before being read spectrophotometrically at 500nm. The concentration of cholesterol was calculated using the formula:

$$\frac{Absorbance\ of\ sample\ x\ Concentration\ of\ the\ standard}{Absorbance\ of\ standard}$$

2.5.2 Microparticles isolated from donor plasma

The manual colorimetric cholesterol assay was not sensitive enough to estimate cholesterol levels in MPs from plasma, so instead the Amplex® Red Cholesterol Assay Kit (A12216, Invitrogen)

was applied to donor plasma fractions. This kit is based on a fluorometric method for detecting very low concentrations of cholesterol. The cholesterol concentration of fractions from all donor samples was determined according to the manufacturer's instructions. Batch analysis was carried out on samples.

2.6 Estimating Triglycerides Concentration in Donor Plasma

Triglyceride levels were estimated in donor plasma using a manual colorimetric triglycerides assay (Triglycerides assay, AUDIT, Diagnostic, Randox). Briefly, 10µl of each plasma /standard was added to a 1ml cuvette followed by 1ml of triglyceride kit reagent. The samples were incubated for 5 minutes at 37℃ before being read spectrophotometrically at 505nm. The concentration of triglyceride in each fraction was calculated using the formula:

$$\frac{Absorbance\ of\ sample\ x\ Concentration\ of\ the\ standard}{Absorbance\ of\ standard}$$

2.7 Microparticle Lipoprotein Estimation

2.7.1 Immunoblotting

Dot blots using antibodies to various APOs were used to evaluate the lipoprotein content of fractions 8-13. A schematic figure of the dot blot technique is shown in Figure 2.5. Briefly, 2µl of each fraction sample from platelet concentrates or donor plasma was spotted onto a nitrocellulose membrane. The membrane was blocked with 5% Bovine Serum Albumin (BSA) for 1 hour at room temperature, followed by incubation with a primary antibody for 1 hour at room temperature. All primary antibodies used were from Mabtech AB, diluted to the following concentrations in 5% BSA: APOA1 (mAb HDL-44-biotin, batch 7,code 3710-6) (1:1000), APOB (mAb LDL-11-biotin code 3715-6 Batch 7) (1:5000), APOH (mAb H464-biotin,Batch 1 3711-6) (1:1000), APOJ (J100-biotin) (1:1000), APOM (M5-biotin) (1:1000), APOD (D544-biotin) (1:1000), APOE (mAbE887-biotin Batch 2 code 3712-6) (1:1000). After washing three times with Tris Buffered Saline with Tween (TBS-T), the membrane was incubated with an avidin-biotinylated secondary antibody

(Vectastain AB Kit, Catalogue Number PK-6100 Series) following the manufacturer's instructions for 30 minutes at room temperature. The membrane was washed three times in TBS-T and incubated with ECL reagent for 1 minute, followed by analysis of chemiluminescent signal using the LI-COR digital imaging system.

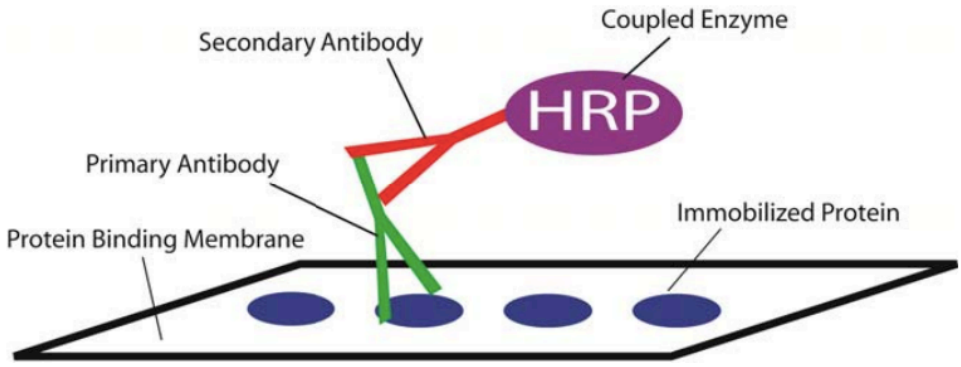

Figure 2.5 Schematic diagram of a dot blot (203)

2.7.2 Enzyme-linked immunosorbent assay

To further confirm there was no lipoprotein contamination in fraction 8-13, an APO Enzyme-linked immunosorbent assay (ELISA) was applied to a representative donor plasma set. This work was carried out by Mabtech, Sweden.

2.8 Sodium Dodecyl Sulfate-Polyacrylamide Gel Electrophoresis and Western Blot Analysis

2.8.1 SDS-PAGE

Discontinuous Sodium Dodecyl Sulfate-Polyacrylamide Gel Electrophoresis (SDS-PAGE) was carried out according to the method of Laemmli (1970) using the Atto Gel Electrophoresis system. Volumes of gel components needed for the various percentages of resolving gels are shown in Table 2.1. The protein concentration was measured using Nanodrop (Thermo Scientific NanoDrop 2000 spectrophotometer). MPs were resolved through the gel at a constant current of 130 voltage per gel. Prestained protein ladders (Fermentas) were run alongside samples as molecular weight standards.

Table 2.1: Composition of Resolving and Stacking SDS-PAGE Gels

Resolving Gel (12%)		Stacking Gel (5%)	
H_2O	3.3ml	H_2O	2.1ml
30% Acrylamide mix (40:1)	4.0ml	30% Acrylamide mix (40:1)	0.5 ml
1.5M Tris Cl pH 8.8	2.5ml	1M Tris Cl pH 6.8	0.38 ml
10% SDS	0.1ml	10% SDS	30 µl
10% APS	0.1ml	10% APS	30 µl
TEMED	5µl	TEMED	3 µl

Tris Cl: Tris hydrochloride, SDS: Sodium dodecyl sulfate, APS: Ammunium persulphate, TEMED: Tetramethylethylenediamine

2.8.3 Transfer of proteins to membrane

The resolved proteins were transferred to a nitrocellulose membrane (Millipore) using a Trans-Blot Electrophoretic Cell (Bio-Rad). All components were soaked in transfer buffer (25mM Tris-HCl pH 8.0, 0.2 M Glycine, 20% methanol). The gel was placed on a layer of filter paper and sponge and overlaid with the nitrocellulose membranes. The second piece of filter paper was placed on top followed by a second sponge. The entire assembly was placed in a cassette, the chamber filled with transfer buffer and a constant current of 80 voltage was applied for 1 hour.

2.8.4 Antibody blotting

Membranes were blocked for non-specific binding by incubation in blocking buffer (TBS-T) at room temperature for 1 hour. The membrane was then incubated at 4°C overnight with a primary antibody directed against human APOA1 (1:1000 dilution). The membrane was washed 3 times for 10 minutes each time in TBS-T and incubated with the appropriate horseradish peroxidase (HRP)-linked secondary antibody for 1 hour at room temperature. Again, the membrane was washed three times for 10 minutes each time in TBS-T. The membrane was incubated with ECL

reagent for 1 minute, followed by analysis of chemiluminescent signal using the LI-COR Digital imaging system.

2.9 Coomassie Staining of Polyacrylamide Gels

To directly visualise the relative presence of proteins in the fractions from platelet concentrates, 10µl of each fraction was mixed with 10µl of 2X concentrated loading buffer (7.5g of Tris-Cl, 20g of SDS, 1g of Bromophenol blue and 6mls of Beta-mercaptoethanol to make 500ml solution), boiled for 10 minutes at 95℃ and loaded on a 12% polyacrylamide gel. After the gel was run as described above in section 2.8.1, staining was carried out overnight using Coomassie blue (1g Coomassie brilliant blue in 1 litre Methanol 50% v/v Glacial Acetic acid 10% v/v H_20 40%). The next day the gel was destained in destaining solution (Methanol 40% v/v, acetic acid 10% v/v, H_2O 10% v/v).

2.10 Cell Culture

2.10.1 Resuscitation of frozen THP-1, HEK 293 and HeLa cell lines

Medium was allowed to warm to 37°C before 10ml of the medium was added to a 25cm^2 culture flask. Using cryo-gloves, an ampoule of cells (THP-1 cells, HEK293 cells and HeLa cells) was removed from liquid nitrogen, sprayed with ethanol, wiped dry and placed in the tissue culture hood. One ml of media from the culture flask was pipetted directly onto the frozen cells and pipetted gently up and down to defrost cells as quickly as possible. Defrosted cells were added to the culture flask which was labelled and placed in the 37°C incubator.

2.10.2 Growth of cell lines

HeLa cells were cultured in RPMI containing a final concentration of 5ml L-glutamine, 10% (v/v) foetal bovine serum (FBS) and 100µg/ml penicillin/streptomycin. THP-1 cells were grown in RPMI containing stable 5ml L-glutamine, 10% (v/v) FBS and 100µg/ml penicillin/streptomycin. HEK293T cells were cultured in Dulbecco's Modified Essential Medium (DMEM) containing

stable 5ml L-glutamine, 10% (v/v) FBS and 100µg/ml penicillin/streptomycin. In all cases, cells were maintained at 37°C in a humidified atmosphere of 5% CO_2. For continuing cell culture, cells were seeded at 1×10^5/ml and sub-cultured two to three times a week. Cells were removed from the surface of the flask by incubation with 3ml trypsin-EDTA (0.05mg/ml) for 5 min at 37°C. Trypsin-EDTA was neutralised by the addition of 7ml of appropriate media.

2.10.3 Cell counting and viability

Estimation of the number of cells present in the cell suspension was carried out using a haemocytometer to ensure a specific number of cells was used in each well for all experiments. Typically, the cell pellet was resuspended in the appropriate media and 10µl of this was added to 10µl of trypan blue. Trypan blue was used to assess the viability of the cells, as it is excluded from healthy cells but is taken up by non-viable cells. This mix of cells and trypan blue (10µl) was then added to the chamber on the haemocytometer with the number of cells present in the central $1mm^2$ grid representing the number of cells in 0.1µl of the cell suspension. The number of cells/ µl was calculated and from this the required volume of cell suspension was seeded in each well.

2.10.4 Differentiating THP-1 cells into macrophages

THP-1 cells were seeded at 0.5×10^6/ml in a 24-well plate before treatment with 100ng/ml phorbol 12-myristate 13-acetate (PMA, Sigma) for 48 hours. After 48 hours, the medium was removed and replaced with fresh medium without PMA. After two to three days, cells had differentiated into macrophages and were ready to be used for experimentation.

2.11 Isolation and Visualisation of Primary Cells

Buffy coats were obtained from the Irish Blood Transfusion Service in St James Hospital. The method used for isolation of monocytes was taken from Repnik *et al* (204).

2.11.1 Peripheral blood mononuclear cell isolation

Buffy coats were diluted in RPMI medium (1:2). The diluted buffy coat (25ml) was layered onto 12.5ml of Histopaque (Histopaque 1077, Sigma-Aldrich) with a density of 1.077g/ml. The

suspension was centrifuged at 950g, 25°C for 15 minutes before the peripheral blood mononuclear cell (PBMC) layer, which interfaced between Histopaque and plasma-medium layers, was collected. The cells were washed three times in PBS by centrifugation at 350g, 25°C for 7 minutes before cells were finally resuspended in RPMI medium.

2.11.2 Human monocyte derived macrophage isolation

PBMCs were layered over 10ml hyperosmotic Percoll (Sigma) before centrifugation at 580g, 25°C for 15 minutes. The hyperosmotic Percoll solution was prepared as follows for 100ml of the solution: 4.85ml of Percoll mixed with 41.5 ml distilled water and 10ml of 1.6 M NaCl. The monocyte layer appeared between the medium layer and Percoll layer. Finally, the harvested monocytes were resuspended in a medium consisting of DMEM with 10% FBS and 1% penicillin/streptomycin before transfer to a 24 well-plate ($0.5 \times 10^6 - 1 \times 10^6$ cells/well) at 37°C in a CO_2 incubation. Cell viability was tested using trypan blue. The day after seeding, non-adherent cells were removed and medium replaced. The cell culture was maintained for at least 14 days in order to obtain human monocyte-derived macrophages (HMDMs). The medium was changed every three or four days.

2.11.3 Visualisation of human monocyte derived primary macrophages

The morphology of HMDMs was assessed using the Zeiss LSM 510 inverted confocal microscope. After HMDMs were harvested, cells were resuspended in 100µl PBS with 2% FBS and stained with 5µl FITC-CD11b antibody (BioLegend) for 45 minutes on ice. Cells were washed twice at 400g, 4°C for 5 minutes each time. Finally, cells were diluted with 300µl PBS/2% FBS and analysed by flow cytometry (BD Accuri C6). Unstained samples were used as negative controls in all measurements.

2.12 Cell treatment

THP-1 cells or HMDMs were treated with LPS (100ng/ml) alone for three hours; and/or MPs (0.1µg, 0.25µg, 0.5µg, 1µg) for one or four hours. The protein concentration was determined using

a BCA protein assay kit according to the manufacturer's instructions (23225, ThermoFisher Scientific). In all cases, untreated cells were included as internal controls.

2.13 Reverse Transcription-qPCR

2.13.1 RNA extraction

1ml of Trizol was added to each well of THP-1 cells or primary HMDMs. After cell lysis, cells were transferred to an RNase-free tube and incubated for 5 minutes at room temperature before 200µl of chloroform was added for a further 5 minutes. Cells were centrifuged at 4℃ at maximum speed for 20 minutes in order to get phase separation. The top layer which contained the RNA was transferred to a clean RNase-free tube. An equal amount of isopropanol was added in order to precipitate the RNA. After 30 minutes incubation, samples were centrifuged at 4℃ at maximum speed for 20 minutes. The supernatant was removed and the RNA pellet washed with 70% ethanol. Finally, the RNA pellet was resuspended in 30µl of RNase-free water. The concentration and quality of RNA were determined by measuring absorbance at 260 and 280nm. A blank solution (RNase-free water) and samples (2µl) were added to the pedestal and measured. The ratio of absorbance at 260nm and 280nm was used to assess the purity of RNA. A ratio of 1.8-2.0 was accepted.

2.13.2 Reverse transcription of RNA to cDNA

RNA (500ng) was reverse transcribed into cDNA using iScript™ Reverse Transcription Supermix kit (Bio-Rad) according to manufacturer's instructions.

2.13.3 Quantitative PCR

A SYBR green-based quantitative PCR kit (Quanta bio) was used according to manufacturer's instructions. Reaction mixture components and PCR conditions are outlined in table 2.2 and table 2.3 below. Primers sequences (Hs18S-r RNA and H-TNFα)used in this study are outlined in table 2.4.

Table 2.2: Reaction Mixture Components for qPCR

Component	Volume per 30µl sample reaction (µl)
PerfeCTa SYBR Green Fast Mix 2X	17.625
Forward primer (10µM)	1.05
Reverse primer (10µM)	1.05
PCR grade water	13.7

Table 2.3: Reaction Protocol for qPCR

	Temperature (°C)	Time (min)
Initial denaturation	95	10
40 cycles:		
Denaturation	95	15
Annealing and extension	60	1
Hold	4	

Table 2.4: Primers Sequences

Genes	Primers sequences
Hs18S-rRNA	F: GCTTAATTTGACTCAACACGGGA R: AGCTATCAATCTGTCAATCCTGC
H-TNFα	F: GAGGCCAAGCCCTGGTATG R: CGGGCCGATTGATCTCAGC

2.14 Cell Line Labelling with 3-NBD-Cholesterol

2.14.1 Fluorescent labelling of HeLa and THP-1 cells

Briefly, 3.5×10^5 of HeLa cells or 1.61×10^6 of THP-1 cells were seeded in a final volume of 2ml in $5cm^2$ dishes. Cells were treated with 1μg/ml of 3NBDC for 0, 1, 3, 5 or 7 hours. At each time point, cells were washed three times with PBS and then measured by flow cytometry (FL1 Emission 530/30nm, Accuri C6 BD).

2.14.2 Fluorescent labelled of extracellular vesicle treated THP-1 derived macrophages

EVs were isolated from PFS by centrifugation at 20,000g for 60 minutes. EV pellets (760 μg) were then resuspended in PBS and incubated with 5μg 3NBDC for 48 hours at 4℃. After 48 hours, EVs were washed twice as above before flow cytometry analysis and cell treatment. THP-1 derived macrophages were incubated with 69μg/ml 3NBDC labelled EVs for 0, 2, 4, 8 and 16 hours. At each time point, the 3NBDC fluorescence intensity was tested by flow cytometry to observe macrophage uptake of EVs.

2.14.3 Fluorescence intensity detection of HeLa cells

HeLa cells were seeded in a black 96-well plate, each well containing 2×10^4 of cells. Cells were treated with 1μg/ml of 3NBDC for 0, 0.5, 1, 2, 5, 7, 10 or 12 hours. At each time point, the supernatant was removed and cells were washed 3 times with PBS. The fluorescence intensity of 3NBDC in the medium and cells was detected by microplate spectrophotometry at a wavelength of 488nm for excitation and 525nm for emission.

2.14.4 Confocal microscopy

THP-1 differentiated macrophages and HEK293T cells were treated with 5μg/ml 3NBDC for 1 hour, HeLa cells and human primary macrophages were treated with 1μg/ml 3NBDC for 18 hours. Cells were washed three times with PBS. Live cells images were acquired using the Zeiss LSM 510 inverted confocal microscope.

2.15 Cholesterol Exchange Assay with 3-NBD-Cholesterol

2.15.1 Preparation of erythrocytes

Venous blood samples were obtained from healthy donors into EDTA vacutainers. Erythrocytes were separated from the plasma by centrifugation at 1,500g for 10 minutes before 1ml of fresh erythrocytes was removed and placed into a 15ml falcon tube. Subsequently, 5ml of flux buffer (150mM NaCl, 5mM NaPi, 5mM glucose) was added and samples were centrifuged three times for a further 5 minutes at 2,000g.

2.15.2 Preparation of exchange plasma

As described in section 2.14.1, plasma was removed after centrifugation at 1,500g for 10 minutes. Plasma was heated at 56°C for 50 minutes and then centrifuged at 15,000g for 30 minutes. Clear central fractions of the plasma (750µl) were removed for plasma exchange experiments.

2.15.3 Cell labelling procedure

Briefly, 500µl of erythrocytes was pipetted into a 1.5ml eppendorf tube and labelling solution (50µl of 3NBDC (1mg/ml) was added to 500µl of flux buffer) was added. Samples were incubated for 90 minutes on ice. After incubation, cells were washed with flux buffer as described above and stored on ice until the exchange experiment was carried out.

2.15.4 Exchange assay procedure

Exchange plasma was diluted 1:1 in flux buffer and warmed to 37°C. Briefly, 10µl of labelled cells was transferred to 90µl of diluted plasma in a 1.5ml eppendorf tube and incubated at 37°C. At each time point (0, 0.5, 1, 2, 5, 7, 10 or 12 hours), the sample was centrifuged at max speed for 15 seconds at 4°C and 45µl of supernatant was transferred into one well of a black 96-well plate. The fluorescence intensity was detected by microplate spectrophotometry at a wavelength of 488nm for excitation and 525nm for emission.

2.16 Statistical Analysis

GraphPad Prism version 7 was used for statistics calculation and plots. The D'Agostino-Pearson test was used to measure data normality. The ROUT method (GraphPad Prism) was used to identify outliers. One-way ANOVA testing was applied for normal distribution data among three groups. The difference among the three groups was determined by one-way Kruskal-Wallis analysis followed by Manny-Whitney U test for data which was not normally distributed. Univariate correlation analysis was performed by Spearman's rank correlation coefficients (r). ROC curve analysis was carried out using SPSS 25.0. p values <0.05 were considered significant. Multiple regression analysis was carried out using SPSS 25.0. A heat map was drawn using Microsoft Excel software. The sample size calculations for the human study was based on an online software (Power Calculator; https://www.anzmtg.org/stats/PowerCalculator/PowerCorrelation), which calculated sample size based on three parameters; power; correlation and significant level. All data is expressed as mean ±SEM or otherwise identified in the figure legends.

3.0 Establishing a Method for the Estimation of Cholesterol in Circulating Microparticles Using a Platelet Concentrate

3.1 Introduction

Accurate identification and quantification of MPs has become increasingly important over recent times and is of great value in uncovering the biological functions of MPs. Within the last fifteen years, it has been shown that MPs are small cell-derived particles which are involved in various biological functions including pro-coagulant activity, pro-inflammatory processes and pro-atherosclerotic processes (205, 206, 207). MPs contain a diverse array of cellular molecules including nucleic acids (DNA, RNA), protein and lipids (cholesterol) (9). In recent years, the interest in studying MPs cargo has increased significantly due to their potential as biomarkers or therapeutic targets. Obtaining samples to analyse the molecular cargo of MPs in blood is a relatively convenient, minimally invasive procedure in a clinical setting. However, the options for MP isolation from sample fluids are relatively limited. To date, there is still no standard method for MP isolation, quantification and characterisation. One widely used method consists of differential centrifugation and/or gradient purification, which often results in impure MP preparations which are contaminated with lipoproteins, apoptotic blebs and protein aggregates, including immune complexes (208). It is generally accepted that using density-gradient centrifugation to isolate MPs from plasma without lipoprotein and protein contamination is particularly challenging, with reports suggesting that EVs (including MPs and exosomes) are often contaminated with HDL from human plasma as the density of HDL overlaps with the density of EVs (209). Furthermore, researchers have demonstrated that using density gradient approaches (sucrose-density gradient ultra-centrifugation in particular) may change the size of MPs and lead to co-isolation of HDL (210). At a recent ISEV meeting, several investigators have also reported that EVs isolated by sucrose-density gradient ultra-centrifugation loose some biological functions (63). Additionally, a further study has reported that when EVs isolated by protein organic solvent precipitation and are placed on THP-1cells or THP-1 cells derived macrophages, cell viability was reduced *in vitro* (57). To this end, the combination of differential centrifugation and SEC has proven to be invaluable for the isolation of relatively pure MP populations, with minimally altered

characteristics, which therefore maintain their biological functions based on several reports (57, 211, 212). For this reason, this was the method of choice selected for this study which set out to investigate the potential role which cholesterol derived from MPs (rather than HDL or LDL) may have in inflammatory processes in autoimmune disease. Work presented in this chapter focused on the optimisation of a method to isolate and purify MPs without lipoprotein contamination. As >70% of circulating MPs originate from platelets, platelet concentrates (obtained from the Irish Blood Transfusion Service) were used for these initial optimisation and characterisation experiments.

3.2 Aims

- Optimise a method for MP fraction isolation from platelet concentrates
- Investigate the size of MPs present in each fraction collected
- Estimate the cholesterol and APO concentration of each fraction collected
- Identify which specific fractions are cholesterol-containing and APO deficient so that these fractions can be selected in further studies

3.3 Results

This study sought to optimise a centrifugation and gradient purification protocol based on a study by Böing *et al* (63). As described in section 2.2, a sepharose (CL-2B 300 cross-linked) column was used to collect 35 fractions from a platelet concentrate. It is widely reported that 70-90% of MPs are derived from platelets in the bloodstream, therefore, the major advantage of using a platelet concentrate was that it was an abundant and readily available source of MPs. Particle size, cholesterol concentration and protein concentration of all fractions was estimated.

3.3.1 Determination of particle size in fractions 1-35

The size of particles present in each of the 35 MP fractions was estimated using a DLS approach. Values obtained were compared to published literature measurements as a way of assessing if particles of the correct size were being purified using this isolation method. In all cases, data

presented is the number of particle size distribution (the relative proportion of the number of different particle sizes) in each fraction. The size of particles in fractions 1-14 fell between 100-1000nm (Figure 3.1A). The size of particles present from fraction 14 onwards were less than 100nm in size (Figure 3.1A). As the size of MPs are 100-1000nm and the size of lipoproteins (HDL, LDL, IDL, VLDL) is ~5-80nm, it was possible that lipoprotein bound APO may be present from fractions 14 onwards. In order to investigate MPs without APO bound, fractions 1-14 was selected initially based on the theory of chromatography, fractions 1-7 mainly contained elution buffer. To confirm that fractions 1-7 did in fact contain elution buffer or contaminated material rather than MPs, a heat map was produced which incorporated both particle size and protein content of fraction (Figure 3.1B). Results demonstrated that fractions 1-7 (Figure 3.1 B yellow to light green colour) contained much lower amounts of protein (0-0.012mg/mL, most likely background reaction as these fractions represent the column's void volume) compared to fractions 8-14 (0.052-1.341mg/mL) (Figure 3.1B green to red colour). In order to ensure that the fractions selected contained MPs and were also free from lipoprotein as much as possible, only fractions 9-12 were used for subsequent investigations in this study.

A

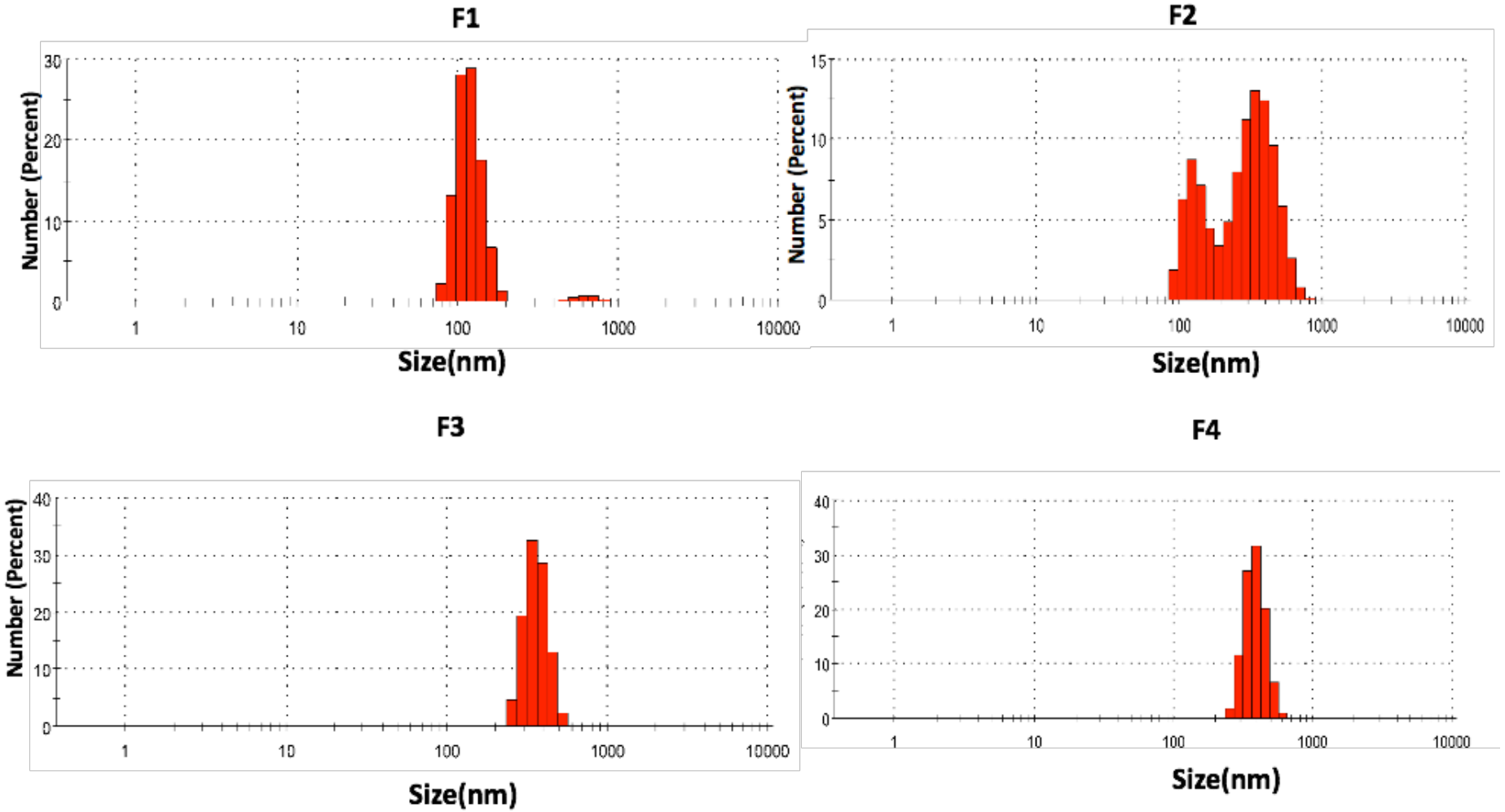
F1
Number (Percent)
30
20
10
0
1
10
100
1000
10000
Size(nm)
F2
Number (Percent)
15
10
5
0
1
10
100
1000
10000
Size(nm)
F3
Number (Percent)
40
30
20
10
0
1
10
100
1000
10000
Size(nm)
F4
40
30
20
10
0
1
10
100
1000
10000
Size(nm)

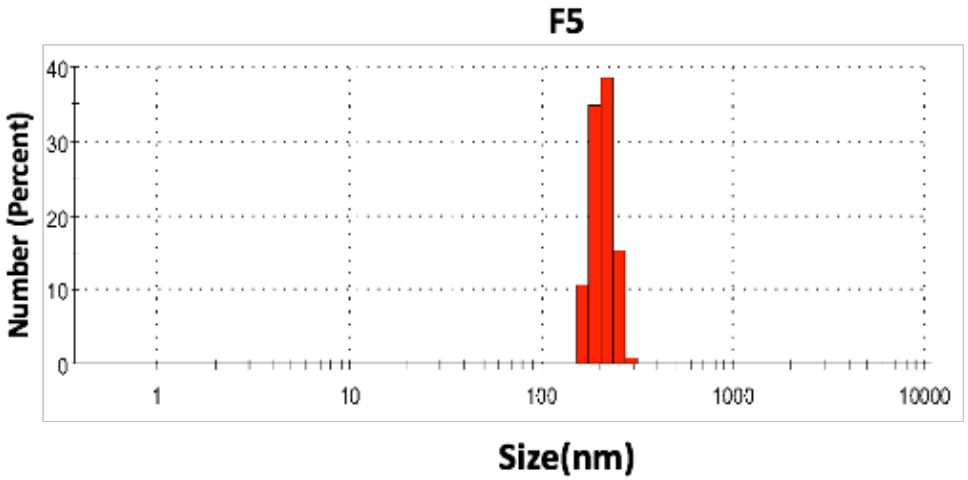
F5
Number (Percent)
40
30
20
10
0
1
10
100
1000
10000
Size(nm)

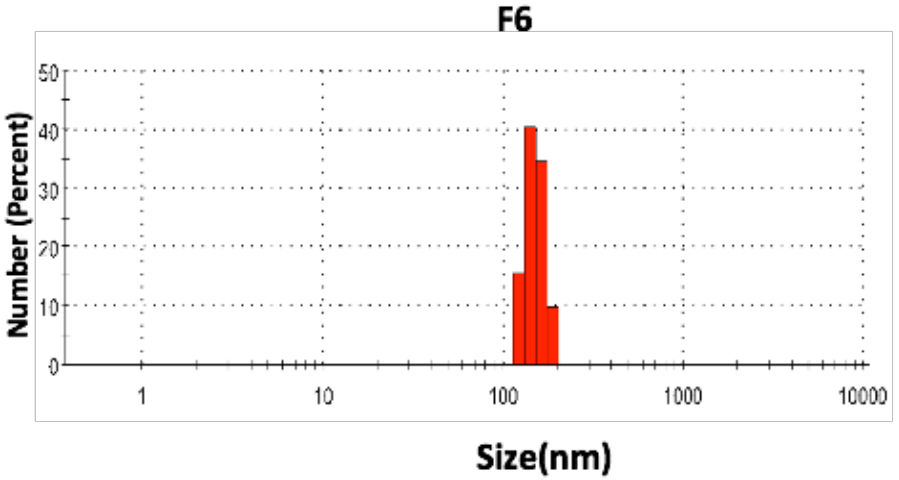
F6
Number (Percent)
50
40
30
20
10
0
1
10
100
1000
10000
Size(nm)

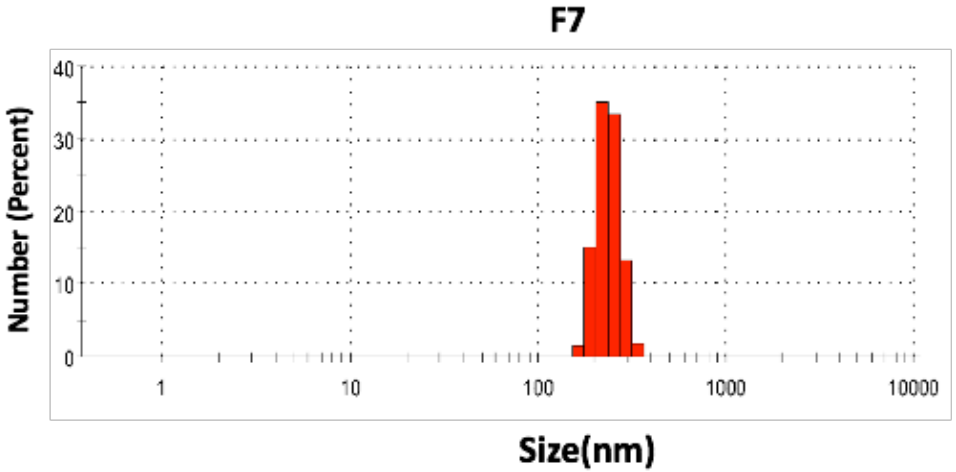
F7
Number (Percent)
40
30
20
10
0
1
10
100
1000
10000
Size(nm)

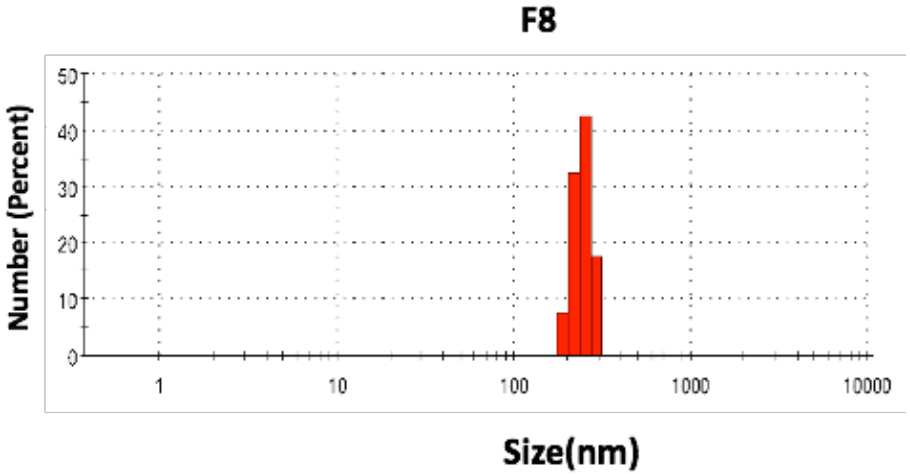
F8
Number (Percent)
50
40
30
20
10
0
1
10
100
1000
10000
Size(nm)

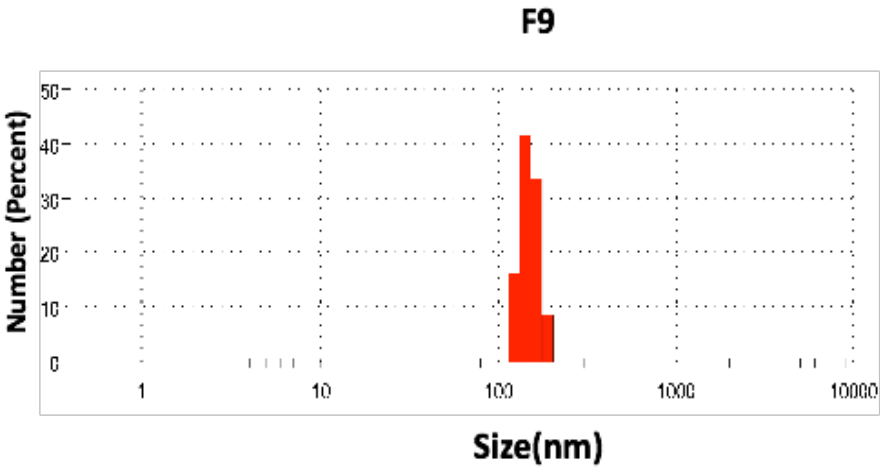
F9
Number (Percent)
50
40
30
20
10
0
1
10
100
1000
10000
Size(nm)

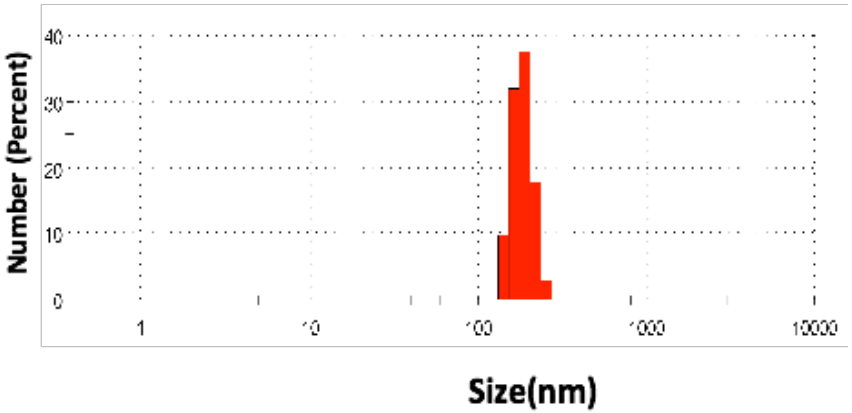
F10
Number (Percent)
40
30
20
10
0
1
10
100
1000
10000
Size(nm)

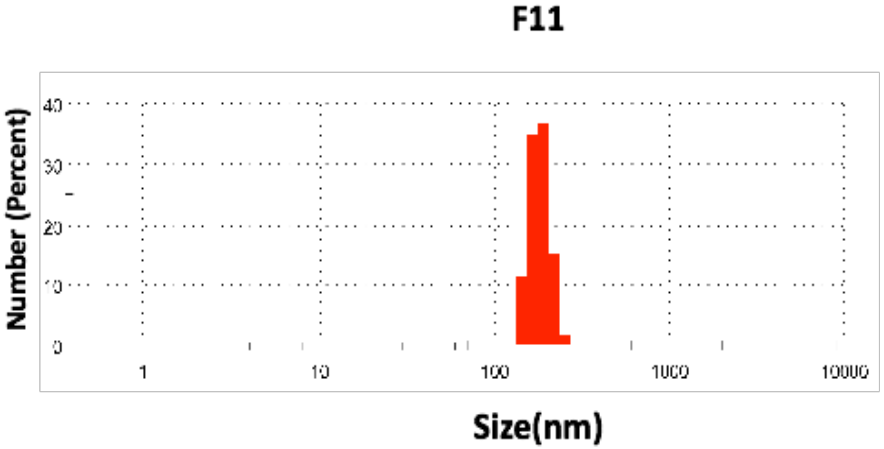
F11
Number (Percent)
40
30
20
10
0
1
10
100
1000
10000
Size(nm)

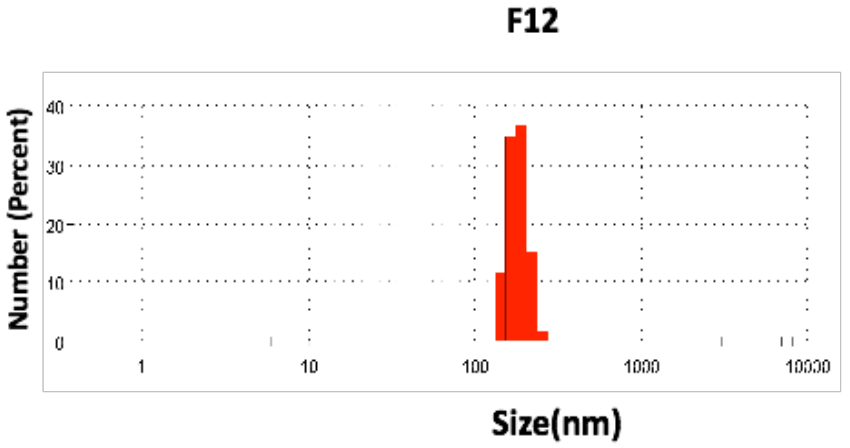
F12
Number (Percent)
40
30
20
10
0
1
10
100
1000
10000
Size(nm)

F13

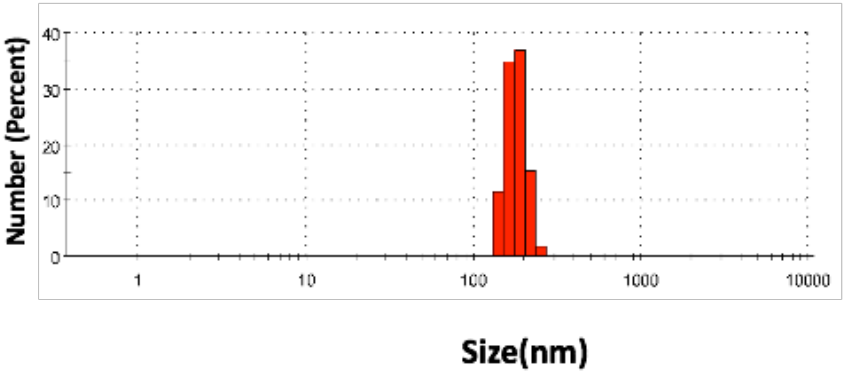

F14

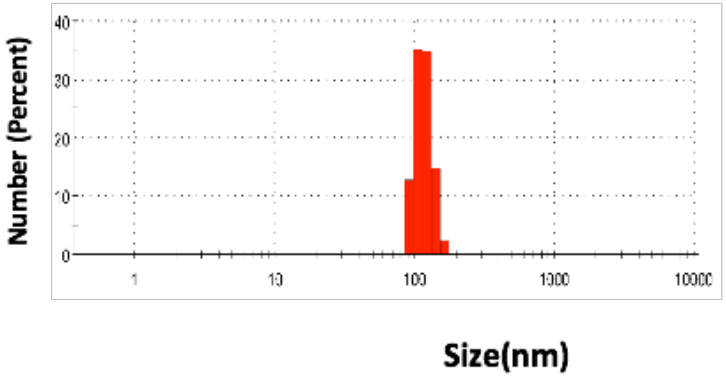

F15

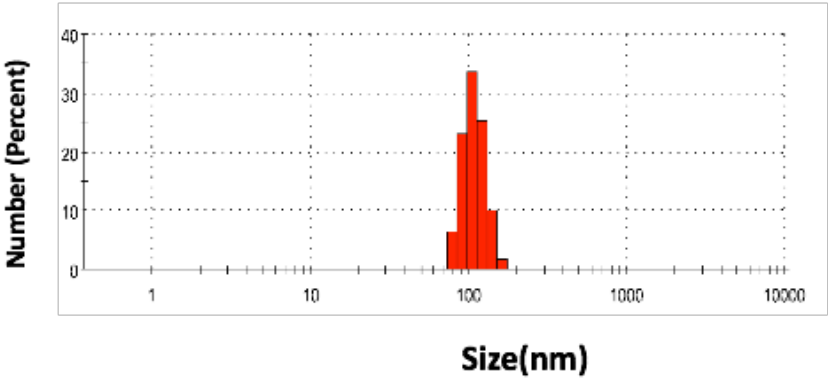

F16

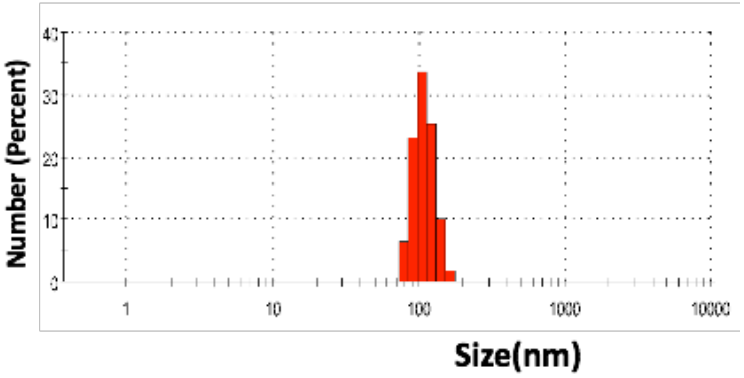

F17

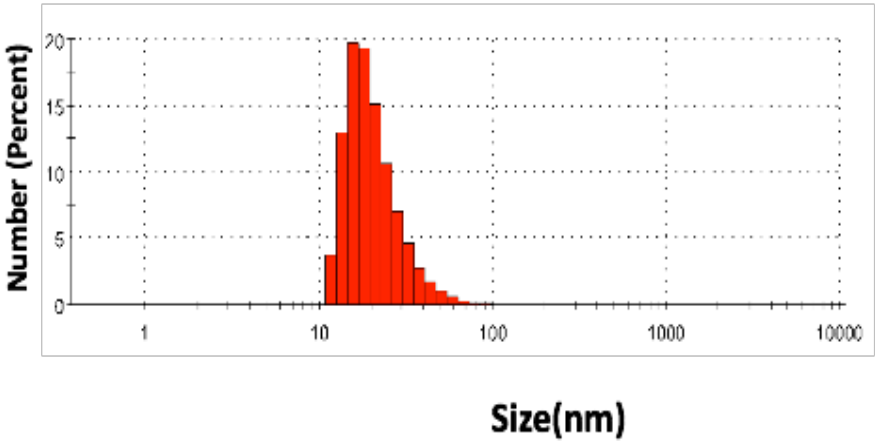

F18

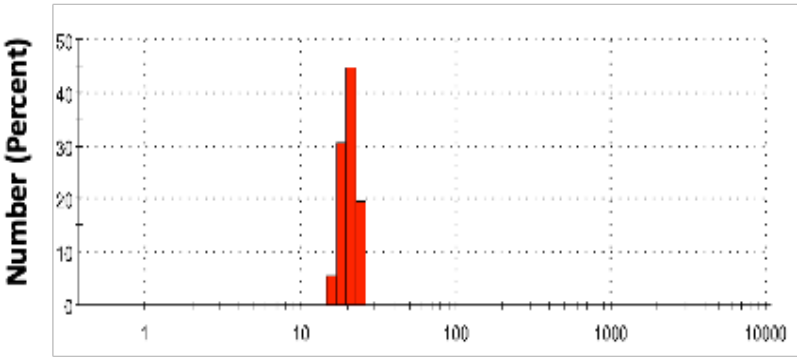

F19

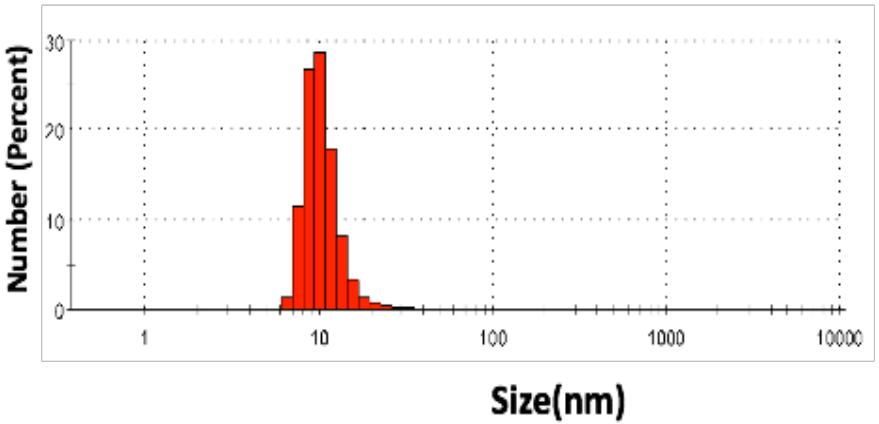

F20

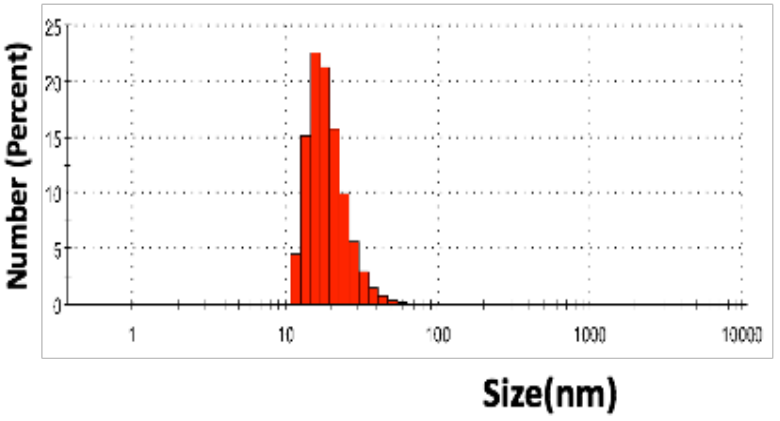

F21

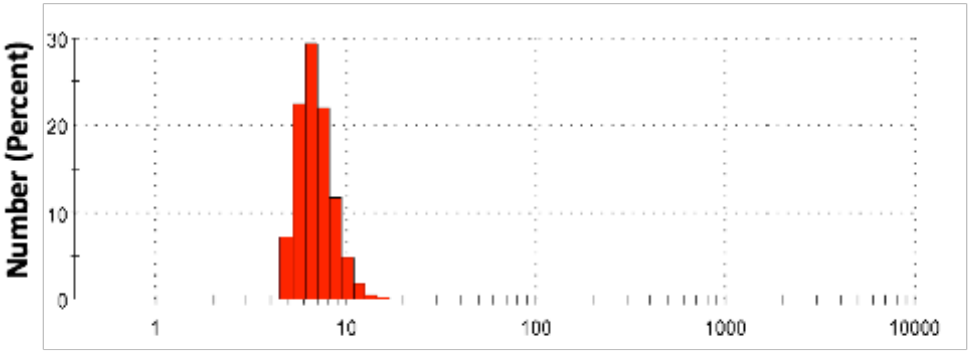

Size(nm)

F22

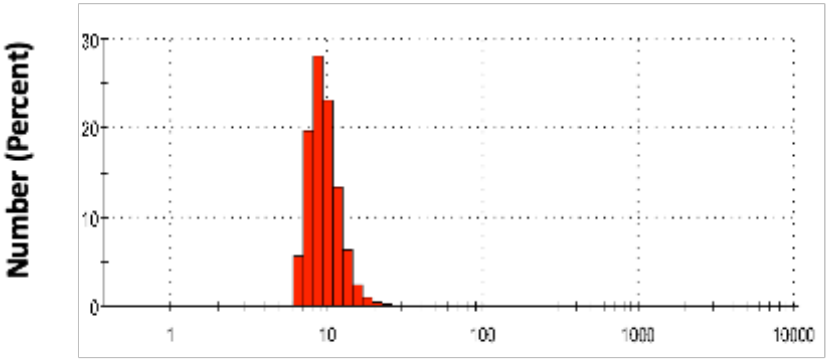

Size(nm)

F23

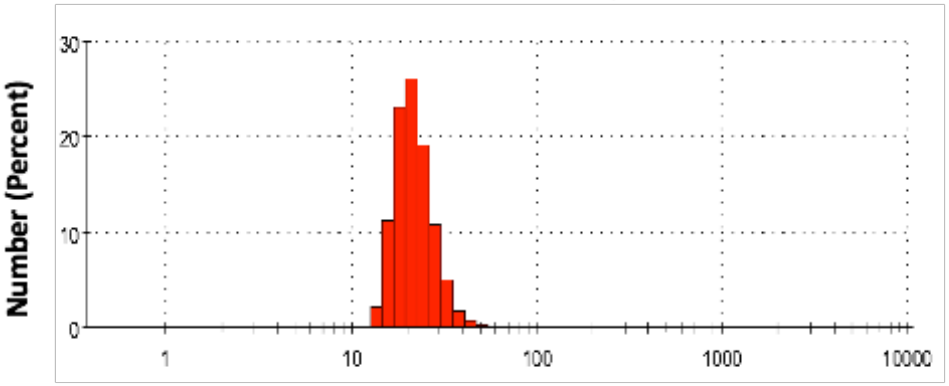

Size(nm)

F24

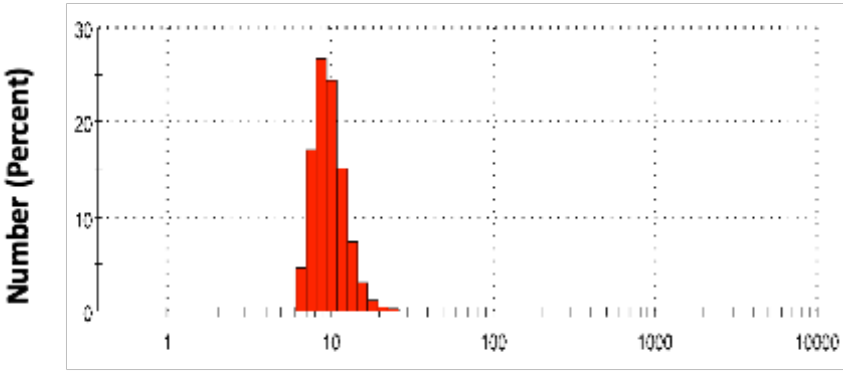

Size(nm)

F25

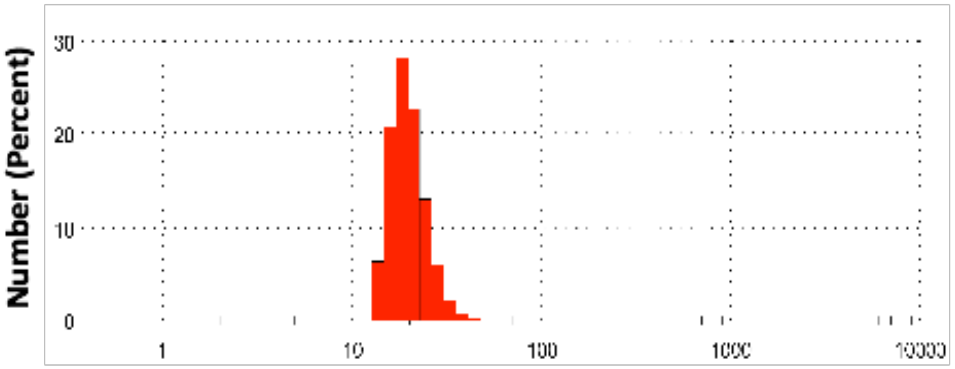

Size(nm)

F26

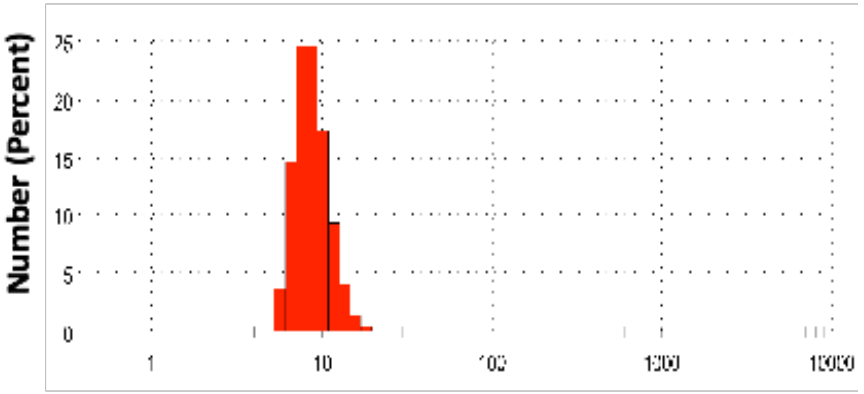

Size(nm)

F27

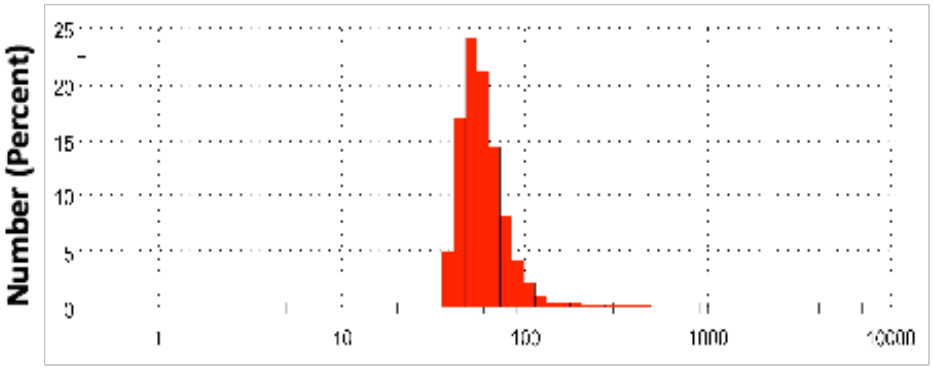

Size(nm)

F28

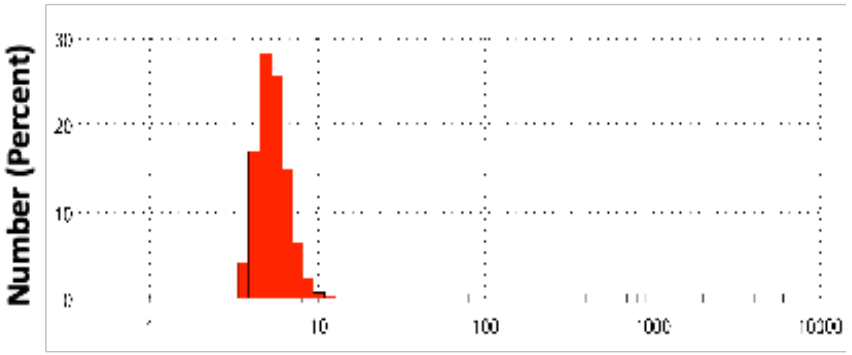

Size(nm)

F29

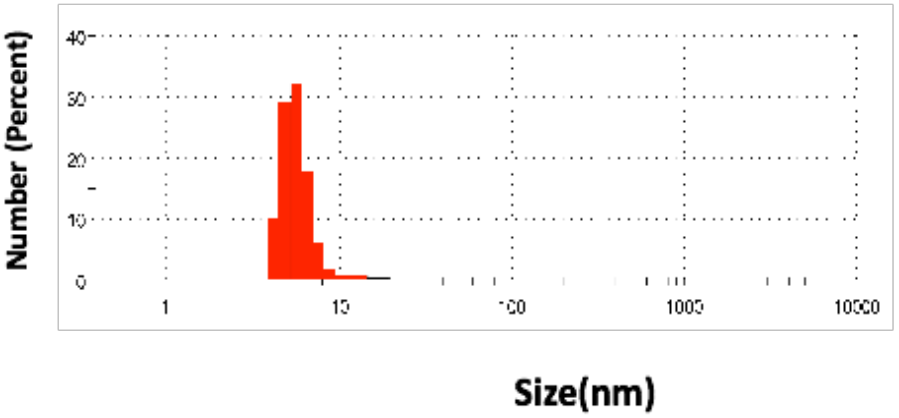

F30

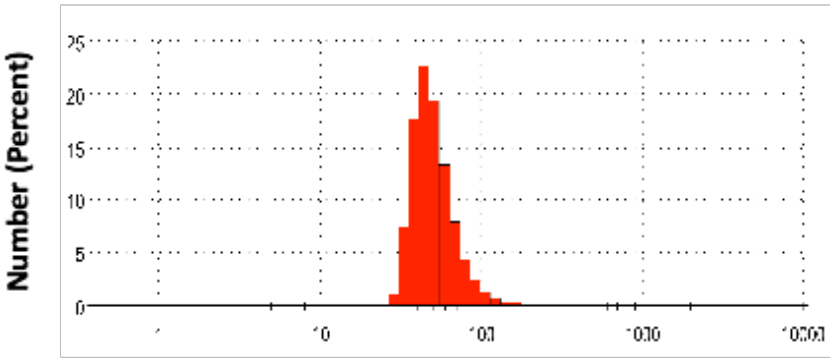

F31

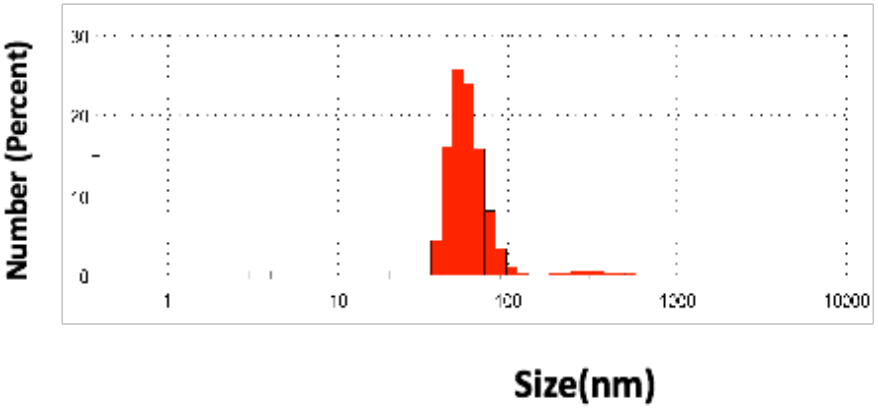

F32

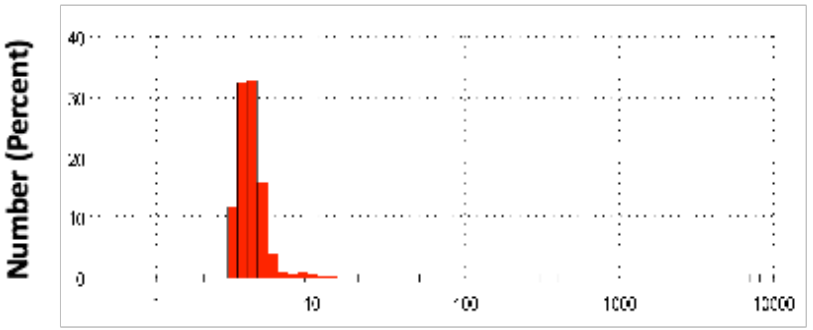

F33

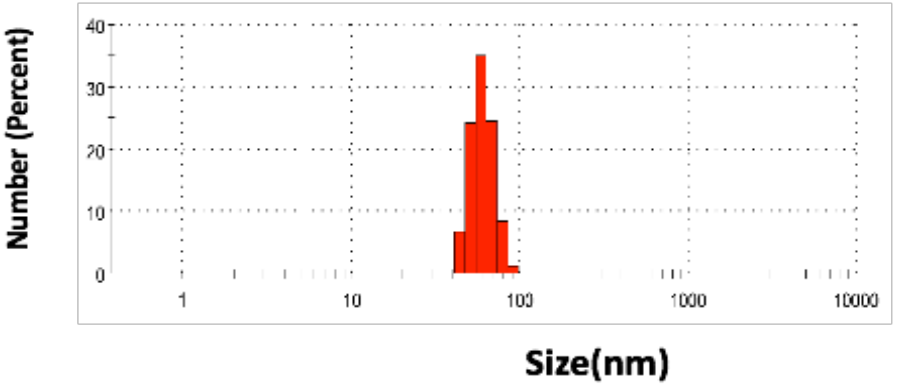
Number (Percent)
40
30
20
10
0
1
10
100
1000
10000
Size(nm)

F34

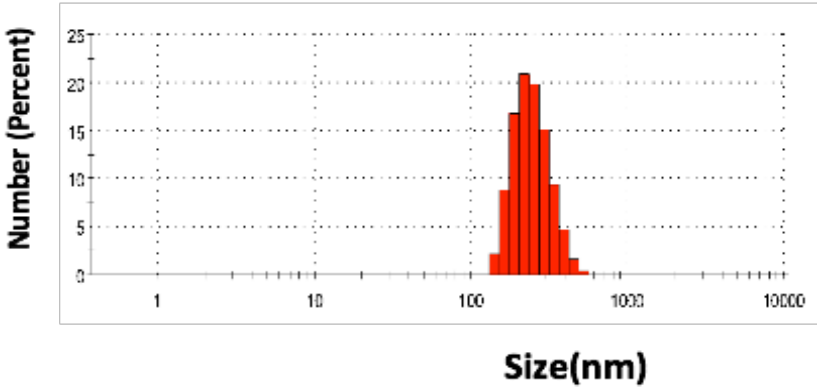
Number (Percent)
25
20
15
10
5
0
1
10
100
1000
10000
Size(nm)

F35

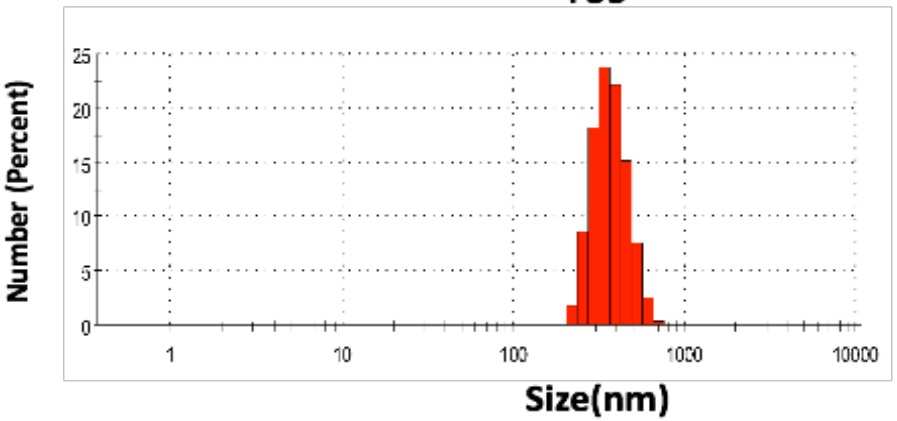
Number (Percent)
25
20
15
10
5
0
1
10
100
1000
10000
Size(nm)

B

Fraction	Protein Concentration (mg/mL)	Size (nm) %<10	%100-300	% 300-500	%500-700	%700-900	%900-1000	%>1000
1	0.001	0	81.8	0.2	1	0.9	0.1	0
2	0.013	0	54.1	35	8.4	0.7	0	0
3	0	0	23.8	73.8	2.4	0	0	0
4	0.011	0	13.4	79	7.5	0	0	0
5	0.005	0	100	0	0	0	0	0
6	0.004	0	100	0	0	0	0	0
7	0.012	0	98.3	1.7	0	0	0	0
8	0.052	0	100	0	0	0	0	0
9	0.442	0	99.8	0	0	0	0	0.2
10	1.064	0	100	0	0	0	0	0
11	1.049	0	100	0	0	0	0	0
12	1.105	0	97.5	2.5	0	0	0	0
13	1.26	0	100	0	0	0	0	0
14	1.341	0	87.3	0	0	0	0	0

Figure 3.1 Determination of microparticle size A): Fractions 1-35 were sized using dynamic light scattering to establish the percentage of particles present at a particular size, ranging from 0.1-10,000nm. The size of particles in fractions 1-14 ranged from 100-1,000nm. The size of particles in fractions 15-35 ranged from 1-1,000nm. In all cases, number (percent) means the percentage of different sized particles in the fraction. B): Heatmap:protein concentration and the percentage of different microparticle size in fractions of 1-14. The size of fractions 1-14 range from 100-1000nm, the protein concentration of fraction 8-14 is much higher (0.052-1.341mg/mL) compared to the protein concentration of fractions 1-7 (0-0.012mg/mL). Yellows means the lowest value both in microparticles size and protein concentration. Red means the highest value both in microparticles and protein concentration. This is representative data from three independent experiments.

3.3.2 Estimation of protein content in fractions 1-35

To investigate the profile of proteins present in fractions isolated using centrifugation followed by SEC, samples from fraction 1-35 were separated by SDS-PAGE and gels were stained with coomassie blue. No protein was detected in fractions 1-7 (Figure 3.2A). Low levels of protein was detectable from fraction 8-14, with the bulk of protein being present from fraction 15 onwards (Figure 3.2B, C, D). The total protein content of each of the 35 fractions was also estimated at A280nm using the nanodrop (Figure 3.3). Results observed were in line with the SDS-PAGE experiments, with minimal protein (<0.01mg/ml) evident in fractions 1-7, suggesting that these fractions do not contain a substantial proportion of MPs and are instead mainly comprised of

eluting buffer. These data also confirmed that protein started to appear in fraction 8, with most protein being present in fractions 24-28 (approx. 12mg/ml) (Figure 3.3). Taken together, these results confirmed that centrifugation followed by SEC was an appropriate method to obtain protein containing fractions from a platelet concentrate.

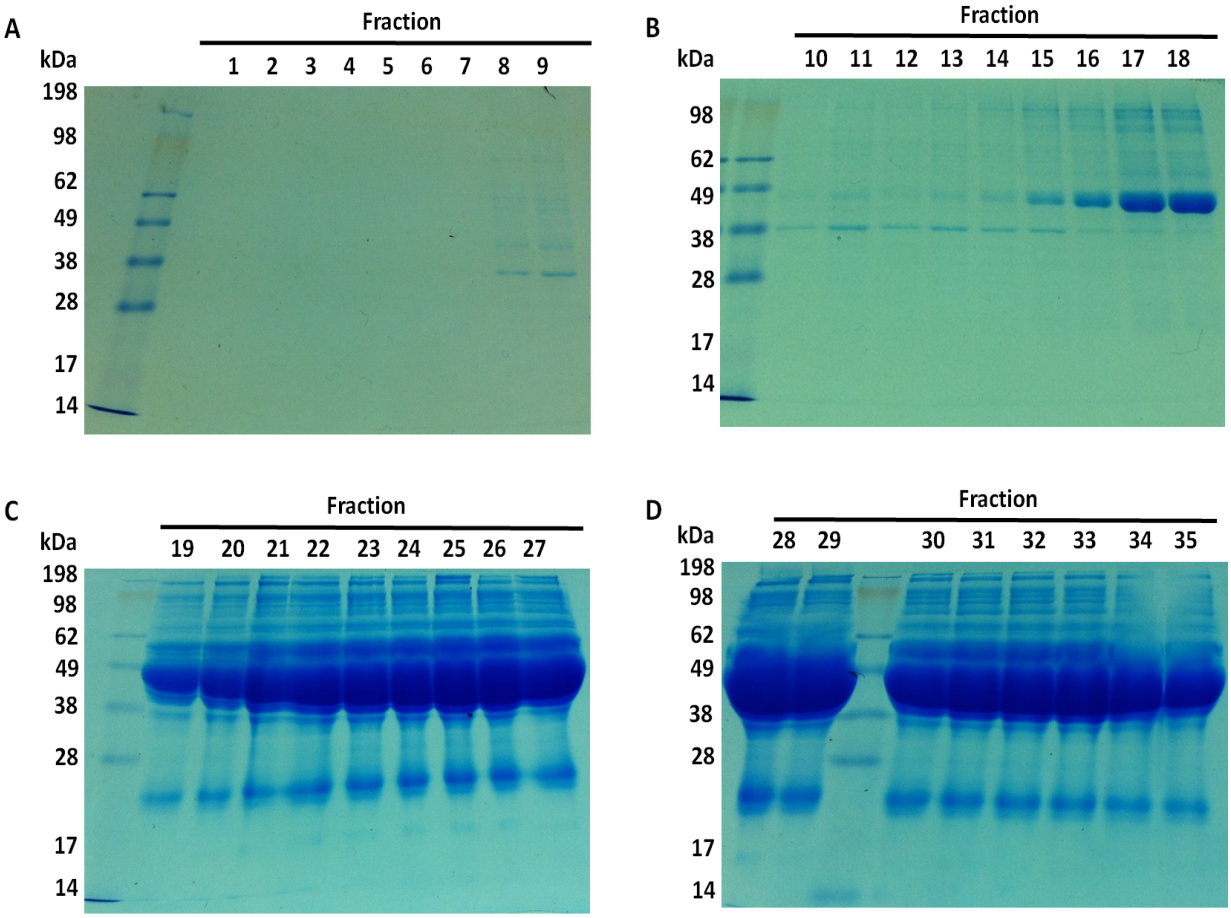

Figure 3.2 Presence of different proteins in fractions using SDS-PAGE and coomassie blue staining. Each fraction (10 µl) was mixed with 2-fold loading buffer and separated by SDS-PAGE before overnight staining with coomassie blue. A) Fractions 1-9, B) Fractions 10-18, C) Fractions 19-27, D) Fractions 28-35. Molecular weight ladder weight in kDa is indicated on each gel. Representative gels shown from three independent experiments.

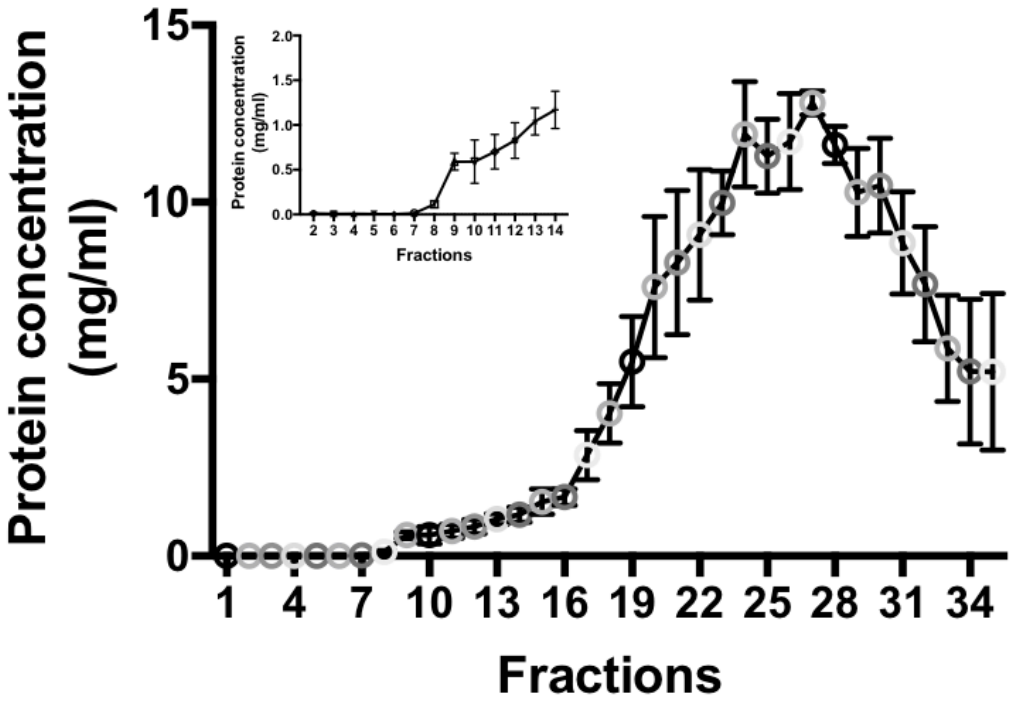

Figure 3.3 Protein concentration in fractions. The protein concentration of each fraction was determined using the nanodrop. Data shown is graphed from the average of three separate experiments ± SEM.

3.3.3 Determination of the presence of Apolipoproteins in fractions 1-35

To establish whether centrifugation followed by SEC resulted in the isolation of fractions without APO contamination, both ELISA and immunoblotting techniques were employed. ELISA results suggested no APOs were present in fractions 1-12, down to a level of sensitivity of less than 78ng/ml (Figure 3.4A). APOB started to appear in fraction 13, peaking in fraction 22 and then decreased in subsequent fractions. APOA1 started to appear in fraction 15. In all other cases, the APO (APOD, E, H, J and M) appeared in fraction 18 and remained until fraction 29 (Figure 3.4A). In agreement with the ELISA data, a western blot for APOA1 further suggested there was no significance APOA1 contamination in fractions 10, 12 or 14 (Figure 3.4B). Taken together, these results indicate that fractions 1-12 are highly APO deficient.

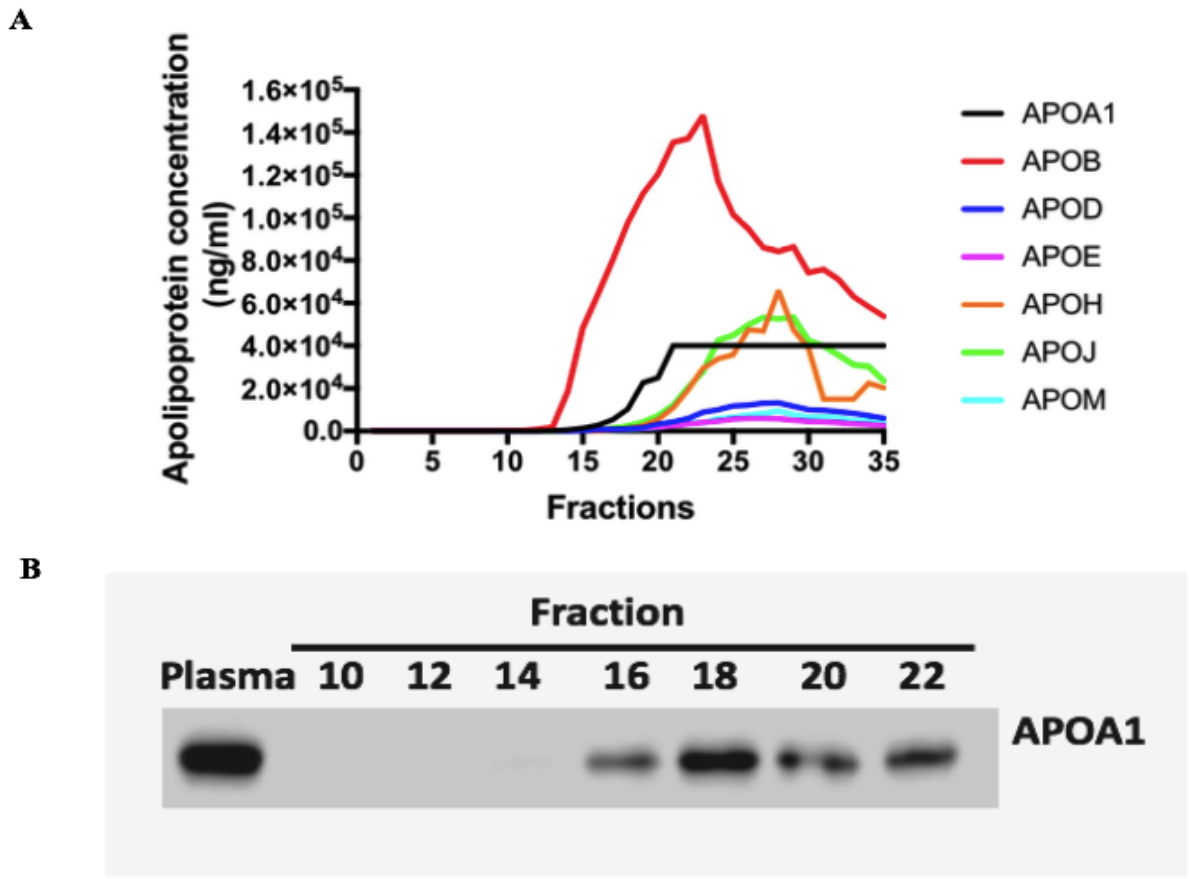

Figure 3.4 Apolipoprotein concentration in fractions. (A) ELISAs were carried out to assess the concentration of APOA1, APOB, APOD, APOE, APOH, APOJ and APOM in fraction 1-35. (B) Western blot showing APOA1 concentration in plasma (positive control) and fractions 10, 12, 14, 16, 18, 20 and 22.

3.3.4 Determination of cholesterol concentration in fractions 1-35

A cholesterol assay was employed in order to establish the concentration of cholesterol in each of the 35 fractions. Cholesterol was detected in all fractions (Figure 3.5). Lower levels were evident in fractions 1-8, with an increase evident until a peak cholesterol concentration was reached in fractions 29-35. Cholesterol was detected in fractions 1-7, which was most likely background as these fractions represent the column's void volume. It must be pointed out that a platelet concentrate was used for these initial optimisation experiments. From a cholesterol point of a view, a platelet concentrate would be expected to contain a greater amount of total cholesterol when compared to a plasma. The platelets are in fact from five donors which have been pooled, so this is probably the reason for the higher cholesterol values seen here compared to subsequent assays.

Going forward, we applied for a more sensitive method (Amplex® Red Cholesterol Assay Kit) to detect cholesterol in donor plasma.

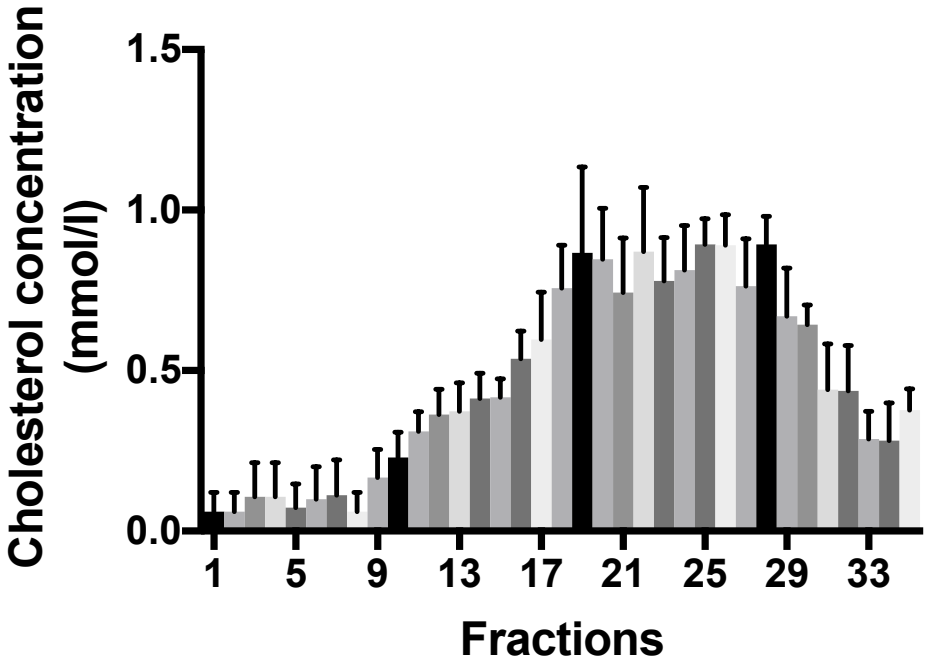

Figure 3.5 Cholesterol concentration in fractions. The cholesterol concentration of each fraction was determined using manual colorimetric cholesterol assay. Data shown is graphed from the average of three separate experiments +SEM.

3.3.5 Determination of the presence of Apolipoproteins in fractions 9-12

Based on the above data, fractions 1-8 were excluded from further analysis as they contained little or no protein, and the 100-200nm material they contain, as evidenced by DLS, is most likely low levels of non-specific artefactual material from the isolation process. Fractions 9-12 were therefore selected as the fractions of interest as they contained protein and were APO deficient. In addition, selection of these fractions also agreed with the report by Boing *et al* in which a similar method was employed (63). In order to confirm the presence or absence of APOs in these and other fractions, a number of fractions were selected and immunoblotted for different APOs. As this study was not primarily interested in the concentration of these APOs but rather if they were present or not, dot blotting was employed to investigate the presence or absence of APOB, E, D, J, M and H (Figure 3.6). In all cases, plasma was used as a positive control. None of the APOs investigated

were evident in fraction 10. Although fraction 12 showed the presence of a small amount of APO B, E, D and J, compared to later fractions, in agreement with the ELISA data there was significantly less APOB, E, D, and J in fraction 12 compared to later fractions. Fraction 17 shows the presence of APOB, E, D, J and M while fraction 22 shows the presence of all APOs investigated (APOB, E, D, J, M and H) (Figure 3.6). While recognising that fraction 12 may contain low amounts of APO, these results confirm that fractions 9-12 are relatively APO deficient.

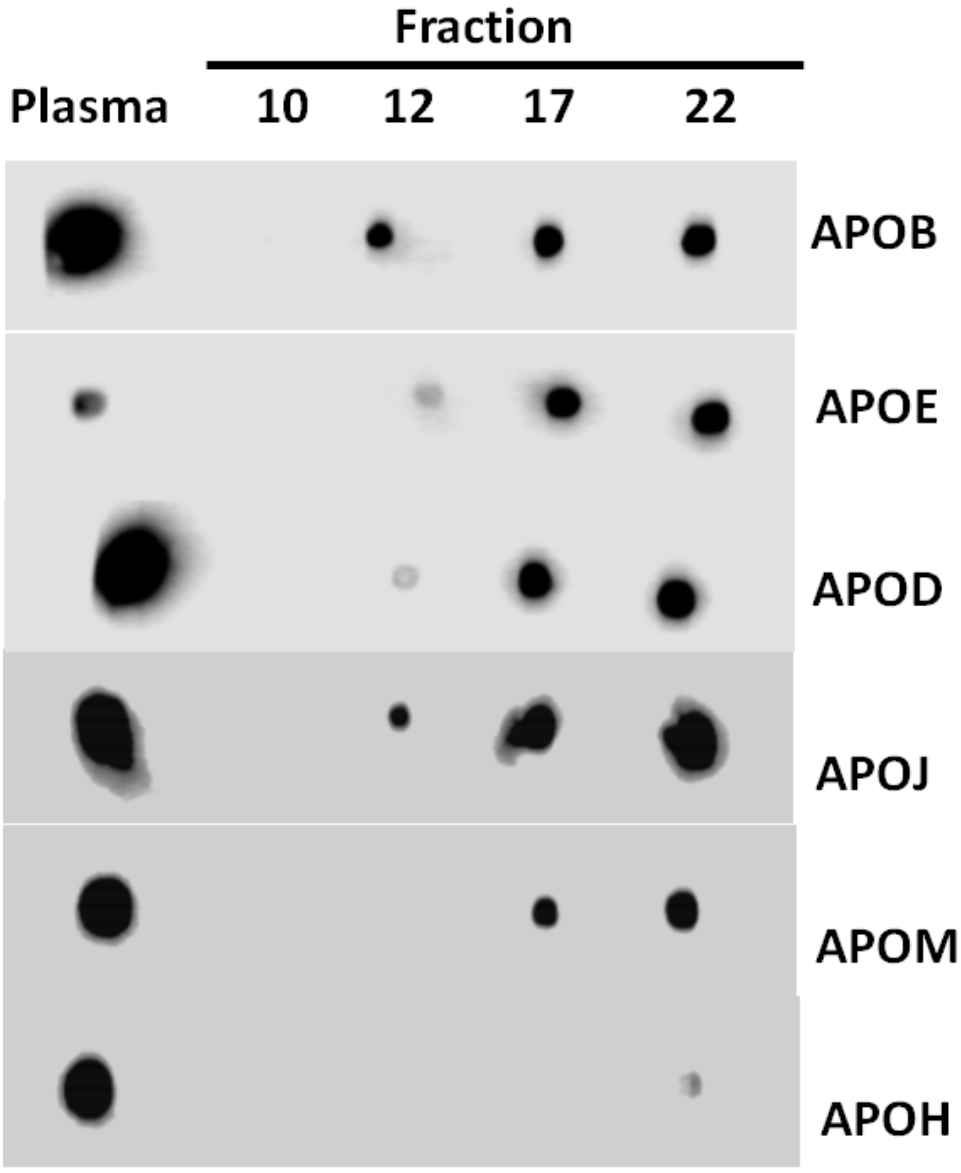

Figure 3.6 Detecting the presence or absence of Apolipoproteins in fractions 10, 12, 17, and 22. Fractions were immunoblotted for APOB, E, D, J, M and H. Plasma was used as a positive control in all cases. This is a representative dot blot from two independent experiments (three independent experiments in the case of APOB).

3.3.6 Determination of particle size in fractions 9-12

DLS (Zetasizer) was employed to further investigate the size of particles in fractions 9-12 and to further confirm that the method of choice (centrifugation followed by SEC) was capable of purifying fractions containing particles of appropriate sizes which were in line with the published literature. Data suggested that the mean size of particles present in these four fractions was between ~150-250nm (Figure 3.7A). A representative read out from the Zetasizer suggested that approx. 35% of particles present in fraction 11 were around 160nm (Figure 3.7B). To further confirm particle size using a different technique, a representative fraction (fraction 11) was chosen for NTA. Results demonstrated that the mode was 144nm, meaning the main size distribution in fraction 11 was 144nm, with particles ranging in size from approx. 197nm to 254nm (Figure 3.7C). These NTA results were similar to the results obtained using DLS. Figure 3.7D depicts an image of particles captured by NTA. These data suggest that particles of the appropriate MP size (approx. 150-250nm) were present in fractions 8-12. Based on equipment availability and the comparability of sizing results using both sizing techniques, DLS was considered suitable to routinely evaluate MP size for the remainder of the study.

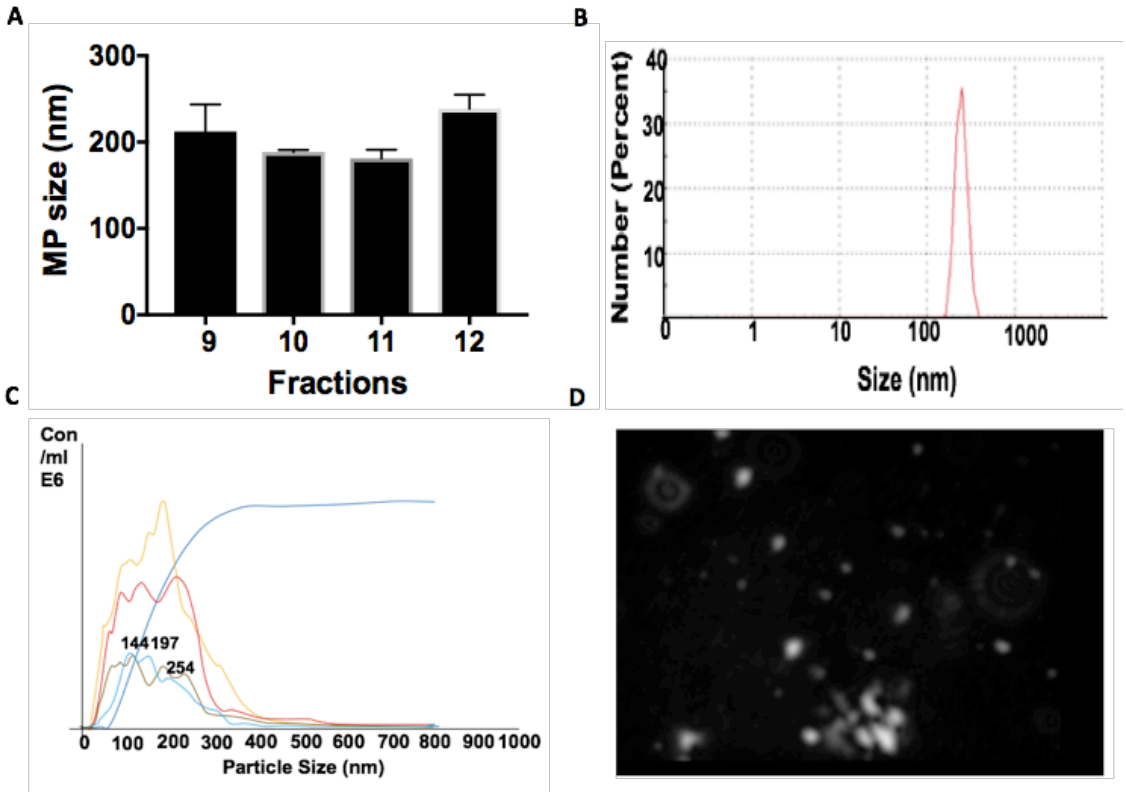

Figure 3.7 Fractions 9-12 size distribution. A) The size of particles present in fractions 9-12 was estimated using DLS (Zetasizer). The mean size distribution was approx. 150-250nm. Data shown is graphed from the average of three separate experiments + SEM. B) A representative read out from the Zetasizer. The peak in this example suggests that approx. 35% of particles present in this fraction are around 160nm in size. C) Particles from fraction 11 were measured by NTA. Three different views were chosen to measure the size. The main size distribution was 144nm, with particle size distribution ranging from 197nm to 254 nm. D) An image of particles captured by NTA. This is a static image of different sized particles which was captured by the machine.

3.3.7 Platelet derived ($CD61^+$) Microparticles are present in fractions 9-12

The most common protocol for analysis of MPs consists of differential centrifugation followed by flow cytometric analysis. It should be noted however that conventional flow cytometry does not allow size distribution determination and is poor at detecting very small particles (<200 nm), such as exosomes and smaller MPs. This is exacerbated by so-called 'swarm' detection of multiple small MPs passing through the aperture as a single event. Consequently, the detected MPs may not always represent the entire population. Despite these limitations, flow cytometry can enable the distinction of MPs of different cellular origins and the analysis of biochemical composition using fluorescently labelled antibodies and other probes. In this part of the study, beads (0.8µm) were used to set up a gate and $CD61^+$ MPs were defined as CD61 positivity with a size ≤0.8µm (Figure

3.8A). Unstained cells and isotype controls were used as negative controls (Figure 3.8B-D). Results indicated that the percentage positivity of $CD61^+$ MPs in fractions 9-12 was between ~60% - 80%, validating that the MP purification technique which was employed in this study could successfully isolate platelet derived MPs (Figure 3.8E-H, Figure 3.9).

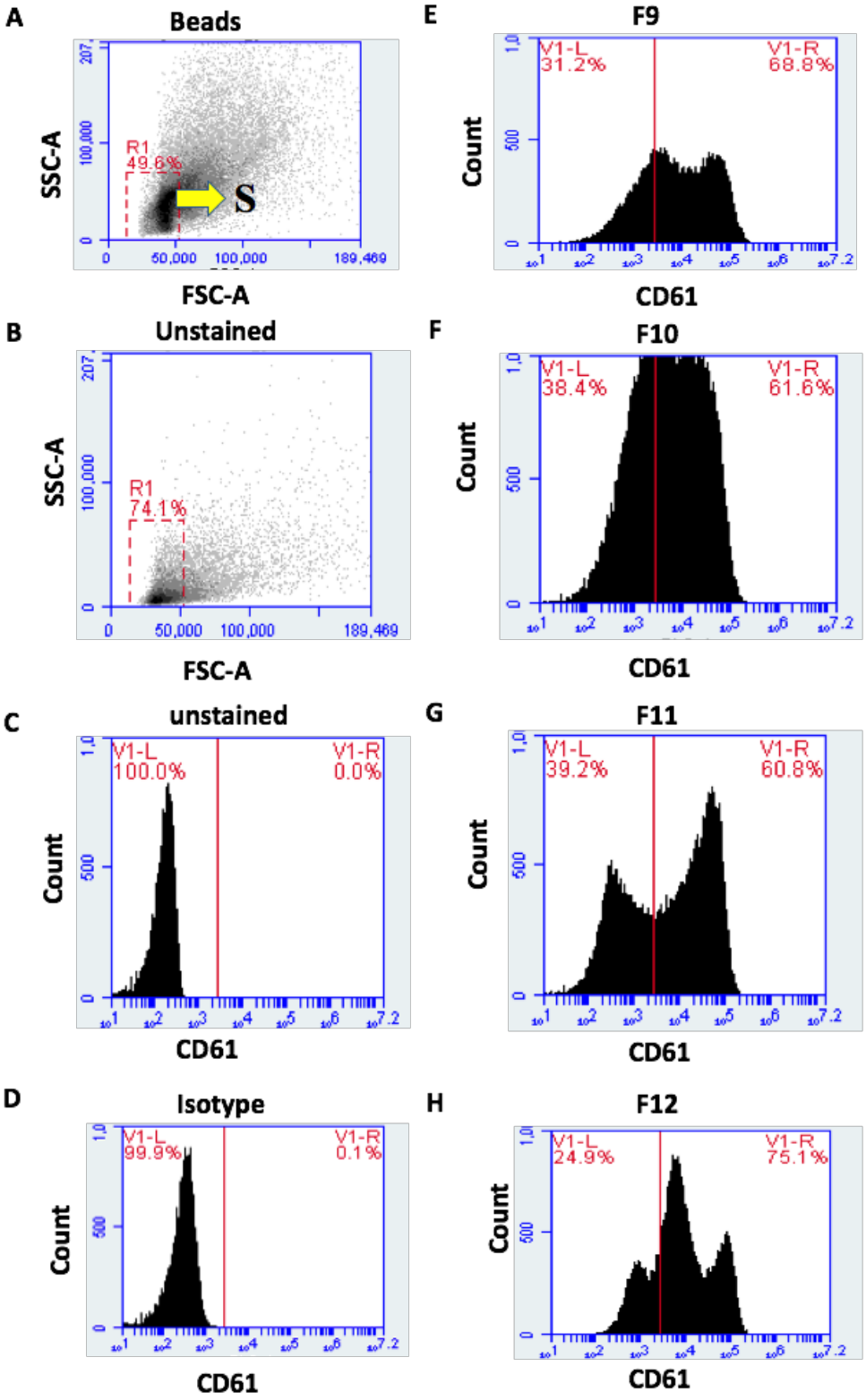

Figure 3.8 Flow cytometry staining for CD61$^+$ microparticles in fractions 9-12. A) Beads ≤0.8µm was applied to set up a gate (S), (B-D). Unstained and isotype control were used as negative controls. (E-H) CD61$^+$ microparticles were detected in fractions 9-12, ranging in percentage positivity from 60.8-75.1%. These are representative plots from three independent experiments.

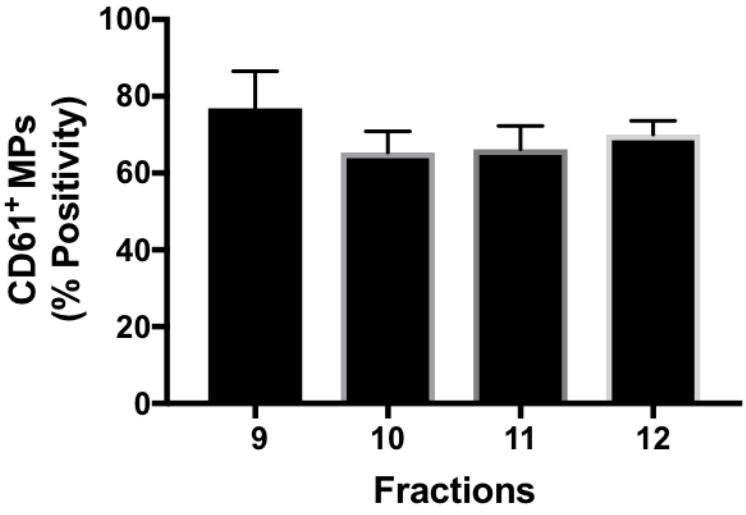

Figure 3.9 The percentage positivity of CD61$^+$ microparticles in fraction 9-12. Fractions 9-12 contained ~ 60% - 80% of CD61$^+$ MPs. Data shown is graphed from the average of three separate experiments +SEM.

3.3.8 Estimation of cholesterol concentration in fractions 9-12

In order to estimate the cholesterol concentration of fractions 9-12, a manual colorimetric assay was used. Results indicated that the cholesterol concentration in these fractions was approx. between 80-170 nmol/fraction (Figure 3.10). It is worth nothing that from a cholesterol point of view, a platelet concentrate would be expected to contain a much higher amount of total cholesterol when compared to a plasma. Each platelet concentrate contains platelets which have been pooled together from five donors, so this is probably the reason for the much higher total cholesterol values observed here when compared to subsequent assays done using donor plasma (Chapter 4).

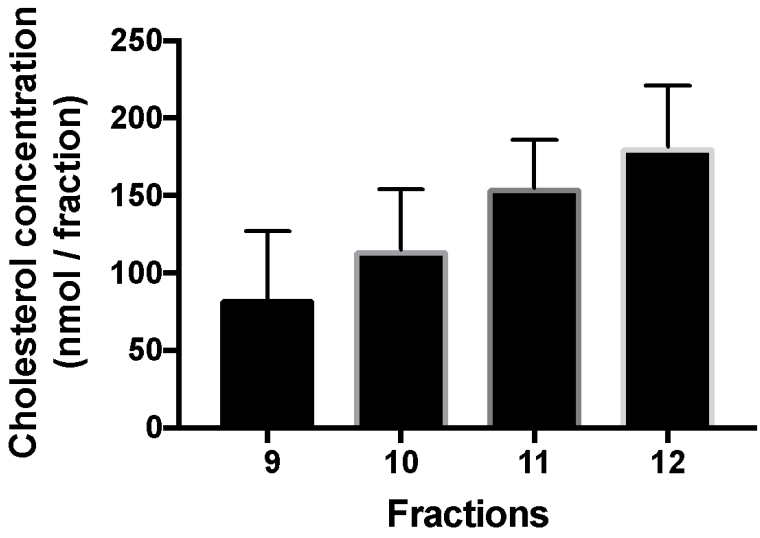

Figure 3.10 Determining cholesterol concentration in fractions 9-12. The cholesterol concentration was measured by a manual colorimetric assay in fractions 9-12. Data shown is graphed from the average of three separate experiments +SEM.

3.4 Discussion

The growing recognition of the biological role of MPs necessitates a standardisation of MP isolation and analysis. This is a *sine qua non* to reliably detect and compare MP numbers, origin and biological activity in health and disease. Initiatives to standardise cross-laboratory MP measurements have already been started by the International Society on Thrombosis and Haemostasis and the International Society for Extracellular Vesicles (213). To this end, in this study a method in which MPs can be purified from platelet-free plasma using a sepharose column was established. More specifically, and of unique interest to this study, cholesterol-containing MPs were isolated without significant HDL contamination in fractions 9-12. Based on immunoblotting results, there was some LDL contamination in fractions 11-12 but compared to LDL concentrations in platelet concentrates, the amount of LDL contamination present in these fractions was considerably less. Compared to other protocols for MP isolation, both differential centrifugation and density gradient ultra-centrifugation often show high lipoprotein contamination (62, 214). The use of SEC in this study has allow us to investigate a unique subset of cholesterol-containing MPs, isolated from a lipoprotein rich environment (platelet concentrate) with little or

no lipoprotein contamination. The principle of SEC is based on different size separation. The sepharose beads pore diameter is around 75nm (63). From our results, we determined the size of MPs was between 150-250nm based on DLS and NTA results. Therefore the time it takes for MPs to pass through the column is quicker compared to HDL and LDL (<80nm). SEC appears therefore to be sufficient to separate MPs from HDL and LDL at >99.95% purity.

Over recent years, methods have been developed to detect even the smallest MPs, enabling reliable semi-quantitative enumeration of MPs in biological fluids (215). These methods employ new flow cytometers equipped with a high-power lasers, high-performance photomultiplier tubes and wide-angle flow scatter measurements, in combination with bright fluorochromes. Since erythrocyte MPs and platelet MPs are easily detectable in the plasma compared with other MPs, and can be obtained in large quantities from transfusion products, these could be used to establish standardised MP measurement protocols. Combining these unambiguous protocols with a selective isolation method, such as FACS or immunoaffinity capture and rapidly expanding proteomic approaches, will provide reliable information on the mechanism(s) involved in MP generation and their biological function. Flow cytometry is a popular method for fast enumeration of MPs and determination of their cellular origin, with forward and sideward light scatter by MPs providing a simple way of discerning different MP populations. Considering this, we sought to determine CD61 positivity of MPs isolated from a platelet concentrate. Analysis of MPs by flow cytometry has been driven mainly by our knowledge of the proteins that are present on the plasma membranes of their parent cells. Inventories of MP proteomes make it possible to overcome this obvious restriction. In a similar fashion, progress is being made in understanding MP formation and pathological function through erythrocyte and platelet MP proteomics (216). It is probable that in the near future, proteomic approach will allow the selection of antibodies for detection of disease-related MP subpopulations. Thus, development of new flow cytometry analytical approaches is dependent on the proteomic analysis of MPs, provided they have been isolated using the same standardised protocols. In this study, flow cytometry was used to confirm fractions 9-12

contain MPs which originated from platelets. In principle, the smallest size which can be detected by flow cytometry is 300nm. We therefore suspect there is a swarm effect present in fraction 10-12 analysis.

In conclusion, this study shows MP isolation using a SEC method significantly reduces lipoproteins contamination. We further confirm MPs contain cholesterol, which supports other studies that have shown cholesterol present in MPs (24, 29, 217). This work establishes a methodological foundation to study the properties and biological importance of MPC.

4.0 Microparticle Cholesterol as a Novel Biomarker in Autoimmune Disorders

4.1 Introduction

There is a growing body of literature that recognises the important role of MPs as a biomarker in autoimmune disorders (218). Numerous studies have shown that circulating MP levels increase in RA or SLE with several papers reporting that MPs can powerfully influence processes such as inflammation, coagulation, thrombosis, antigen presentation and apoptosis in autoimmune disorders (177, 219, 220). A recent study has shown that the combination of apoptotic cell derived MPs and IFN-α resulted in an increase in pro-inflammatory cytokine (TNF, IL-6, IL-8) secretion in SLE (221). Furthermore, Nielsen *et* al has shown relative numbers of IG-positive MPs significantly increased in well-characterised SLE patients. In this study, IG-positive MPs were significantly associated with anti-dsDNA autoantibodies (221). Laura *et al* have reported MPs and MP immune complexes from SLE and RA patients increase adhesion molecules expression (CD54, CD102), chemokine production (CCL2, CCL5) and structural alterations in macrovascular and microvascular endothelial cells (222). Some recent studies show that circulating MPs play a protective role in autoimmune diseases. A paper has reported neutrophil-derived MPs can inhibit the release of proinflammatory factors by macrophages (IL-8, 10 and TNFα) and increase the anti-inflammatory cytokine TGFβ in the early phase of an inflammatory response (223). EVs can also suppress NK and $CD8^+$ cytotoxic functions (223). Taken together these studies suggest that MPs can impact the pathogenesis of autoimmune disease and serve as biomarkers for underlying cellular disturbance. Circulating or membrane cholesterol imbalance is associated with a high risk of developing autoimmune disorders (189, 224). The potential connection between cholesterol and autoimmunity was strengthened by a study by Ronda *et al* in which serum cholesterol efflux capacity was shown to be impaired in RA and SLE patients, which further increased atherosclerotic risk in these patients (225). Other evidence suggests that the abnormalities of monocyte-cholesterol interaction leads to an insufficiency of anti-infectious defence and further promotes the aggravation of infectious syndrome, which is a known risk factor in later RA development (226).

Taken together, these studies suggest that interplay between imbalanced cholesterol and abnormal immune cells can accelerate the inflammation process seen in autoimmune disorders, however there is no published study to date which has investigated the role of MPC in autoimmune disorders. Having already optimised a method to isolate lipoprotein deficient MPs from a platelet concentrate in Chapter 3, this part of the study set out to investigate the possibility of MPC as a novel biomarker in autoimmune diseases.

TLRs are widely expressed on the surface of monocytes and macrophages, cells which are important components of the innate immune system and play a key role in host defence against infection through immune-inflammatory response (227). TLR4 acts as a receptor for lipopolysaccharide (LPS) by associating with the myeloid differentiation protein 2 (MD2) to form a complex to interact with LPS. The formation of the TLR4-MD2-LPS complex activates the adaptor molecules Myd88 or TRIF and drives pro-inflammatory signalling cascades (227). In this chapter, we also investigated the role of MPs on TLR4 signalling responses using MPs isolated from healthy control and SLE and RA patient plasma samples in an *in vitro* (human monocytic cell line: THP-1) and *ex-vivo* (HMDMs) model.

4.2 Aims

- Establish a reference range for MPC in healthy controls and autoimmune patients (SLE and RA)
- Investigate the possibility of MPs isolated using SEC as a biomarker in autoimmune disease diagnosis and patient stratification.
- Characterise inflammatory properties of MPs isolated from autoimmune disease patients

4.3 Results

4.3.1 Characterisation of microparticles isolated from healthy control plasma

As outlined in chapter 3, the platelet concentrates used for MP isolation in the study to this point were from five donors pooled together and so hence we hypothesised that these MP fractions

contained a higher amount of total cholesterol compared to MP fractions isolated from a single donor plasma. In order to investigate this and to further validate the reproducibility of the isolation method, MP fractions were purified from 16 healthy control plasma samples. As the platelet concentrate was from multiple donors, it was necessary to look at individual donors to establish a range for MPC in a healthy control population. In each case, 1.5ml of donor PFP was loaded onto a sepharose column and 30 fractions were collected for characterisation studies. DLS was used for sizing, TEM for determining their structure and immunoblotting and ELISAs to assess and quantify the presence of APOs.

Based on previous results, fractions 8-13 were selected for analysis to allow for one fraction either side of fractions 9-12. Results suggested that MPs in fraction 8-13 were of the correct size, ranging in size between 100-1000nm (Figure 4.1A). Approx. 73% of MPs present in fractions 8-13 were between 100-300nm (Figure 4.1A black bars), ~25% of MPs between 300-500nm (Figure 4.1A red bars), and the remaining ~2% of MPs were between 500-1000nm in size (Figure 4.1A blue bars). To investigate the structure of MPs isolated from donor plasma using SEC, fractions were visualised by TEM. Results suggested that the starting material (i.e. plasma loaded onto the column) contained structures of various shapes and sizes (Figure 4.1B, panel A). Fraction 2 did not contain any material whereas fractions 8-13 contained mostly large particles with very few smaller particles evident in the background (Figure 4.1B, panel C-H). The size and structure of particles appeared to be consistent with the presence of MPs. Later fractions 16, 18, 20, 22, contained MPs of various sizes and had a lot more very small particles evident in the background (Figure 4.1B, I-L). The smaller particle numbers were increased in the later fractions compared to the early fractions (fraction 8-13). It is notable that fractions 8-13 mainly contained large particles with few small particles, however, small particles gradually increased and large particles gradually decreased in the later fractions. This further confirmed that fractions 8-13 was a relatively uniform subset of fractions, free from a significant proportion of very small particles with a size consistent with that of lipoproteins and were therefore appropriate for further investigations.

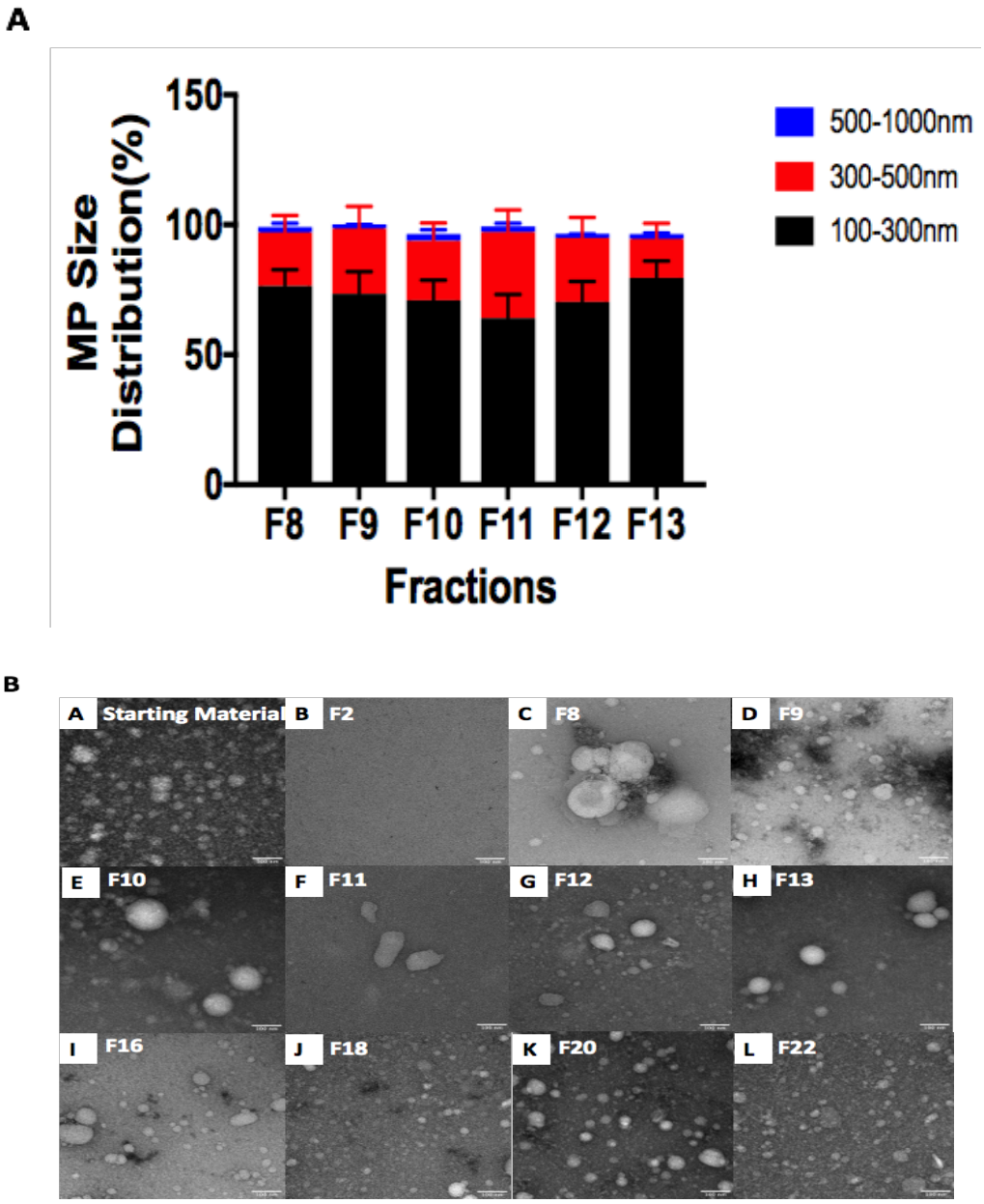

Figure 4.1 Biophysical characterisation of healthy control microparticles. A) MP size distribution in fraction 8-13 as determined by DLS, data expressed as mean +SEM. Data is from 16 healthy people. Around 73% of MPs present in fraction 8-13 were between 100-300nm (black bar), around 25% MPs size in 300-500nm (red bar), only around 2% MPs size fell into 500-1000nm (blue bar). B) Representative images from one healthy person: starting material (A), negative control (B), fraction 8-13 (C-H), fraction 16, 18, 20, 22 (I-L) detected by TEM. Each fraction contained different numbers of particles. Scale bar = 100nm.

Immunoblotting and ELISAs were used to investigate the presence of APOs in various fractions. Dot blots showed fractions 8-13 were free from APOA1, B, E, D, H, M and J (Figure 4.2A). As quality control for apolipoprotein content, an APOA1 and APOB immunoblot was conducted for each donor plasma. An APOA1 and APOB ELISA further confirmed that fraction 8-13 are

expected to contain less than 0.01% lipoprotein (Figure 4.2B). A zoomed in image of ELISA results from fractions 10-16 (Figure 4.2B top left) clearly shows that fraction 10-13 did not contain significant detectable APOA1 and APOB. This further confirmed that fractions 8-13 were a subset of fractions that were MP-containing and lipoprotein deficient and for this reason were the fractions which would be used for subsequent studies in both healthy control and autoimmune disease patient plasma.

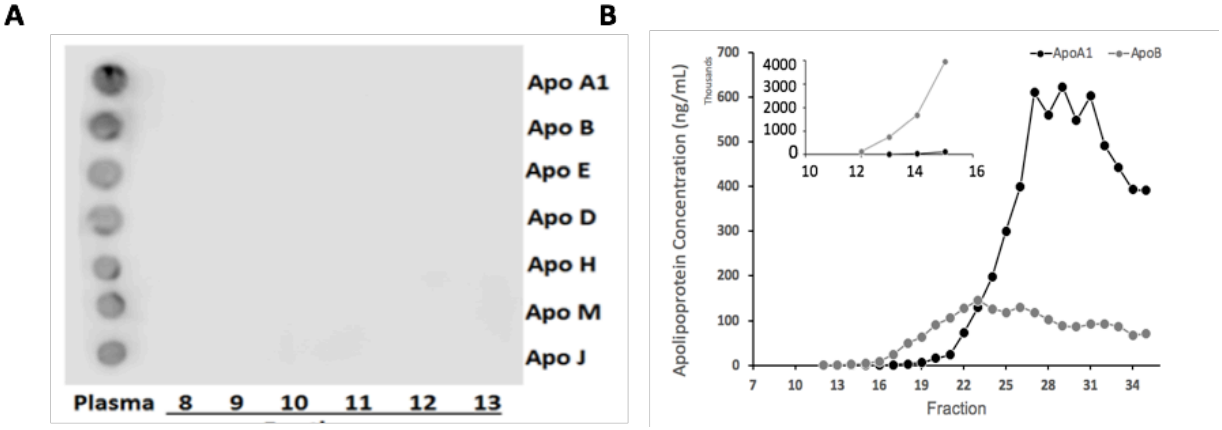

Figure 4.2 Investigating the presence of apolipoproteins in donor plasma fractions. A) Immunoblot for APOA1, B, E, D, H, M and J in fraction 8-13, with plasma functioning as a positive control. B) APOA1 and APOB ELISAs on fractions 1-35. Fractions 8-10 were undetectable for APOB and fractions 8-11 were undetectable for APOA1. The limitations of ELISA: APOA1 is 4ng/mL and APOB is 78ng/mL.

For subsequent patient studies, each donor donated only 3.5ml of whole blood which yielded approx. 1.5ml of PFP. In order to ensure that there was enough material for all investigations going forward, it was decided that 0.5ml of plasma would be loaded onto the sepharose column for fraction collection. All data presented from this point applies to fractions isolated from 0.5ml of plasma.

4.3.2 Population Demographics

Information relating to healthy controls, SLE patients and RA patients is outlined in table 4.1 below. Thirteen healthy controls who met the selection criteria of no hypertension or inflammation and had a normal lipid profile without using cholesterol-lowering medication) were recruited to

the study. Fourteen SLE patients were recruited to the study, of which two had no clinical information provided. Fifteen RA patients were recruited based on seropositive for cyclic citrullinated peptide (CCP) or rheumatoid factor (RF). RA patients (57.8 ± 12.46) were significantly older than SLE patients (46.9 ± 13.23, $p<0.05$) or controls (43.3 ± 11.38, $p<0.01$). There was no statistical difference between female/male ratios between healthy controls (10/3) and patient sets (SLE: 10/2, RA: 11/4) although females predominated in each group (Table 4.1, third row). Again this was not surprising as the autoimmune conditions being discussed here have a known female prevalence (228). The mean disease duration between both SLE and RA patient sets was also comparable, with a median value of 10 and 11 years respectively (Table 4.1, fourth row). Data shows that 7.7% (1/13) of healthy controls, 0% (0/14) of SLE patients and 13.3% (2/15) of RA patients smoked at the time of the study (Table 4.1, fifth row). The autoantibody, complement and medical treatment profile for the SLE patients is included in table 4.1 (middle lighter grey section). Laboratory results (RF, CCP, ESR, CRP and DAS28 CRP), Disease-Modifying Anti-Rheumatic Drugs (DMARDS) and X-ray information for RA patients in outlined in table 4.1 (lower darker grey section).

Table 4.1: Basic Clinical Information of Donors

	Healthy Controls	SLE Patients	RA Patients	Statistical Differences
Number	13	14	15	
Age mean (SD)	43.3 (11.38)	46.9 (13.23)	57.8 (12.46)	HC versus SLE: ns HC versus RA: p<0.01 SLE versus RA: p<0.05
Gender (F/M)	10/3	10/2	11/4	ns
Diseases duration, years median (Min - Max)	N/A	10 (2 - 25)	11 (1 - 36)	ns
Current smokers (n)	1	0	2	ns
SLE Patient Cohort				
Autoantibodies at inclusion				(n)
ANA Positive				12
Anti-Ro				9
Anti-La				4
Anti-Sm				2
Anti RNP/SM				2
dsDNA				9
Complement				
C3(g/L) (meanSD)				0.920.29
C4(g/L) (mean SD)				0.1550.08
Medicine				
Mycophenolate				3
Prednisolone				3
Plaquenil				6
Azathioprine				1
Valacylovir				1
RA Patient Cohort				
RF (IU/ml)(median[min-max])				124 (0-5350)
CCP (U/ml) (median[min-max])				219 (1-600)
ESR (mm/hr) (median[min-max])				14.5 (4-52)
CRP (mg/L) (median[min-max])				5.5 (0.5-29)
DAS28 CRP (median[min-max])				2.71 (1.35-4.62)
DMARDS				
MTX 12.5mg weekly PO				2
MTX 15 mg weekly PO				3
MTX 20 mg weekly PO				2
HCQ 200mg OD				2
HCQ400mg OD				2
SSZ				4
Etanercept				1
Xrays				
Erosion small joints/swollen				8

N/A: Not applicable, RF: Rheumatoid factor, CCP: Cyclic Citrullinated Peptides, ESR: Erythrocyte Sedimentation Rate, CRP: C-reactive protein, DAS28 CRP: Disease Activity Score-28 for Rheumatoid Arthritis with CRP, DMARDS: Disease-Modifying Anti-Rheumatic Drugs, MTX: methotrexate, HCQ: Hydroxychloroquine, SSZ: Sulfasalazine.

4.3.3 Microparticle size in patients and controls is not different

MPs isolated from 0.5ml of citrate plasma from controls, SLE or RA patients using a SEC method has a size profile consistent with that described in the literature. The majority of MPs from each fraction were in the 100-300nm size range, with a significant minority in the 300-500nm range. Less than 10% of particles were between 500 and 1000nm. Results demonstrate that approx. 70% of MPs, derived from either the healthy control group or the patient groups, ranged in size from 100-300nm (Figure 4.3, black bars). Approx. 20%-30% of MPs isolated from the healthy control group and both patient groups were between 300-500nm in size (Figure 4.3, red bars), with less than 10% of all group's MPs falling within the 500-1000nm size range (Figure 4.3, blue bars). Taken together, these data suggested that there was no obvious difference in MP size in fractions isolated from healthy control or SLE and RA patient plasma.

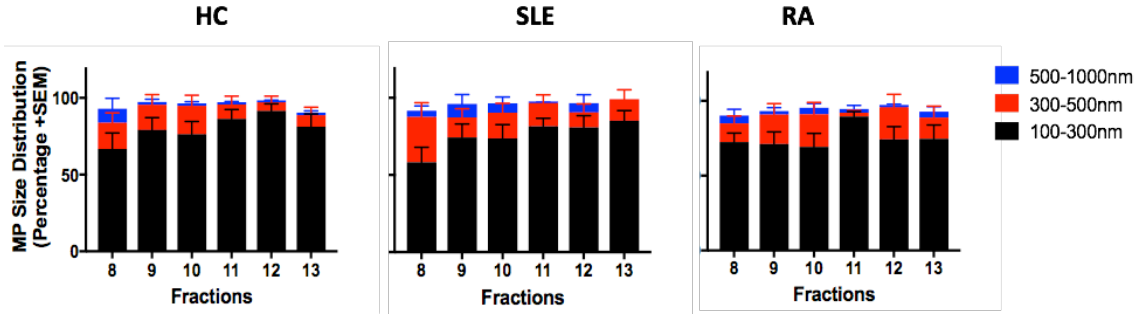

Figure 4.3 Microparticle size distribution in fractions 8-13 as determined by DLS. MPs from (A) healthy control group (n=13), (B) SLE patients (n=14) and (C) RA patients (n=15) percentage size distribution. Data expressed as mean +SEM.

To further confirm MPs were of the correct size range, the size of MPs derived from one representative healthy person was measured using a different sizing technique, NTA (Figure 4.4). In agreement with the DLS results, MP size distribution was observed to be between 100-1000nm, with the majority of MPs (the peak) size range falling between 100-300nm (Figure 4.4). Fraction 8 and fraction 13 were diluted five times before analysis and fraction 9-12 were diluted 10 times before analysis. Figure 4.4 shows the concentration increased from fraction 8 and reached a peak in fraction 11 and then decreased again.

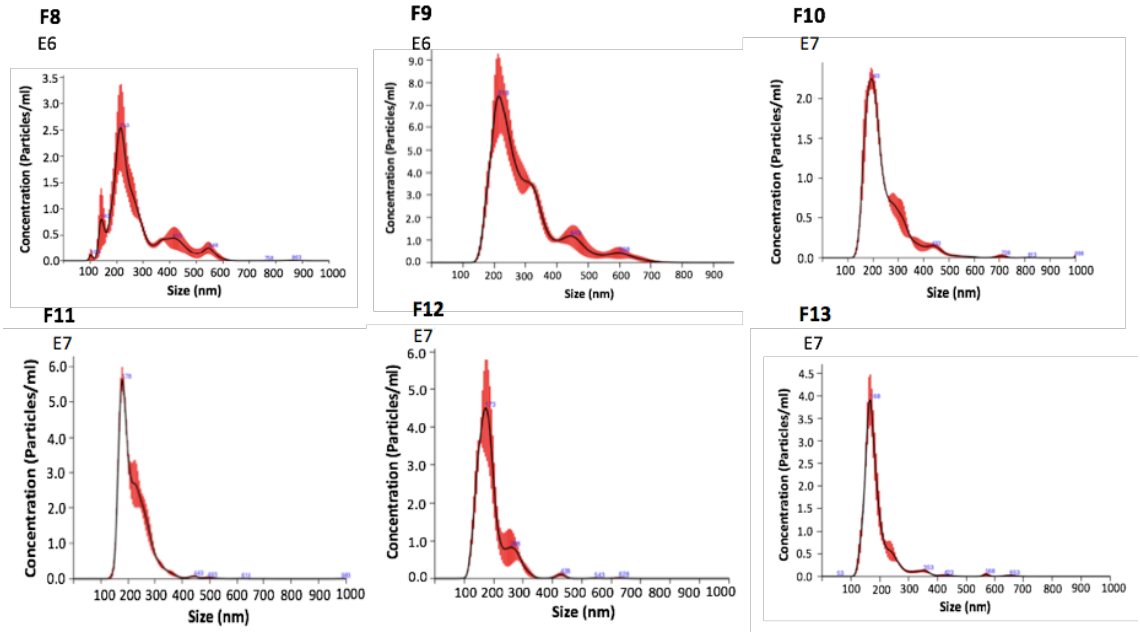

Figure 4.4 Microparticle size distribution in fraction 8-13 as determined by NTA. A representative size distribution analysis of MPs from a healthy control. MP size distribution was between 100-1000nm, with the majority of MPs (the peak) size range being between 100-300nm.

4.3.4 Investigation of the structure of microparticles in isolated fractions

TEM was employed to confirm the presence of MPs in different fractions derived from healthy control or patient plasma. Some representative TEM images from healthy control and SLE patients are presented in figure 4.5. Fraction 10 and fraction 11 isolated from healthy control plasma contained large vesicles (>100nm), which are similar in shape and size (Figure 4.5A, panel A, B), however, fraction 18 and fraction 20 which were also isolated from healthy control plasma contain numerous smaller vesicles (<100nm), which are assumed to be small exosomes and lipoproteins (Figure 4.5A, panel C, D). These healthy control images are consistent with the images of the same fractions isolated from 1.5ml of plasma which are shown in figure 4.1B. Representative images of fractions isolated from SLE patients are also shown in Figure 4.5. Fraction 2 (Figure 4.5A, panel E) did not contain any material whereas fractions 11, 12 and 13 contained particles of similar shape and size (100-1000nm) (Figure 4.5A, panels F-H). Later fractions 16, 18, 20 and 22 contained some larger particles but were mainly made up of smaller particles of similar size (5-80nm) which can be seen in the background (Figure 4.5A panels I-L). We assume these to be lipoprotein. Furthermore, dot blots confirmed that fractions 8-13 from healthy controls, SLE and RA patients

did not contain APOA1 and APOB (Figure 4.5B). Results therefore confirmed that fractions 8-13 were relatively uniform in structure, contained particles of similar shape and size and were lipoprotein deficient.

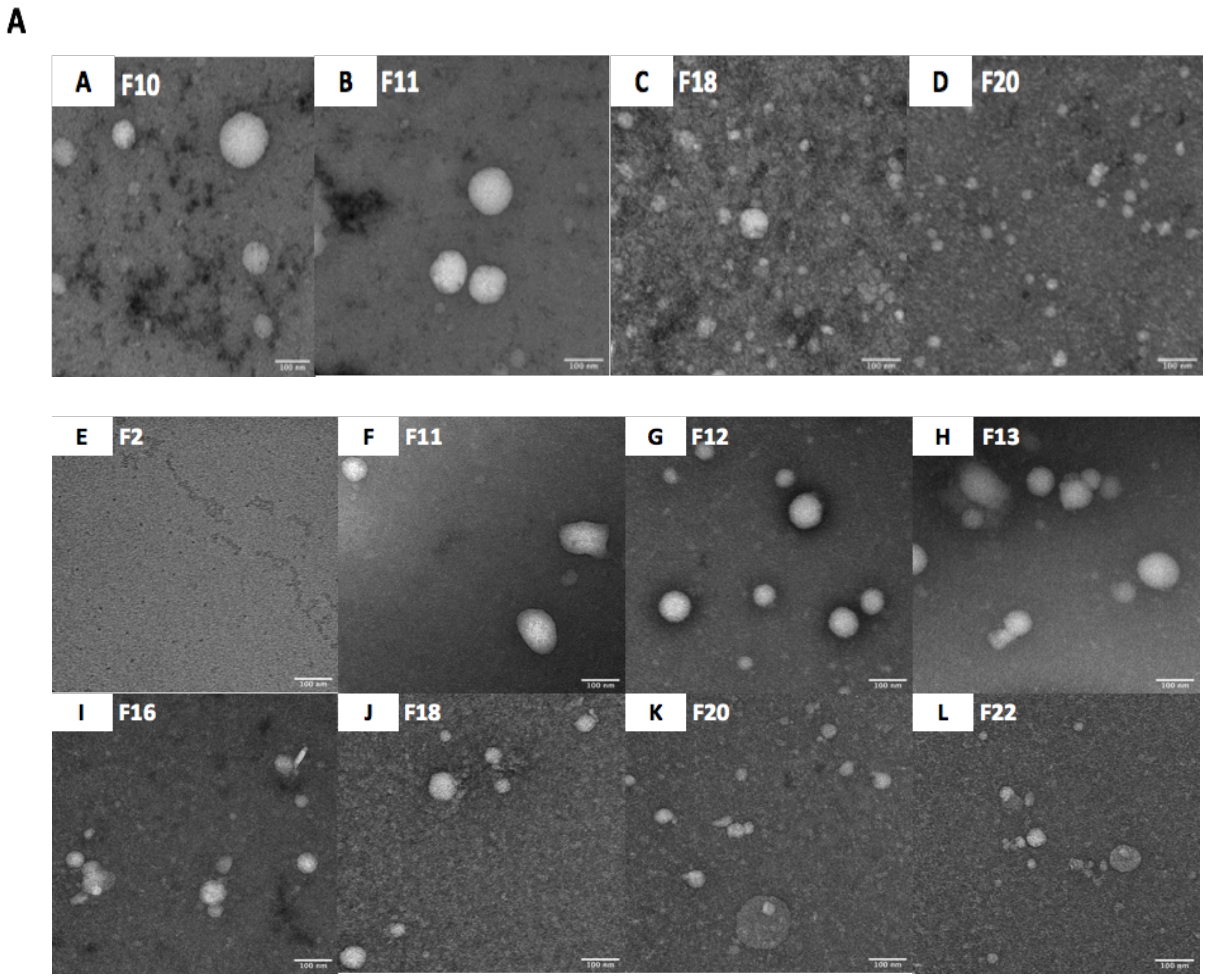

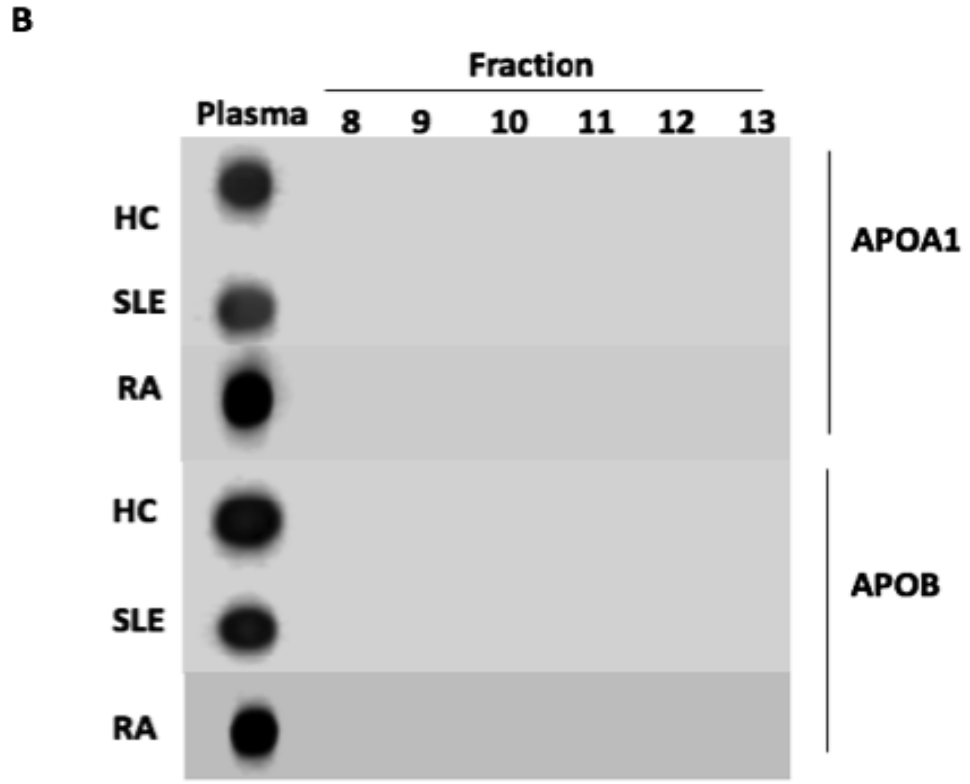

Figure 4.5 Determination of structure and apolipoprotein content in representative fractions. A) Representative TEM images of fraction 10, 11, 18 and 20 from a healthy control (A-D). Representative TEM images of fractions 2, 11, 12, 13, 16, 18, 20, 22 from two SLE patients (E-L). Scale bar =100nm. B) Immunoblot for APOA1 and APOB in fractions 8-13 from healthy control (HC), SLE and RA patients, with plasma functioning as a positive control. This is a representative immunblot. All samples were examined by dot blot.

4.3.5 Determination of the cell of origin of microparticles in fractions 8-13

Flow cytometry was used to investigate the cell of origin of MPs present in fractions 8-13 isolated from healthy control, SLE patient and RA patient plasma. In all cases, fractions were stained with platelet markers ($CD61^+/CD42b^+$), endothelial cell markers ($CD31^+CD42b^-$) and a leucocyte marker ($CD45^+$) in order to establish the MP cell of origin. The numbers of MPs originating from different cells in healthy controls and patients groups was investigated. Results showed that there was no significant difference in the amount of resting platelet derived ($CD42b^+$) MPs observed between each group (Figure 4.6A). There was however a significant difference in the amount of platelet derived ($CD61^+$) MPs in SLE ($p<0.001$) and RA patients ($p<0.01$) compared to healthy controls, with both patient groups showing an increased amount (Figure 4.6B). Neither SLE or RA patients contained significantly more leucocyte ($CD45^+$) derived MPs compared to healthy

controls, although RA patients were shown to have significantly more ($p<0.05$) of this type of MP compared to SLE patients (Figure 4.6C). Both SLE and RA patient groups contained more endothelial cell ($CD31^+CD42b^-$) derived MPs compared to healthy controls, with p values of $p<0.05$ and $p<0.001$ respectively (Figure 4.6D). Our results are consistent with several studies which have reported that there is increased levels of active platelet ($CD61^+$) derived and endothelial ($CD31^+CD42b^-$) derived MPs in autoimmune diseases patients (166, 229, 230).

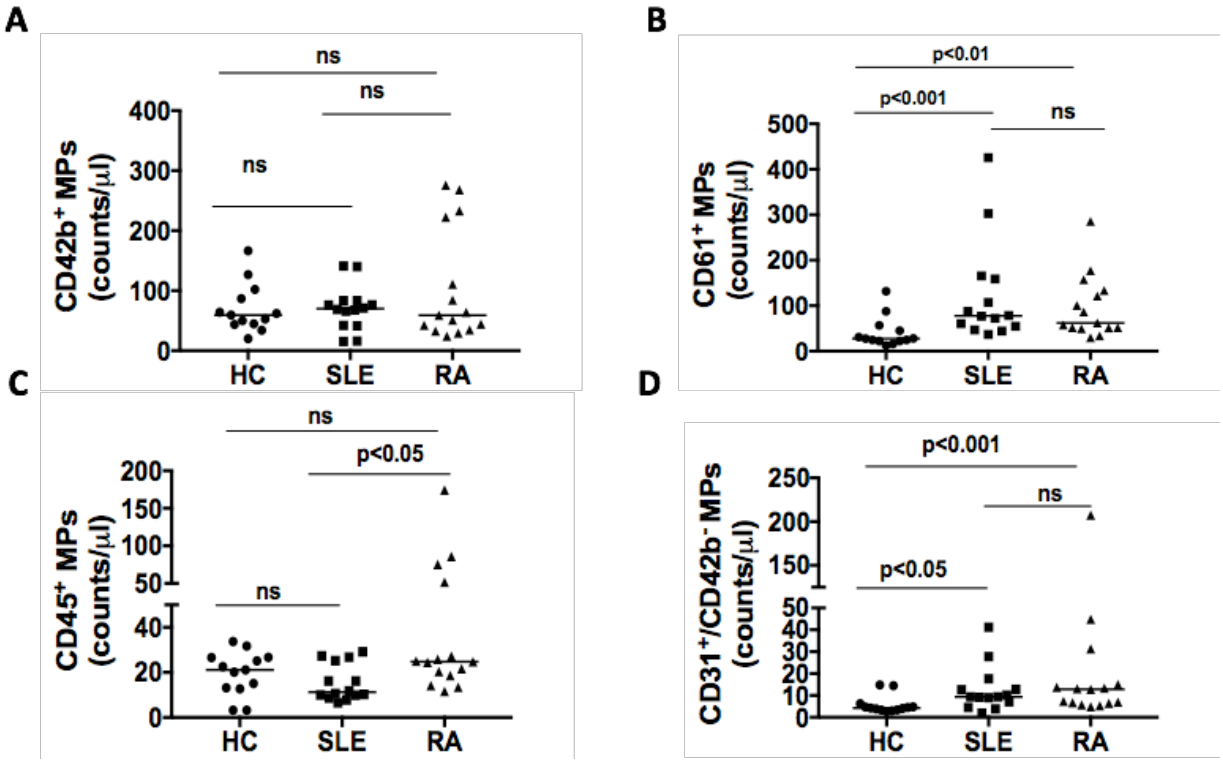

Figure 4.6 Characterisation of circulating microparticles from healthy control, SLE and RA. A) The number of general platelets derived MPs ($CD42b^+$). B) The number of active platelets derived MPs ($CD61^+$). C) The number of leucocyte derived MPs ($CD45^+$). D) The number of endothelial cell dervied MPs ($CD31^+$ $CD42b^-$) in healthy control, SLE patients group and RA patients group. Each data point presents an individual participant, and the median shown as a black line. All comparisons not specified in the figures were not significant (ns). All of data are based on 13 healthy controls, 14 SLE patients and 15 RA patients.

4.3.6 Investigation of the lipid profile of donors and cholesterol content of microparticles in fractions 8-13

Total cholesterol and triglyceride levels were estimated in both healthy controls and patients subsets. D'Agostino-Pearson testing was used to measure data normality. Total cholesterol values

in the healthy control and patient groups were all within the normal range. One-way ANOVA testing indicated that there was no significant difference in total plasma cholesterol levels between the three groups (Figure 4.7A). The rest of the data presented in figure 4.7 (B-D) was found to not be normally distributed. Kruskal-Wallis testing revealed that there was no significant difference in triglyceride concentration among groups (Figure 4.7B). The cholesterol content of MPs from fractions 8-13 was estimated. RA patients had significantly greater cholesterol content in MP compared to healthy controls and SLE patients ($p<0.01$), (Figure 4.7C). There was no difference in the MPC content between healthy controls and SLE patients. Outlier identification analysis (ROUT method) was applied to discover any potential outliers within the three groups. One outlier was identified in the healthy control group (Figure 4.7C, red dot). In all cases, the outlier was excluded in statistical analysis. Statistical analysis confirmed that RA patients had significantly more ($p<0.01$) MPC as a percentage of total plasma cholesterol when compared to both healthy controls and SLE patients (Figure 4.7D). There was no difference in MPC expressed as a percentage of total plasma cholesterol values between healthy controls and SLE patients. Although MPC accounted for approximate 1.5% of total cholesterol in RA patients, that was almost three times higher than the percentage in healthy controls (approx.0.5%) and SLE patients (approx. 0.5%). Again, the ROUT method identified one outlier in the healthy control group (Figure 4.7D, red dot).

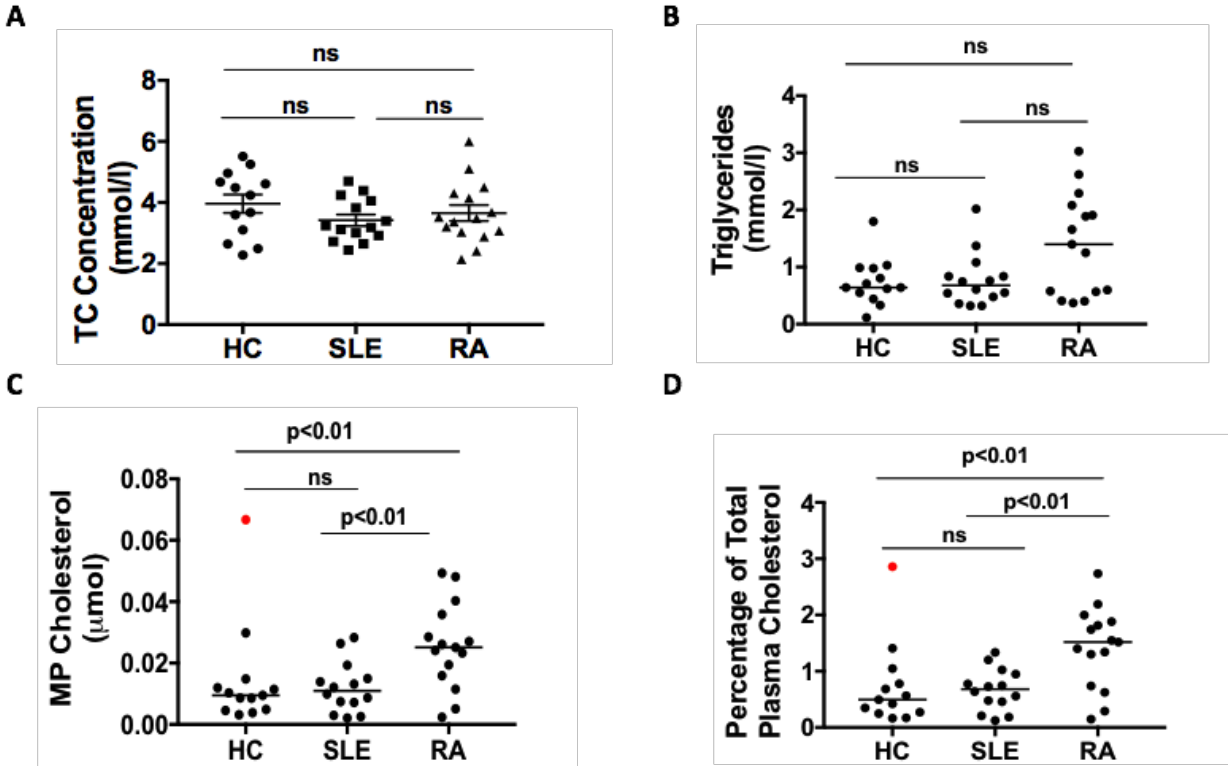

Figure 4.7 Autoimmune patients have increased microparticle cholesterol compared to healthy controls. A) Total cholesterol concentration in healthy control and patient groups. Data was expressed as mean ±SEM. B) Triglyceride concentration in healthy control and patient groups. Data was expressed as median with black dots. C) Microparticle (MP) cholesterol in healthy control and patient groups, Data was expressed as median with black dots. Red dot symbolises outlier. D) MP cholesterol expressed as a percentage of total plasma cholesterol in healthy control and patient groups. Data was expressed as median with black dots. Red dot symbolises outlier. In all cases, these data are based on 13 healthy controls, 14 SLE patients and 15 RA patients.

4.3.7 Investigation of potential correlations between microparticle, microparticles cholesterol and clinical parameters

As MPs can reflect the inflammatory state observed in SLE or RA patients (231), we hypothesised that MPs derived from different cells of origin could be associated with some clinical inflammatory indexes, such as C3, C4, CRP, CCP and RF. Spearman correlation was used to investigate the association between MPs and clinical parameters. In the case of RA patients, CRP levels were shown to positively correlate with the number of active platelet derived ($CD61^+$) MPs present (Figure 4.8A, p=0.052, R=0.51). CCP levels were shown to positively correlate with the number of leucocyte derived ($CD45^+$) MPs present (Figure 4.8B, p=0.048, R=0.52), and RF levels were shown to positively correlate with the number of endothelial derived ($CD31^+CD42b^-$) MPs present (Figure 4.8C, p=0.0040, R=0.73). This suggests that MPs derived from RA patients are related to

the clinical parameters from RA diseases, which indicates the inflammatory status of diseases. Furthermore, There is no correlation between MPC derived from RA patients and any clinical parameter investigated (Figure 4.9A-E). Likewise, there is no correlation between MPC and total cholesterol in RA patients (Figure 4.9F).

In the case of SLE patients, serum C3 levels were shown to negatively correlate with the number of endothelial derived ($CD31^+CD42b^-$) MPs present (Figure 4.8D, p=0.038, R=-0.6). Generally, the typical pattern in active SLE patients is low C3 levels, with C3 levels rising after treatment. In our study, only two SLE patients were active, with the rest being inactive. This is the reason that C3 levels are in the normal range (0.8-1.6g/L). However, $CD31^+CD42b^-$ MPs increased in inactive SLE patients and was negatively correlated with C3 levels, which suggests $CD31^+CD42b^-$ MPs is a more useful biomarker to diagnose inactive SLE patients than C3 levels.

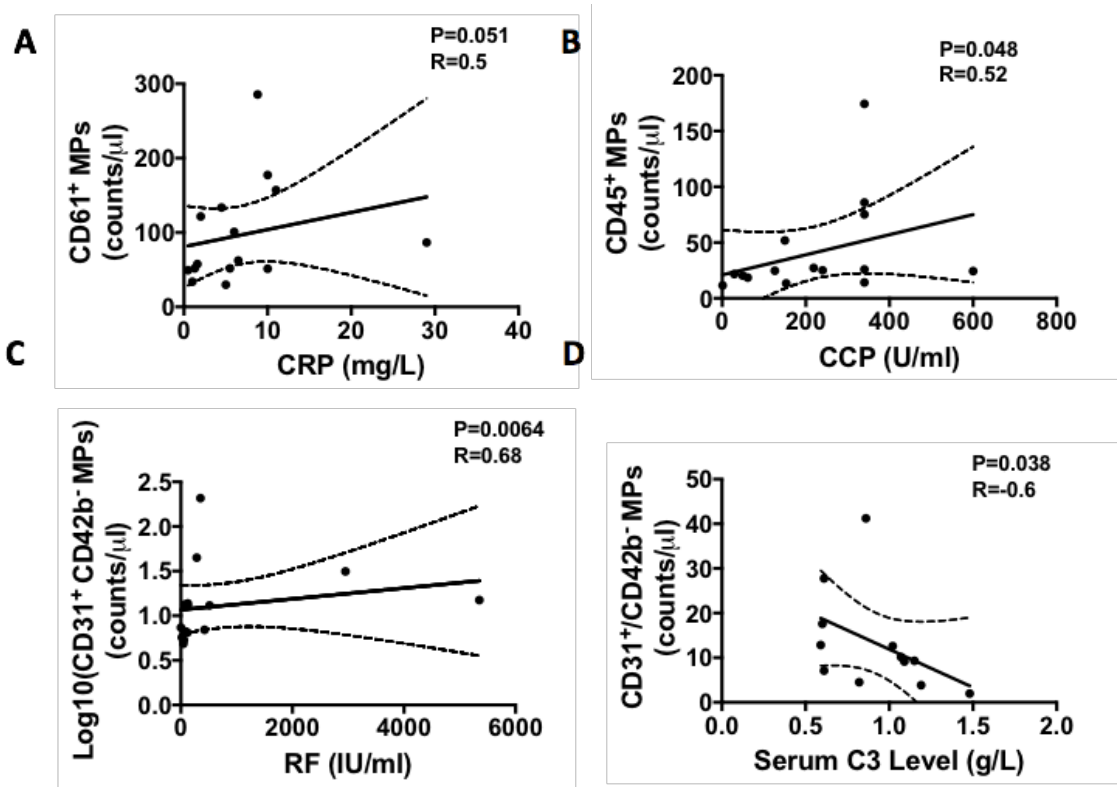

Figure 4.8 Correlations between microparticles derived from different cell types and clinical parameters in patient groups. A) Correlation between active platelet derived ($CD61^+$) MPs and CRP level in RA patients B) Correlation between leucocyte derived ($CD45^+$) MPs and CCP level in RA patients C) Correlation between endothelial cell derived ($CD31^+CD42b^-$) MPs and RF level. Log10 = logarithm (base 10) in RA patients. D) Correlation between endothelial cell derived ($CD31^+CD42b^-$) MPs and serum C3 level in SLE patients.

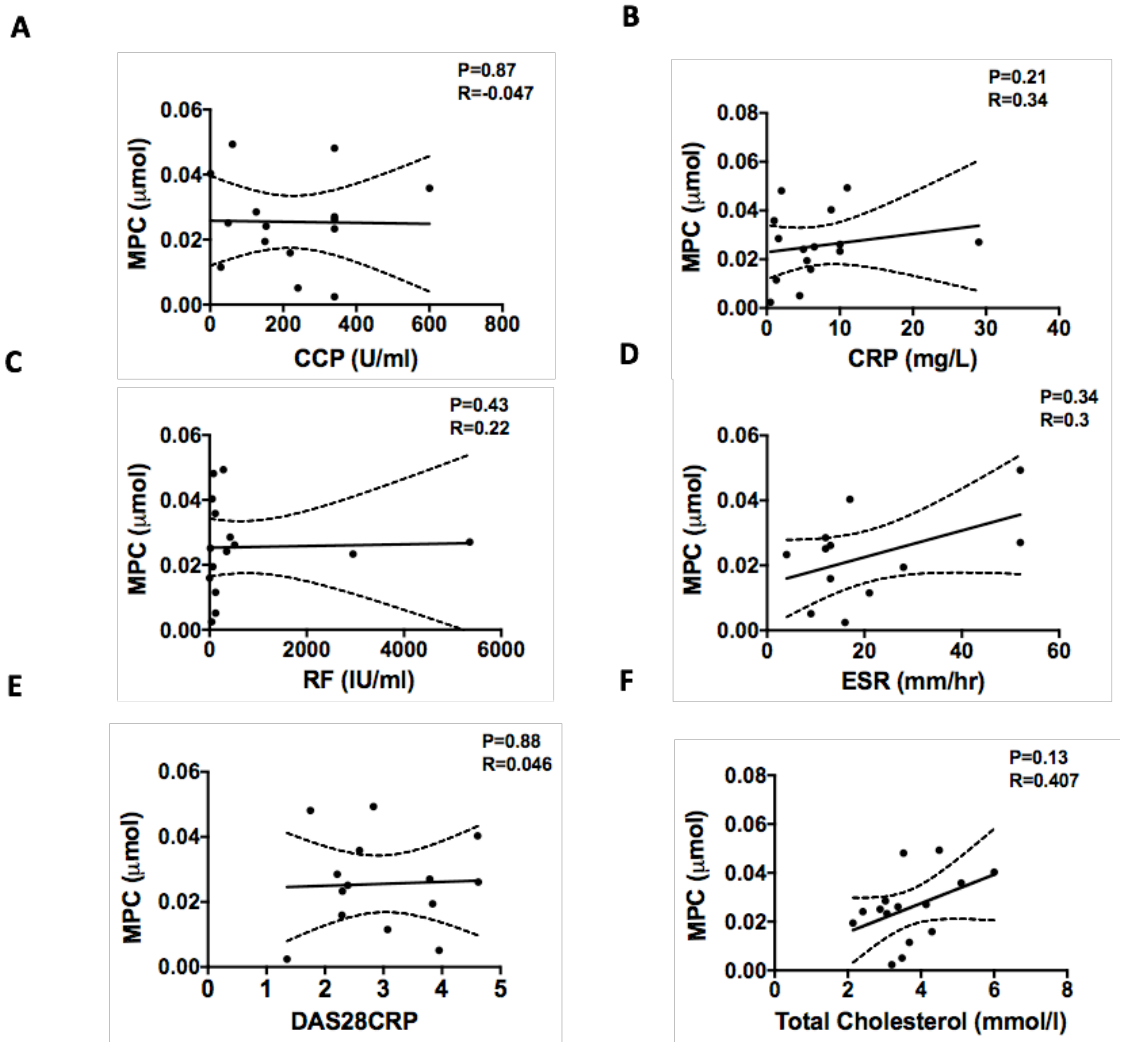

Figure 4.9 Correlations between microparticle cholesterol (MPC) and clinical parameters in RA patients. A) Correlation between MPC and CCP levels. B) Correlation between MPC and CRP levels. C) Correlation between MPC and RF levels. D) Correlation between MPC and ESR levels. E) Correlation between MPC and DAS28 CRP score. F) Correlation between MPC and total cholesterol.

4.3.8 Using microparticle cell of origin numbers and microparticle cholesterol levels to define diagnostic parameters in healthy control and patient groups

Receiver Operating Characteristic (ROC) analysis was performed to identify the cut-off values for $CD61^+$ MPs, $CD31^+CD42b^-$ MPs, $CD45^+$ MPs and MPC in order to distinguish each donor group from one another. The area under the ROC curve (AUC) was used to estimate the accuracy of the diagnostic test for the discrimination between RA patients, SLE patients and healthy controls. AUC values range from 0 to 1. Generally, an AUC of 0.5 suggests that patients with or without

the disease cannot be classified by this biomarker, an AUC of 0.7 to 0.8 is considered acceptable, an AUC of 0.8 to 0.9 is considered excellent and more than 0.9 is considered outstanding. The main limitation of AUC does not account for different misclassification which arise from false-negative and false-positive diagnoses. Table 4.2 shows AUC, 95% confidence interval (CI), cut off, sensitivity, specificity and p-value for all parameters tested.

AUC values (>0.7) and sensitivity and specificity values from table 4.2 were used to assess the potential diagnostic value of different parameters. Analysis of healthy controls versus RA patients demonstrated AUC values for $CD31^{+}CD42b^{-}$ MP number, $CD61^{+}$ MP number and MPC amount were more than 0.8, which suggests that these three biomarkers were capable of classifying patients with or without RA diseases (Figure 4.9A). Analysis of healthy controls versus SLE patients suggested that $CD31^{+}CD42b^{-}$ MP number and $CD61^{+}$ MP number were useful biomarkers in distinguishing patients with or without SLE (Figure 4.9B). $CD61^{+}$ MPs numbers had a higher AUC value (0.881) than $CD31^{+}CD42b^{-}$ MP number (0.756), which suggests $CD61^{+}$ MP number was more accurate at diagnosing SLE when compared to $CD31^{+}CD42b^{-}$ MP number (Table 4.2, Figure 4.9B). $CD45^{+}$ MP number and MPC amount were both considered to be useful biomarkers to distinguish SLE from RA based on AUC values >0.7 (Figure 4.9C). Furthermore, results suggested that MPC, $CD31^{+}CD42b^{-}$ MP number or $CD61^{+}$ MP number was capable of classifying patients with or without autoimmune diseases, however, $CD31^{+}CD42b^{-}$ MP number or $CD61^{+}$ MP number was not able to distinguish SLE from RA disease, with only MPC showing promise in this regard. This suggests MPC to be a promising biomarker to diagnosis SLE and RA patients, who often present with overlapping symptoms.

Table 4.2: ROC Curve Analysis to Define Diagnostic Parameters in Healthy Control and Patients Groups

Biomarker	AUC	95% CI	Cut off	Sens.	Spec.	p value
Healthy Controls and RA Patients						
$CD31^{+}CD42b^{-}$MPs	0.861	0.698-1	4.84 counts/µl	1	0.750	0.002
$CD61^{+}$ MPs	0.872	0.722-1	47.33 counts/µl	0.867	0.833	0.001
$CD45^{+}$ MPs	0.661	0.453-0.869	23.53 counts/µl	0.600	0.670	0.157
$CD42b^{+}$ MPs	0.533	0.311-0.756	194.54 counts/µl	0.267	1	0.770
MPC	0.828	0.655-1	0.015 µmol	0.800	0.917	0.004
Healthy Controls and SLE Patients						
$CD31^{+}CD42b^{-}$ MPs	0.756	0.554-0.795	6.68 counts/µl	0.786	0.833	0.027
$CD61^{+}$MPs	0.881	0.735-1	33.97 counts/µl	1	0.750	0.001
$CD45^{+}$MPs	0.387	0.156-0.618	4.89 counts/µl	1	0.167	0.328
$CD42b^{+}$MPs	0.583	0.345-0.822	65.08 counts/µl	0.714	0.750	0.471
MPC	0.565	0.336-0.795	0.012 µmol	0.500	0.833	0.572
SLE Patients and RA Patients						
$CD31^{+}CD42b^{-}$ MPs	0.560	0.340-0.779	12.96 counts/µl	0.467	0.786	0.585
$CD61^{+}$ MPs	0.438	0.224-0.652	48.08 counts/µl	0.867	0.214	0.570
$CD45^{+}$ MPs	0.771	0.593-0.950	17.42 counts/µl	0.8	0.714	0.013
$CD42b^{+}$ MPs	0.514	0.289-0.739	181.94 counts/µl	0.267	1	0.896
MPC	0.786	0.611-0.961	0.019 µmol	0.733	0.857	0.009

CI: Confidence interval, Sens: Sensitivity, Spec: Specificity, AUC: Area under the curve; MPC: Microparticle cholesterol

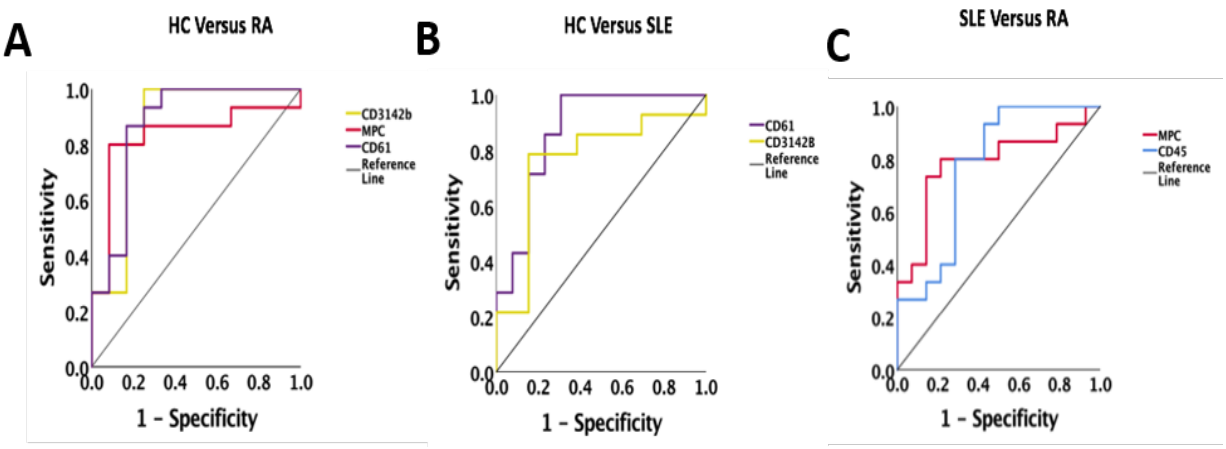

Figure 4.10 ROC curve analysis in healthy control and patient groups. A): ROC curve analysis results of $CD61^+$ MPs (purple line), $CD31^+$ $CD42b^-$ MPs (yellow line) and microparticle cholesterol (MPC) (red line) in healthy controls versus RA patients. B): ROC curve analysis results of $CD61^+$ MPs (purple line) and $CD31^+$ $CD42b^-$ MPs (yellow line) in healthy controls versus SLE patients. C) ROC curve analysis in $CD45^+$ MPs (blue line) and MPC (red line) in SLE versus RA patients.

4.3.9 Microparticles attenuate TNFα and TLR4 expression in LPS-induced inflammation

Preliminary experiments have been carried out to explore the role of MPs in inflammatory responses. MPs isolated from healthy controls, and SLE and RA patient subsets were used to treat cells (THP-1 cells, HMDMs) and TNFα and TLR4 expression was measured. The availability of SLE and RA patients in an "active" disease status often hampers these types of investigations. Initial experimental work in this area was carried out in collaboration with Prof. Caroline Jefferies at her laboratory in Cedars-Sinai Hospital, where plasma was available from SLE patients with active and inactive disease. To investigate the effect of MPs on LPS induced responses, cells were pre-treated with MPs for 1 hour and then treated with LPS for a further 3 hours. Some optimisation experiments in which cells were treated with MPs for 3 hours rather than 1 hour showed similar results so as a starting point a 1 hour treatment time was selected. However, further experiments are needed to investigate the effect of MPs on TLR4 and TNFα responses over a longer MP pretreatment time course. Three hour LPS treatment is a standard treatment length to see both surface protein changes and gene expression of both early and later acting inflammatory genes such as TNFα. A longer LPS treatment time of 24 hours will be needed in future experiments when cytokine release is being investigated.

Results show that treatment of THP-1 cells with a high concentration (13μg total protein) of MPs for one hour, followed by LPS stimulation for three hours, lead to alterations in LPS induced TNFα mRNA levels (Figure 4.10). Notable differences were observed in cells which were pretreated with MPs derived from an active SLE patient almost completely obliterating the LPS induced expression of TNFα mRNA compared to MPs derived from both healthy controls and an inactive SLE patient. Although these treatment conditions may be considered supraphysiological, these initial data provided insight and direction into the design of subsequent experiments and verified the importance of having both disease active and inactive donors.

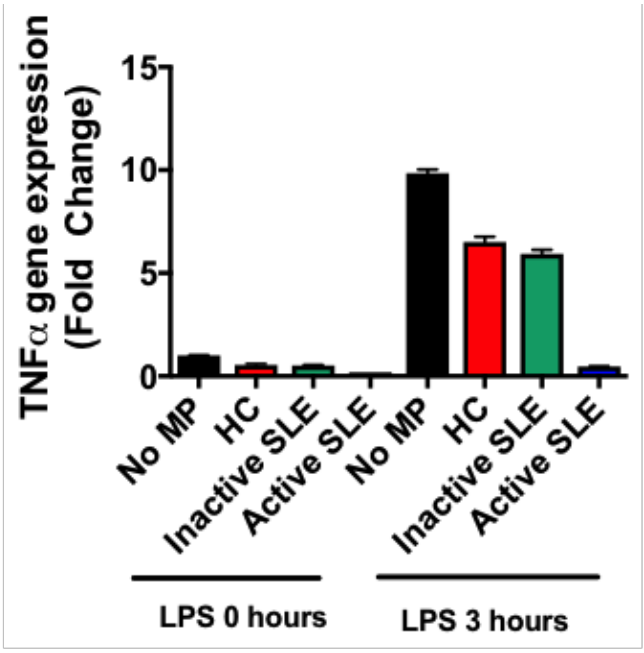

Figure 4.11 Pretreatment of THP-1 cells with microparticles from active SLE patients downregulates LPS induced TNFα mRNA expression. TNFα mRNA levels were measured in THP-1 cells which had been pretreated with MPs from 2 healthy controls (HC), 1 inactive or 1 active SLE patients for 1 hour with/without LPS treatment for a further 3 hours. Data is expressed as mean +SEM.

In order to mimic normal pathophysiological levels, a lower concentration of MPs was used for subsequent cell treatment experiments. As normal human plasma contains 2 to 4μg/ml of MP protein, THP-1 cells were pretreated with 1μg of MPs (concentration 2μg/ml) for subsequent experiments. As TNFα is produced downstream of TLR signaling, therefore the effects of MPs effect on TLR4 surface expression was assessed by flow cytometry. Results show that pretreatment with MPs derived from healthy controls did not reduce basal or LPS induced TLR4 expression

whereas this was reduced after pretreatment with MPs derived from both active SLE and RA patients (Figure 4.12). Although these results are preliminary, interestingly MPs from the inactive RA patient had no downregulating effect on LPS induced TLR4 expression, again suggesting the differences from a functional point of view between MPs produced in active versus inactive disease (Figure 4.12, red dot).

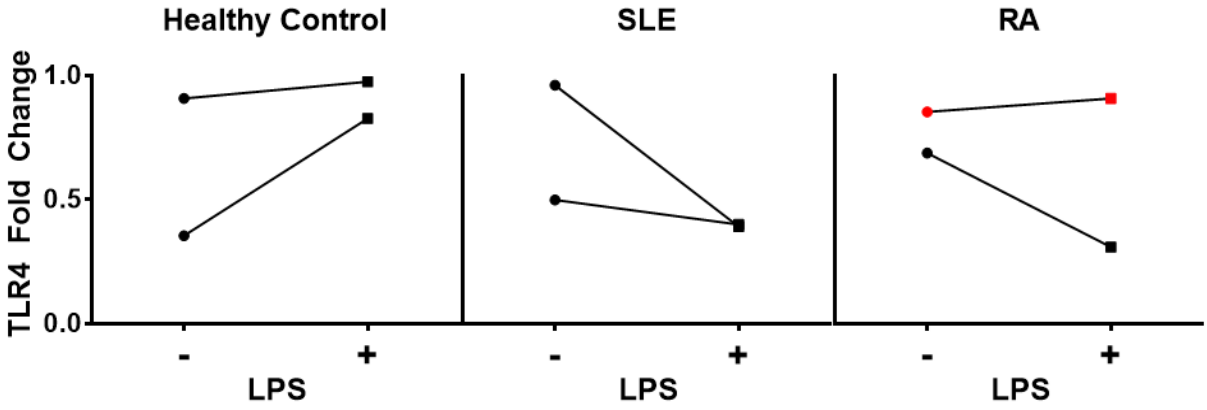

Figure 4.12 Pre-treatment of THP-1 cells with microparticles from autoimmune patients downregulates LPS induced TLR4 expression. THP-1 cells were pre-treated with 1µg of microparticles (2µg/ml) derived from two healthy controls, two active SLE patients, one active RA patient and one inactive RA patient (red dot) for 1 hour followed by +/- LPS treatment for a further 3 hours. TLR4 protein expression was analysed by flow cytometry. All data was normalised to cells which had been treated with LPS only for 3 hours.

To further investigate the preliminary data acquired from the THP-1 cell line above, experiments were repeated in HMDM primary cells. In all cases, HMDMs were isolated from buffy coats obtained from the Irish Blood Transfusion Service. A representative image of HMDMs isolated from a buffy coat is shown in figure 4.13A. Once purified, HMDM CD11b (macrophage marker) expression was assessed by flow cytometry (Figure 4.13, C).

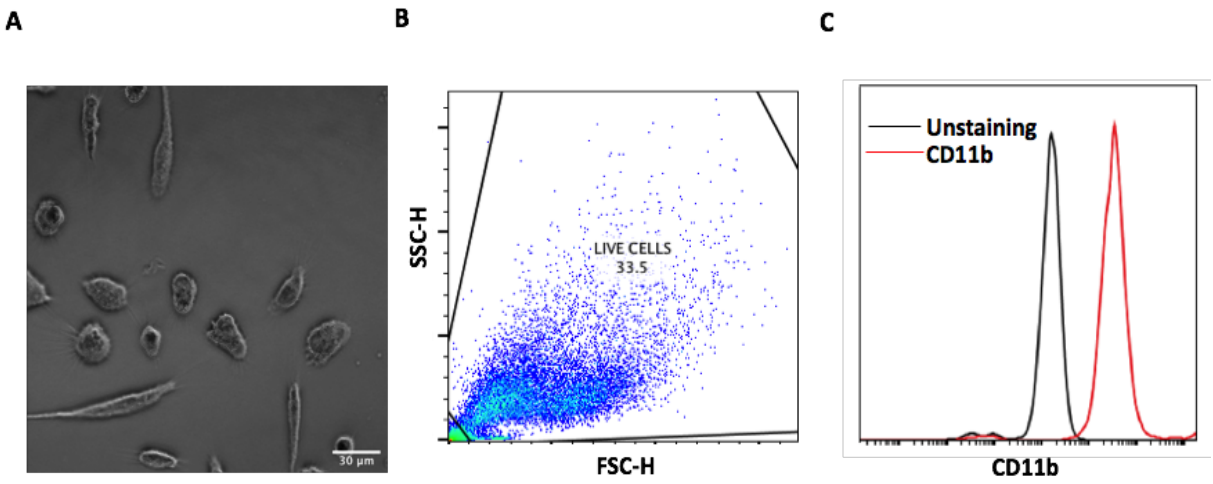

Figure 4.13 Characterisation of human monocytes derived macrophages. A) A representative image of HMDMs isolated from a buffy coat. Scale Bar=30µm. B) Gates were set up on the flow cytometer to exclude debris and dead cells. C) HMDMs express CD11b (Red line). FSC: forward scatter. SSC: side scatter.

Treatment of HMDMs was according to an identical protocol to that described above with the exception of a lower amount (0.1µg) of MPs being used in these experiments in order to investigate how potent the MPs were. Treatment with MPs from two active RA patients lead to a 50% reduction in surface expression of TLR4 as judged by flow cytometry, under both basal and LPS stimulated conditions (Figure 4.14A). This reduction in LPS induced TLR4 expression was not observed post treatment with MPs from the inactive RA patient (Figure 4.14A, red dot). Assessment of TNFα mRNA levels under similar experimental conditions revealed a MP dependent reduction in LPS induced TNFα mRNA expression. MPs from both SLE and RA had similar impacts on mRNA levels, but there was no impact under basal conditions (Figure 4.14B). This is most likely due to the low basal expression of TLR4 and therefore the limited scope to observe a reduction in gene expression. Although these results are provisional, they do uncover a novel mechanism of immunomodulation which may be of importance under *in vivo* conditions.

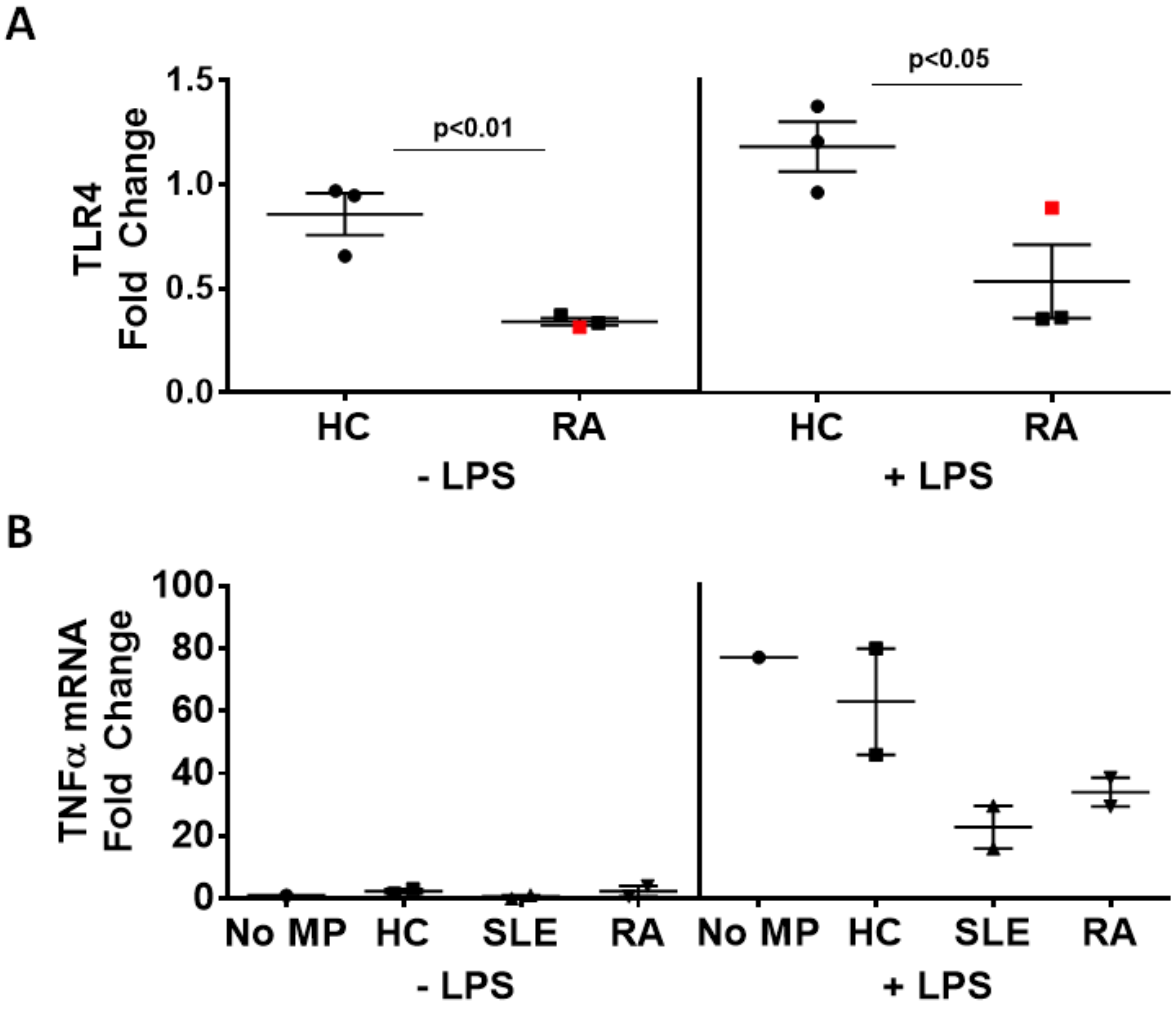

Figure 4.14 Microparticles from autoimmune patients reduce basal and LPS induced TLR4 and TNFα expression. In all cases, HMDMs were pretreated with 0.1µg of MPs from either three healthy controls, three RA patients (two active and one inactive (red spot)) or two active SLE patients for 1 hour followed by LPS treatment for 3 hours. A). TLR4 protein expression was measured by flow cytometry. Data was expressed as mean ±SEM. All data was normalised to cells which had been treated with only LPS for 3 hours. B) TNFα mRNA levels were measured by q-PCR. Data expressed as mean ±SEM.

4.4 Discussion

Consistent with similar reports, in this study, MPs originating from platelets ($CD61^+$) and endothelial cells ($CD31^+CD42b^-$) were significantly higher in SLE and RA patients compared to healthy controls (166, 229, 230). Furthermore, this study provides new insights into MPC levels in SLE and RA and demonstrated for the first time that MPC in RA patients is significantly increased compared to healthy controls and SLE patients. Above all, our results demonstrated how

an increased level of MPC could provide a valuable platform for distinguishing SLE and RA disease and holds promise as a new biomarker.

Our findings around increased $CD61^{+}$MPs and $CD31^{+}CD42b^{-}$MPs in both patient groups compared to healthy controls, with no difference in $CD45^{+}$MP or $CD42b^{+}$MP levels is in line with other studies (166, 229, 230, 231). Our results demonstrate that RA patients had an increased number of $CD45^{+}$ MPs compared to the SLE patient group. One reason for this could be related to disease status, as the SLE group contained only two patients with active disease (SLEDAI score>6).

Our results showed the level of MPC to be significantly increased in RA patients compared to both SLE patients and healthy controls. Uzma *et al* have reported that dyslipidaemia is observed in active RA disease, with patients often having low cholesterol levels yet high CVD risk (232). The paradoxical lipid changes observed in RA are not fully understood. Due to the nature of the disease, RA patients were significantly older than SLE patients and controls but we found no correlation between MPC and age. Furthermore, multiple regression analysis was applied to evaluate clinical and biochemical variables age, gender, smoking, total cholesterol, triglycerides, CRP, CCP, RF, ESR, DAS28 as independent variables in regression models of the dependent variable MPC. Results showed MPC to be an independent risk factor. This is the first study to our knowledge to demonstrate cholesterol accumulation in MPs derived from RA patients, with MPC derived from RA patients showing potential as a novel biomarker to diagnose RA disease.

It is widely accepted that MPs can function as biomarkers in autoimmunity, with increased levels being observed in many diseases (23, 218, 231, 233). However, these studies have focused on using MPs to diagnose autoimmunity in general, rather than classifying autoimmune diseases. In this study, $CD61^{+}$MPs and $CD31^{+}CD42b^{-}$MPs could separate autoimmune patients and healthy controls, while MPC could further distinguish RA from SLE. Several studies report MPs derived from autoimmune diseases patients as having pro-inflammatory effects (234, 235). Recently, one study has reported platelet-derived MPs have anti-inflammatory effects in human plasmacytoid dendritic cells. Platelet-derived MPs decreased TNFα and IL-8 secretion after platelet-derived

MPs uptake by human plasmacytoid dendritic cells (236). Another study further reports that EVs derived from endothelial cells can reduce proinflammatory responses by inhibiting NF-κB signalling pathways (237). The precise mechanism of action is still unclear. The authors suggest that proteins or lipids contained within the EVs contribute to their anti-inflammatory and immunomodulatory effects (237). Another study by Čebatariūnienė *et al.* reports that EVs purified from periodontal ligament stem cells can suppress LPS-induced NF-κB signalling pathways (238). Our preliminary results in this study suggest that the anti-inflammatory effects of MPs may be involved in TLR4 - NF-κB -TNFα signalling pathways.

In conclusion, in this pilot study, we establish a candidate reference range of MPC (0.003μmol -0.03μmol) in a representative healthy control population. Furthermore, we report striking differences in MPC levels among patients and age matched controls, suggesting its potential as a novel biomarker and usefulness in patient stratification. Despite these promising results, further work is required to fully elucidate MPs exact mechanism of action in inflammatory responses.

5.0 3-Hexanoyl-NBD-cholesterol is a versatile membrane cholesterol tracer

5.1 Introduction

Cholesterol is a fundamental component of the cell membrane and plays an important part in maintaining cell membrane integrity and fluidity (80). Cholesterol is transported in plasma as a component of lipoproteins due to very low water solubility (110). The basic cholesterol structure and biosynthesis were described in chapter 1 (section 1.3). Cholesterol is not homogenously distributed in mammalian cells. Depending on cell types, it is widely accepted that the cell membrane contains most of the cellular cholesterol (110). The endoplasmic reticulum is the organelle which synthesises cholesterol but in fact contains very low cholesterol as the cholesterol is rapidly transferred from the endoplasmic reticulum to other organelles once synthesised (110). Excess cholesterol is known to have cytotoxic effects in cells, therefore, the exact amount of cholesterol the cells need for physiological functions needs to be very tightly regulated (110). Cells are adept at removing excess cholesterol in several ways which involve the liver X receptor family, ATP binding cassette transporters (ABCA1, ABCG1) and other binding proteins (110, 239). Therefore, robust and efficient sensors and tracers of cholesterol are needed to support research into different aspects of cholesterol behaviour, including localisation, uptake, diffusion and efflux (110, 240) Previous studies have shown that fluorescent cholesterol analogues could be investigated in lipid trafficking as cholesterol is not fluorescent (107, 241). Fluorescent analogs of cholesterol can be divided into intrinsically fluorescence sterols and extrinsic or tagged sterol probes (110). Intrinsically fluorescent cholesterol analogs include dehydroergosterol, cholestatrienol, cholestatrienol esters and cholesteryl parinaric acid as lipoprotein probes. Extrinsic cholesterol analogs include boradiaza-indacene-tagged cholesterol, 6-Dansyl-cholesterol, NBD-tagged cholesterol and pyrene-tagged cholesterol (110). The advantages and disadvantages of commonly used fluorescence sterol probes as described in Table 5.1 (110).

In this project, we are more interested in studying NBD-tagged cholesterol analogy. In most research 22NDBC has been used as the cholesterol probe (108, 109), however, a recent study has suggested that insertion of the fluorescence tag of 22NBDC in the membrane can change the

ability of cholesterol to move (111). The rate of 22NBDC exchange between the cells and the acceptor is much faster when compared to the normal cholesterol exchange rate. The chemical structure of different NBD-cholesterol is shown in Figure 5.1. As can be seen in this figure, the fluorescent tag (Figure 5.1, red box) of 22NBDC and 25NBDC are inserted into the membrane bilayer. By contrast, the fluorescence tag of 3NBDC is attached to carbon 3 via a C6 spacer, at the hydrophilic end of cholesterol (Figure 5.1, red box), which is outside the membrane bilayer (110, 111, 112). This structure would thus be anticipated to more appropriately mirror the normal orientation of cholesterol in the membrane and recapitulated the interactions with other membrane components, such as phospholipids. Traditionally, radioisotope-labelled cholesterol is used as a cholesterol tracer for metabolic studies in cells and whole organisms, as well as to determine the exchange rate between cells and acceptors (242, 243). However, this method is not feasible in every lab and there are safety and regulatory issues with the use of radioactivity. In many fields, radioactive molecules have been replaced with fluorescent tracer molecules, which are easier to use and amenable to high throughput screening platforms. Although there are a number of fluorescent cholesterol analogs (labelled on the side chain) in current use, they suffer from different biophysical and technical limitations. Thus this study aims to explore the use of a recently described fluorescent analog, 3NBDC, as a biochemical tool to track cholesterol dynamics, with a particular interest in evaluating its use in studies on MPC.

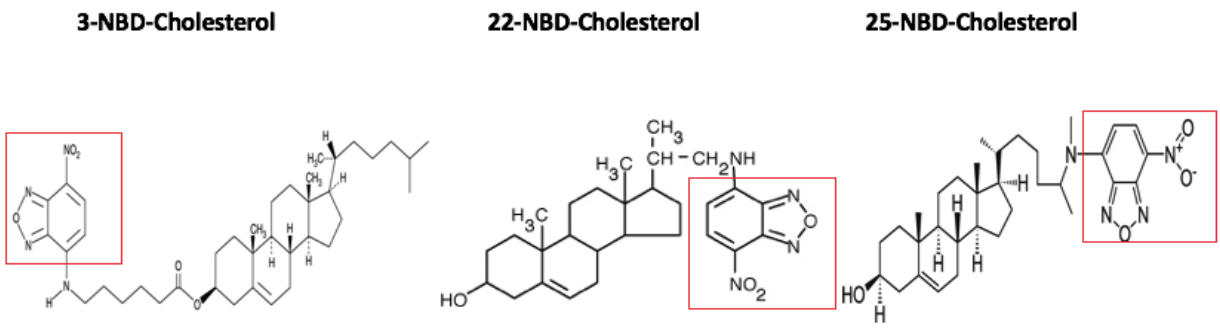

Figure 5.1 Chemical structure of 3-NBD-Cholesterol, 22-NBD-Cholesterol and 25-NBD-Cholesterol. The fluorescence tag NBD group is shown in the red box.

Table 5.1 Advantages and disadvantages of commonly used fluorescent cholesterol probes

Cholesterol probe	Advantages	Disadvantages
Fluorophore bound to bacterial toxins as perifringolysin O	Used to assess threshold concentrations of cholesterol in models & cell membranes. Partly useful for super-resolution microscopy.	Cannot track inter-organelle transport nor sterol diffusion, do not bind esters. Trafficking studies only infixed cells, unless genetically encoded.
Filipin	Reliable quantitative measure of cholesterol. Partition into lo phase in model membranes. Useful for assessing cholesterol content in tissue samples.	Cannot track inter-organelle transport or be used in living cells. Do not bind esters. Requires UV optics. Cross-reactivity to gangliosides.
Dehydroergosterol	Closest analogue to ergosterol followed by cholesterol; gets bound and transferred by sterol transfers proteins. Induces and partitions into lo phase in model membranes Can replace cholesterol or ergosterol in sterol-auxotroph organisms.	Low brightness, requires UV optics, bleached easily, limited substrate for acyl-coenzyme A acyl transferase 1 in mammalian cells.
Cholestatrienol	Closest analogue of cholesterol; gets bound and transferred by sterol transfers proteins. Partitions into lo phase in model membranes & orders phospholipids almost as good as cholesterol.	Low brightness, requires UV optics, bleached easily.
Parinaric acid cholesteryl esters	Does not alter sterol structure.	Cannot track cholesterol after hydrolysis. Requires UV optics.
Broadiaza-indacene cholesterol	High brightness and good photostability. Partitions into lo phase in model membranes. Ease of use in conventional fluorescence microscopy. Partly useful for dynamic super-resolution microscopy.	High affinity to lipid droplets, thereby partial miss-targeting in cells. No ordering of fatty acyl chains in model membranes. Usability in yeast is questionable. Not substrate for all known sterol transfers proteins.
Dansyl-cholesterol	High brightness, small molecule. Ease of use in conventional fluorescence microscopy.	Partitions into ld phase in model membranes. Prone to bleaching. Not substrate for all known sterol transfers proteins.
Pyrene-cholesterol	Forms excimers with potential use in membrane sterol aggregation.	No esterification. Requires UV optics. Partition preference and binding to sterol transfers proteins not known.
Dye-linked polyethylene glycol-cholesterol	Very photostable. Very useful for dynamic super-resolution microscopy.	No flip-flop & no non-vesicular transport. No metabolism.
Click chemistry substrates	Mimic cholesterol very well before click reaction, many possible analytical enhancers to optimize fluorescence. Useful for super-resolution microscopy.	Cannot be used in living cells. Behaviour of fluorescent analogue after click reaction is poorly characterized.
22/25-NBD-cholesterol	Easily absorbed from media. Ease of use in conventional fluorescence microscopy.	Prone to bleaching orientation in membranes opposite to cholesterol. Partitions into ld phase in model membranes. Not substrate for all known sterol transfers proteins.

5.2 Aims

- Confirm that 3NBDC replicates the biophysical behaviour of cholesterol using an intramembrane exchange model
- Characterise the uptake of 3NBDC in cell systems
- Evaluate the potential of 3NBDC to label and track MP uptake under *in vitro* conditions

5.3 Results

5.3.1 Cholesterol exchange between erythrocytes and autologous plasma

Previous research has established that radioisotope-labelled cholesterol may be used to study the rate of cholesterol exchange between donor erythrocytes and acceptor plasma (243, 244). To assess if 3NBDC could replace radioisotope cholesterol based methods, we carried out studies of the 3NBDC exchange rate between erythrocytes and autologous plasma under similar conditions to that used for radiolabelled cholesterol. This cell model was used to ensure that there was no possible metabolism of cholesterol in the experimental system and ensure that the results were based on the partition of cholesterol between the donor cellular membrane and the acceptor lipoprotein. Cholesterol efflux from labelled erythrocytes to plasma lipoproteins led to a time dependent and the equilibration of the label between the two different compartments (erythrocytes membrane and plasma lipoprotein), as assessed by the appearance of the fluorescent label (Figure 5.2). Similar to previous studies using radiolabelled cholesterol, an initial fast phase was followed by a plateau after 7 hours (245, 246). These data are consistent with the expected behaviour of radiolabelled cholesterol under similar conditions (247).

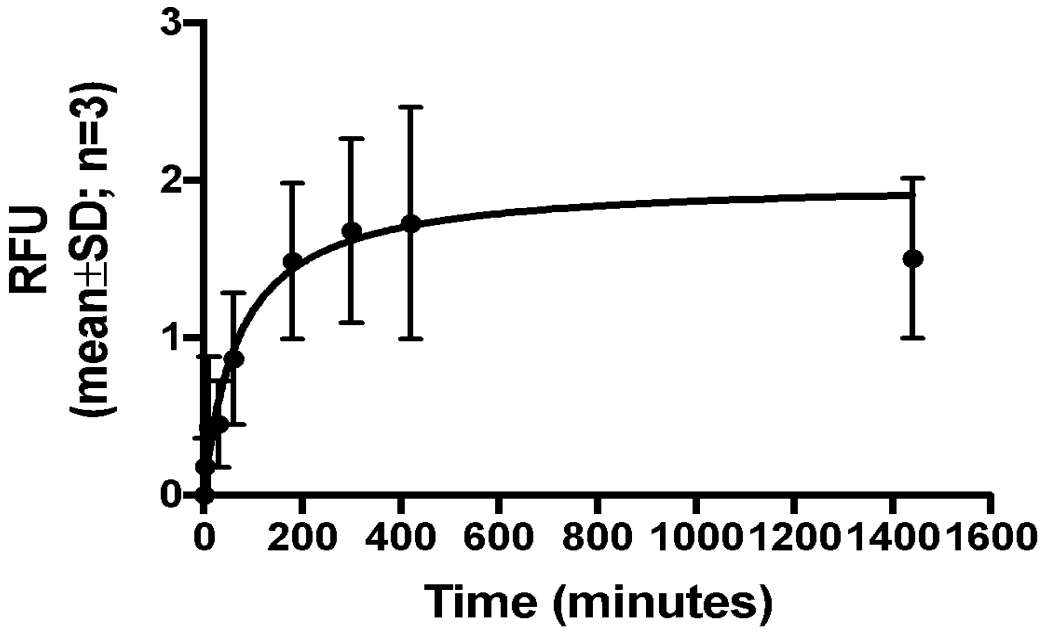

Figure 5.2 3-NBD-cholesterol exchange between erythrocytes and plasma. The exchange rate was measured by increasing the 3NBDC fluorescence intensity of unlabelled plasma. The rate of exchange increased dramatically in the first half an hour and reached a plateau at 7 hours. Data are expressed as mean ±SD. The data is based on three healthy donors and four independent experiments. This experiment has been carried out by multiple experimenters with similar results in every case.

5.3.2 Uptake of 3-NBD-Cholesterol using *in vitro* cell systems

To confirm 3NBDC uptake by different cell lines, HeLa cells were stained with 3NBDC (1µg/ml) for different durations. Confocal microscopy and flow cytometry were then used to characterise uptake by HeLa cells. The ability to use flow cytometry to track the uptake of 3NBDC is an advantage of this sensor. Data from flow cytometry revealed a time-dependent uptake by HeLa cells (Figure 5.3A). After 7 hours, almost 80% of HeLa cells were labelled to some extent by 3NBDC. Figure 5.3B shows a representative flow data of 3NBDC uptake in HeLa cells after five hours incubation. In parallel experiments, labelling of HeLa cells with 3NBDC was evaluated by live cell microscopy. Again, time-dependent cell labelling is evident, with initial scattered labelling (Figure 5.3D, E) followed by widespread labelling of cells after 18 hours of incubation (Figure 5.3F). Labelling of cells in this case is expected to proceed by at least two mechanisms - i) direct update of 3NBDC from the bulk media by HeLa cell membranes and ii) labelling of lipoproteins present in the medium followed by uptake of labelled lipoproteins by receptor mediated processes.

Similar time-dependent uptake results were obtained from THP-1 cells (results not shown). Taken together, results from live cell imaging and flow cytometry further support the contention that 3NBDC is a viable cholesterol tracer.

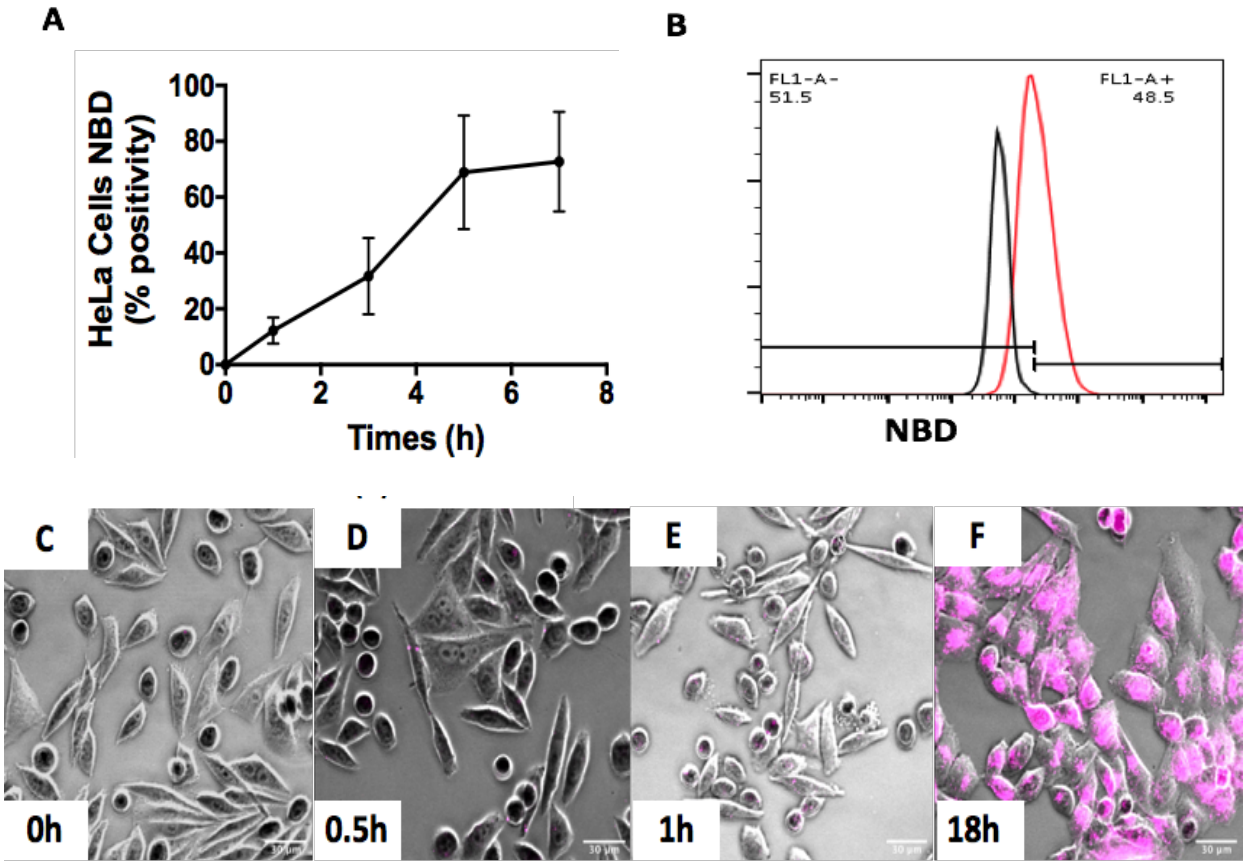

Figure 5.3 HeLa cell uptake of 3-NBD-Cholesterol. A) HeLa cells were incubated with 1µg /ml of 3-NBD-Cholesterol (3NBDC) for 1, 3, 5 and 7 hours and analysed by flow cytometry. Cell uptake of 3NBDC was time-dependent with around 80% of HeLa cells labelled with 3NBDC after 7 hours incubation. The data is based on three independent experiments and is expressed as mean ±SEM. B) A representative flow plot of 3NBDC stained HeLa cells after five hours incubation. C-F) 3NBDC stained HeLa cell (purple) live images were taken by confocal microscopy at different time points. Scale bar = 30µm.

Additional studies were carried out on PMA differentiated THP-1 cells and HMDMs. Live cell images were taken by confocal microscopy. Figure 5.4 shows that THP-1 derived macrophages were labelled by 3NBDC after one hour incubation (Figure 5.4B) while HMDMs were labelled following overnight incubation. It should be noted that studies on the metabolic transformation of 3NBDC by both THP1 cells and HMDMs have been carried out at time points up to 48 hours, and no significant metabolism of transformation of the 3NBDC has been observed. Taken together these results suggest that 3NBDC can readily label a variety of different cell types.

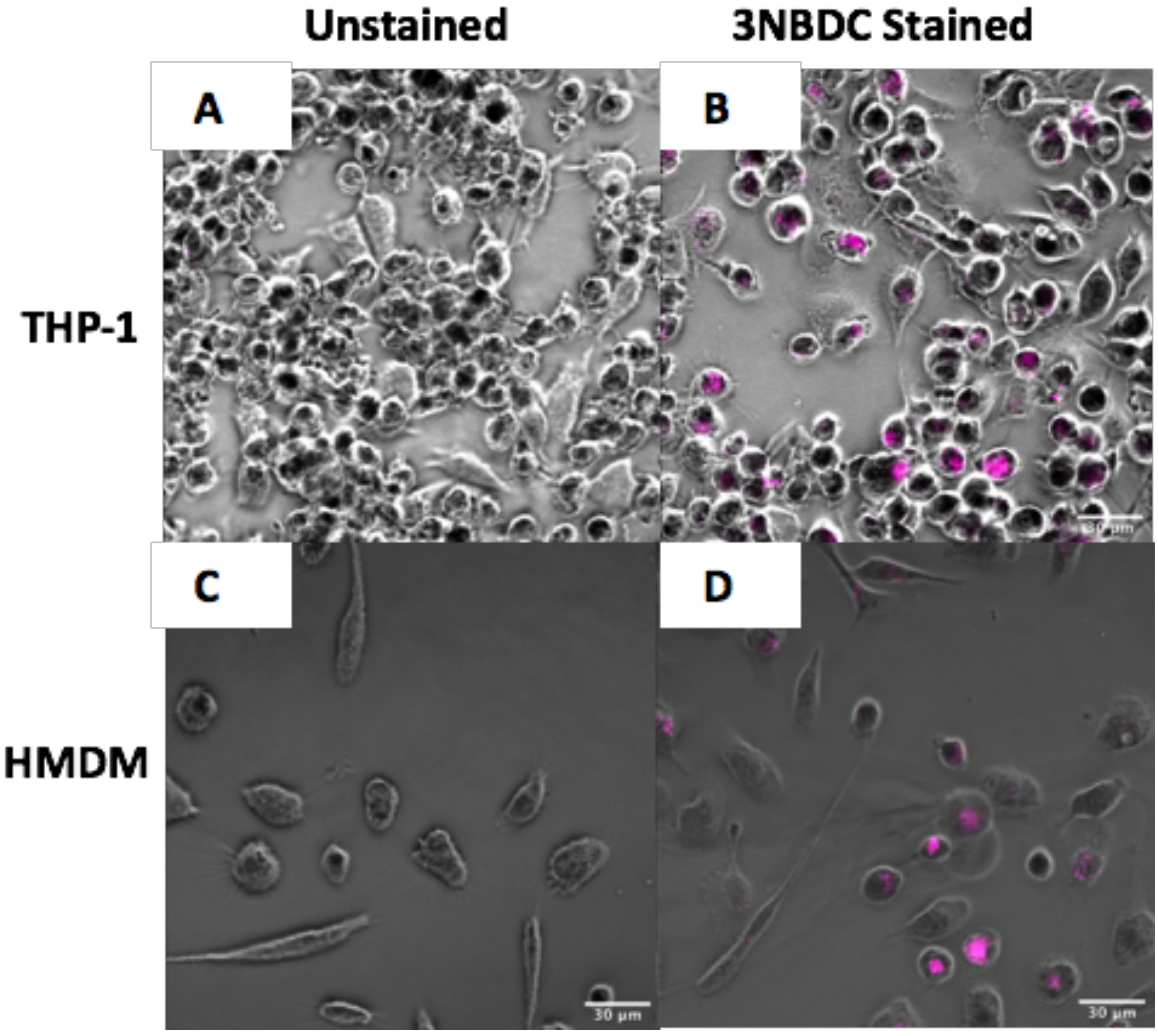

Figure 5.4 THP-1 cell derived macrophages and human primary monocyte derived macrophages uptake of 3-NBD-Cholesterol. A) THP-1 cell derived macrophages (THP-1) were labelled with 3-NBD-Cholesterol (3NBDC) and images were taken by confocal microscope (a is control, b is stained). n=3. B) Human primary monocyte derived macrophages (HMDMs) were labelled with 3NBDC and images were taken by confocal microscope (c is control, d is stained). n=1. Scale bar = 30 µm.

5.3.3 Treating THP-1 derived macrophages with labelled extracellular vesicles

To further explore the 3NBDC application, EVs were isolated from platelet concentrates and labelled with 3NBDC. EV surface markers were characterised by flow cytometry and, as expected, were derived from platelets (Figure 5.5A). Isolated EVs were labelled with 3NBDC for 48 hours and analysed by flow cytometry. Following washing of the cells, approximately 40% of EVs were labelled with 3NBDC (Figure 5.5B). Co-incubation of THP-1 cell derived macrophages and 3NBDC labelled EVs revealed a time-dependent increase in cellular fluorescence, with an observed plateau at approximately 16 hours (Figure 5.5C). As noted above, there are a number of mechanisms for the uptake of the 3NBDC labelled EVs - i) direct exchange between EVs membranes and cellular plasma membranes, ii) exchange between EVs and lipoproteins present in the medium followed by uptake of labelled lipoproteins by receptor mediated processes and iii) uptake of labelled EVs by phagocytosis. To estimate the magnitude of phagocytic versus other forms of uptake, parallel experiments with a non-phagocytic cell line (HEK-293T cells) were completed. Based on these experiments, HEK293T cell labelling was approximately 40% of that of the THP-1 cell derived macrophages, indicating that non-phagocytic processes account for about 40% of the labelling following incubation with 3NBDC labelled EVs. Taken together these results suggest that 3NBDC is a promising marker to label and track EVs in cell systems.

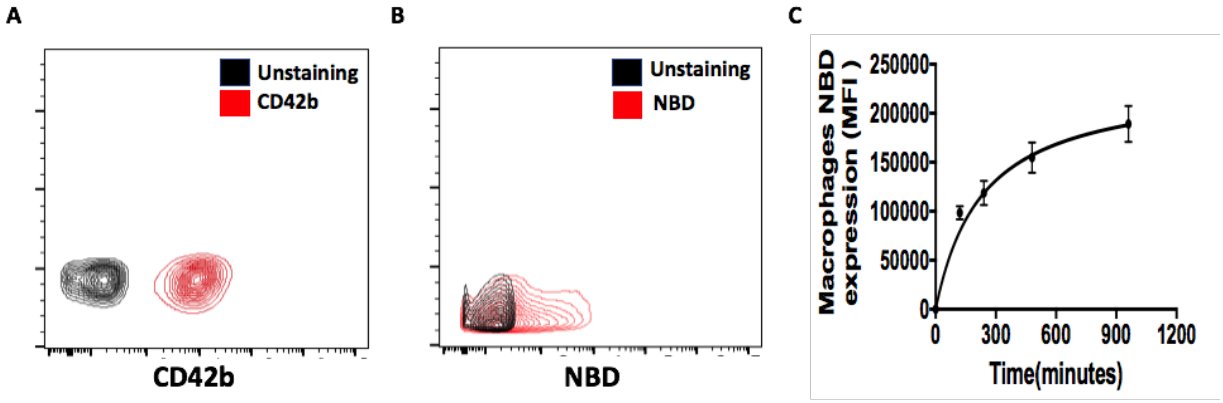

Figure 5.5 THP-1 derived macrophage uptake f 3-NBD-Cholesterol labelled extracellular vesicles. A) A representative flow plot showing CD42b^{+} EVs (100% positive) derived from platelet concentrate. B) A representative flow plot showing around 40% EVs express 3-NBD-Cholesterol (NBD) after 48 hours incubation. C) THP-1 derived macrophages uptake of 3-NBD-Cholesterol labelled EVs was time-dependent. The data is based on five independent experiments and is expressed as mean ±SEM.

5.4 Discussion

Fluorescent cholesterol analogs, can closely mimic the properties of natural cholesterol and permit detection by microscopic techniques, therefore, a series of cholesterol probes with NBD fluorescence analogs have been widely studied to investigate the intracellular distribution and membrane organisation of cholesterol (110). These fluorescence cholesterol analogs have also demonstrated their potential as replacements for traditional radioisotope-labelled cholesterol for investigating lipids trafficking such as cholesterol efflux (248). Cholesterol efflux plays a key step in reverse cholesterol transport to remove excess cholesterol from the cell membrane (248). Previous studies have investigated HDL-mediated cholesterol efflux by applying 22NBDC (249, 250). Other reports have also examined their ability to mimic the behaviour of natural cholesterol in the cell membrane by studying 22NBDC or 25NBDC (108, 109). However, there are no studies which have reported on the application of 3NBDC. Furthermore, reports have shown the half- time of transfer between liposomes or cells membranes by 22NBDC or 25NBDC is much faster than the half-time of transfer between liposomes or cell membranes for natural cholesterol (110, 111). It is worth nothing that the majority of biophysical studies have shown 22NBDC or 25NBDC as poor mimics of cholesterol in biological membranes (110). In this study, we tested the exchange time between the red cell membrane and plasma by 3NBDC labelling. The results have shown it takes around 7 hours to reach a plateau, which is consistent with the data obtained by radioisotope-labelled cholesterol methods (245, 246). In addition, different cell lines are easily labelled with 3NBDC and labelling may be readily observed by confocal microscopy and flow cytometry. In our studies, 3NBDC does not have the problem of photobleaching, which is a good advantage for dynamic measurements of cholesterol transport.

EVs are lipid bilayer-enclosed vesicles released by cells. Currently, one of the main obstacles in the field of EVs is to develop a strategy to label all EVs instead of a subpopulation of EVs. Furthermore, EV tracking plays an important role in understanding the molecular biology, as well as therapeutic potential of EVs. There are some organic fluorescent dyes used for EV labelling

such as PKH dyes, however, it has been reported that these days have an *in vivo* half life ranging from 5 to >100 days (251), which may mislead the *in vivo* distribution of EVs. Furthermore, aggregation and micelle formation of lipophilic dyes may yield false signal of EVs (251). Therefore, new fluorescent dyes need to be developed to enable accurate, long-term imaging of EVs. In the present study, our data shows that 3NBDC labelled EVs are readily taken up by both phagocytic and non-phagocytic models. Although, the precise mechanism of uptake of EVs is not clear, a literature review suggested that cells take up EVs by several endocytic pathways, such as phagocytosis, lipid raft-mediated internalisation, caveolin-mediated and micropinocytosis uptake (252, 253). Our data of EV uptake, although limited to two cell lines, indicate that phagocytic processes are responsible for at least 60% of the uptake of labelled EVs. Further investigation to compare different NBD fluorescent analogs with traditional radioisotope-labelled methods such as [^{3}H]-cholesterol may assist in determining the potential of 3NBDC as a cholesterol tracer.

In conclusion, the results of this study indicate that 3NBDC has the potential to be used as a cholesterol biosensor in multiple applications.

6.0 General Discussion and Future work

MPs are small vesicles released from the plasma membrane under normal physiological conditions. MPs contain active bio-lipids (such as cholesterol). Increased MPs levels and lipid abnormalities are observed among patients of autoimmune diseases (such as SLE and RA), however, no previous study has measured cholesterol levels derived from circulating MPs in healthy people and autoimmune diseases patients. To address this deficit, this thesis developed a method to measure MPC in circulating plasma. Furthermore, the reference value of MPC from a representative healthy population was established and we also demonstrated that MPC is a promising novel marker in autoimmune disorders. In addition, a novel cholesterol sensor (3NBDC) was studied in multiple applications.

We demonstrated that MPs, with a significantly reduced lipoprotein amount can be effectively purified from human PFS of platelet concentrates and human plasma by the combination of centrifugation and SEC methods. The centrifugation method enables the removal of platelets which avoids MP activation by platelets. SEC is the most widely used method for MP isolation. Compared to classical time-consuming differential centrifugation, there is also reduced risk of protein aggregation or huge lipoprotein co-isolation, which often hampers the study of biological functions of MPs. In addition, differential centrifugation often results in low recovery of MPs due to the high viscosity of plasma (59). Other methods including precipitation and density gradient ultracentrifugation possess different drawbacks as mentioned in the introduction chapter. Recently, microfluidic devices have been added to the list of methods used for EV isolation, however, this application is limited due to the low yield EVs often obtained (59).

The principle of SEC is separation based on a difference in size. The main advantage of SEC is that it can separate large and small molecules. As mentioned previously, the fact that cholesterol-carried lipoprotein size (HDL, LDL, IDL, VLDL) is around 5-80nm and MPs range in size from 100-1000nm enables MPs with reduced lipoprotein content to be isolated using SEC. Also, the SEC method only needs a small amount of plasma, which is feasible from a clinical

application point of view. The combination of centrifugation and SEC is therefore the most feasible method to study cholesterol contents of MPs.

Based on robust and reproducible method development, we established a reference value for MPC in a healthy representative population. Furthermore we demonstrated that MPC is a novel biomarker in autoimmune diseases. Several studies have reported MPs contain cholesterol (24, 29, 217), however, there is no study to date which has measured the level of MPC in circulating plasma. A number of studies report that MPs derived from platelet and endothelial cells hold diagnostic value in autoimmune disorders (166, 229, 230). Our results are consistent with previous studies, however, MPs derived from platelets or endothelial cells cannot classify different autoimmune disorders (such as SLE and RA) due to similar clinical symptoms. Instead, our results demonstrate that MPC is able to distinguish SLE from RA. One possible mechanism is that the serum cholesterol efflux capacity is impaired in autoimmune disorders which leads to cholesterol enrichment within the cell membrane, therefore, an increase in MPC is observed. A study has reported that microvesicles shed from the cell membrane can help cells to efflux cholesterol (218). Microvesicles were shown to be released from a monocyte cell line and primary human macrophages when cell membranes area enrich with cholesterol (254). The study has demonstrated overexpression of the cholesterol transporter ABCA1 contributes to cholesterol-rich EV release from human THP-1 macrophages, BHK and HepG2 cells (254). In our study, it is noticeable that MPC is not increased in SLE patients. The possible reason is related to disease status as most SLE patients were inactive which makes it challenging to find a difference from a diagnostic point of view. In addition, our preliminary data suggests that MPs, derived from SLE or RA patients, play an anti-inflammatory role by reducing TLR4 and TNFα expression. Although a number of studies have reported MPs derived from autoimmune diseases have pro-inflammatory effects, increasing evidence suggests they also contain anti-inflammatory properties (234, 235). Studies report the protective effects of MPs derived from leucocytes, which carry an endogenous anti-inflammatory protein (Annexin 1) and release the anti-inflammatory cytokine transforming growth factor β1,

which also inhibits TNFα (255). However, certain methodologic differences including MPs isolation methods and timing of cell stimulation may lead to different results.

In addition, we demonstrate 3NBDC is a versatile membrane cholesterol sensor. Cholesterol plays a key role in maintaining the biophysical properties of the cell membrane and the amount of membrane cholesterol is tightly controlled by lipid metabolism. Although, the intracellular transport of cholesterol is widely studied, the mechanisms regulating this transport are not fully understood. The NBD-group is linked to two main positions on the cholesterol backbone: 1). The NBD group is esterified to the hydroxyl group of cholesterol; 2). NBD group is covalently attached to the branched alkyl chain of cholesterol (241). Valid fluorescent analogs of cholesterol should closely mimic cholesterol. The chemical structure of 3NBDC allows the cholesterol to properly orient in the membrane bilayers, with the fluorescence tag outside the membrane. In addition, 3NBDC preferentially localises in the cell membrane, which has led to an application in monitoring membrane cholesterol. As is widely published, one of the main obstacles in the field of MPs is the development of a strategy to label all of the MPs instead of subpopulations of MPs. MPs released from the cell membrane contain cholesterol, which makes 3NBDC an attractive candidate to detect and track MPs.

In summary, this is the first report on the reference value of MPs cholesterol in healthy people, and investigation into the use of MPC as a novel biomarker to diagnose and classify SLE and RA. Furthermore, the work on 3NBDC applications lays the groundwork for future research on tracking both cell membrane cholesterol and EVs.

Study limitation and Future direction

A major limitation of this work was the number of patients and their disease status. The results should be considered only as preliminary because the number of patients was relatively small, therefore studies covering larger number of patients are needed to confirm these results. Regarding diseases status, only two SLE patients were active. This limited the assessment of the utility of

MPC to distinguish between SLE and healthy people. Another limitation was the cost of sepharose -CL2B. In our study, each sepharose column was used only for one donor to avoid cross-contamination and lipoprotein contamination, which added to the cost of testing each sample considerably. For the 3NBDC study, there are two main limitations. One is that only three cell models (Erythrocytes, THP-1 derived macrophages and HEK293T cells) were studied. In order to fully confirm these findings, more cell models need to be explored. Another limitation is that these 3NDBC data would need to be compared to the action of other NBD labelled fluorescence analogs in our hands, in order to make a truly informed comparison with 3NBDC.

Future work should focus on the validation of the diagnostic value of MPC in RA patients. The validation method would need to involve a larger group of RA patients from multiple sites. It would be interesting to include RA patients with cardiovascular diseases in order to establish if MPC may be a potential biomarker in this regard. In addition, MPC needs to be investigated as a potential biomarker in other autoimmune disorders (eg. pSS) and other non-autoimmune diseases (eg. cancer). A considerable amount of work is needed to unravel the precise mechanisms of action of MPs on inflammatory responses in autoimmune. Ultimately a RA mouse model is needed to explore the immunomodulatory effects of MPs *in vivo* and fully identify new therapeutic targets. It would be valuable to combine 3NBDC labelling and different cells marker staining to identify the amount of MPC in various cells types using flow cytometry. This could be useful in diagnosing diseases by comparing the amounts of MPC from different cells in different diseases, but this also needs to be confirmed in a larger population. Tracking MPC with 3NBDC will help to elucidate the mechanisms of MPs uptake and metabolism in various cell and animal models. Additionally, comparison studies need to be applied to compare the application of 3NBDC and other cholesterol sensors (like radioactive cholesterol) to track cell membrane cholesterol.

7.0 References

1. Chargaff E, West R. The biological significance of the thromboplastic protein of blood. J Biol Chem. 1946.
2. Wolf P. The nature and significance of platelet products in human plasma. Br J Haematol. 1967.
3. Xu X, Lai Y, Hua Z-C. Apoptosis and apoptotic body: disease message and therapeutic target potentials. Biosci Rep. 2019. doi:10.1042/bsr20180992
4. Raposo G, Stoorvogel W. Extracellular vesicles: Exosomes, microvesicles, and friends. J Cell Biol. 2013;200(4):373-383. doi:10.1083/jcb.201211138
5. Crescitelli R, Lässer C, Szabó TG, et al. Distinct RNA profiles in subpopulations of extracellular vesicles: Apoptotic bodies, microvesicles and exosomes. J Extracell Vesicles. 2013. doi:10.3402/jev.v2i0.20677
6. Burnouf T, Chou ML, Goubran H, Cognasse F, Garraud O, Seghatchian J. An overview of the role of microparticles/microvesicles in blood components: Are they clinically beneficial or harmful? Transfus Apher Sci. 2015 Oct; 53(2):137-45. doi:10.1016/j.transci.2015.10.010.
7. Rubin O, Canellini G, Delobel J, Lion N, Tissot JD. Red blood cell microparticles: clinical relevance. Transfus Med Hemother. 2012 Oct; 39(5): 342-7. doi:10.1159/000342228.
8. Stern JN, Duckett L, Fasler-Kan E, et al. Circulating microparticles: square the circle. BMC Cell Biol. 2013;14(1). doi:10.1186/1471-2121-14-23
9. Gustafson D, Veitch S, Fish JE. Extracellular Vesicles as Protagonists of Diabetic Cardiovascular Pathology. Front Cardiovasc Med. 2017 Nov 9;4:71. doi:10.3389/fcvm.2017.00071
10. Witwer KW, Buzás EI, Bemis LT, et al. Standardization of sample collection, isolation and analysis methods in extracellular vesicle research. J Extracell Vesicles. 2013. doi:10.3402/jev.v2i0.20360

11. McGinn CM, MacDonnell BF, Shan CX, Wallace R, Cummins PM, Murphy RP. Microparticles: A Pivotal Nexus in Vascular Homeostasis and Disease. Curr Clin Pharmacol. 2016;11(1): 28-42.

12. Kalra H, Drummen GPC, Mathivanan S. Focus on extracellular vesicles: Introducing the next small big thing. Int J Mol Sci. 2016. doi:10.3390/ijms17020170

13. Headland SE, Jones HR, D'Sa AS, Perretti M, Norling LV. Cutting-edge analysis of extracellular microparticles using ImageStream(X) imaging flowcytometr y. Sci Rep. 2014 Jun 10;4:5237.

14. Shet AS. Characterizing blood microparticles: technical aspects and challenges. Vasc Health Risk Manag. 2008;4 (4):769-74.

15. França CN, Izar MC, Amaral JB, Tegani DM, Fonseca FA. Microparticles as potential biomarkers of cardiovascular disease. Arq Bras Cardiol. 2015 Feb;104(2):169-74. doi:10.5935/abc.20140210.

16. Berckmans RJ, Nieuwland R, Kraan MC, et al. Synovial microparticles from arthritic patients modulate chemokine and cytokine release by synoviocytes. Arthritis Res Ther. 2005.

17. Fadeel B, Xue D. The ins and outs of phospholipid asymmetry in the plasma membrane: roles in health and disease. Crit Rev Biochem Mol Biol. 2009 Sep-Oct; 44(5): 264-77. doi:10.1080/10409230903193307.

18. Olivier Morel, Laurence Jesel, Jean-Marie Freyssinet, Florence Toti. Cellular Mechanisms Underlying the Formation of Circulating Microparticles. Arteriosclerosis, Thrombosis, and Vascular Biology. 2011;31:15-26. doi:10.1161/ATVBAHA.109.200956.

19. Latham SL, Tiberti N, Gokoolparsadh N, et al. Immuno-analysis of microparticles: Probing at the limits of detection. Sci Rep. 2015. doi:10.1038/srep16314

20. Waehrens LN, Heegaard CW, Gilbert GE, Rasmussen JT. Bovine lactadherin as a calcium-

independent imaging agent of phosphatidylserine expressed on the surface of apoptotic HeLa cells. *J Histochem Cytochem*. 2009. doi:10.1369/jhc.2009.953729

21. Connor DE1, Exner T, Ma DD, Joseph JE. The majority of circulating platelet-derived microparticles fail to bind annexin V, lack phospholipid-dependent procoagulant activity and demonstrate greater expression of glycoprotein Ib. Thromb Haemost. 2010 May;103 (5):1044-52. doi:10.1160/TH09-09-0644.
22. Perez-Pujol S, Marker PH, Key NS. Platelet microparticles are heterogeneous and highly dependent on the activation mechanism: studies using a new digital flow cytometer. Cytometry A. 2007 Jan;71(1):38-45
23. Mobarrez F, Vikerfors A, Gustafsson JT, et al. Microparticles in the blood of patients with systemic lupus erythematosus (SLE): Phenotypic characterization and clinical associations. Sci Rep. 2016;6(August):1-10. doi:10.1038/srep36025
24. Record M, Silvente-Poirot S, Poirot M, Wakelam MJO. Extracellular vesicles: lipids as key components of their biogenesis and functions. J Lipid Res. 2018;59(8):1316-1324. doi:10.1194/jlr.e086173
25. Palviainen M, Saari H, Kärkkäinen O, et al. Metabolic signature of extracellular vesicles depends on the cell culture conditions. J Extracell Vesicles. 2019. doi:10.1080/20013078.2019.1596669
26. Buratta S, Urbanelli L, Sagini K, et al. Extracellular vesicles released by fibroblasts undergoing H-Ras induced senescence show changes in lipid profile. PLoS One. 2017. doi:10.1371/journal.pone.0188840
27. Weerheim AM, Kolb AM, Sturk A, Nieuwland R. Phospholipid composition of cell-derived microparticles determined by one-dimensional high-performance thin-layer chromatography. Anal Biochem. 2002 Mar 15;302 (2):191-8.
28. Hu Q, Wang M, Cho MS, et al. Lipid profile of platelets and platelet-derived microparticles in ovarian cancer. BBA Clin. 2016 Jun 30;6:76-81. doi:10.1016/j.bbacli.2016.06.003.

29. Biró É, Akkerman JWN, Hoek FJ, et al. The phospholipid composition and cholesterol content of platelet-derived microparticles: A comparison with platelet membrane fractions. J Thromb Haemost. 2005. doi:10.1111/j.1538-7836.2005.01646.x

30. Brzozowski JS, Jankowski H, Bond DR, et al. Lipidomic profiling of extracellular vesicles derived from prostate and prostate cancer cell lines. Lipids Health Dis. 2018 Sep 8;17 (1):211. doi:10.1186/s12944-018-0854-x.

31. Skotland T, Sandvig K, Llorente A. Lipids in exosomes: Current knowledge and the way forward. Prog Lipid Res. 2017 Apr;66:30-41. doi:10.1016/j.plipres.2017.03.001.

32. Min-Dan Xu, Xian-Zheng Wu, Yun Zhou, Ying Xue, Ke-Qin Zhang. Proteomic characteristics of circulating microparticles in patients with newly-diagnosed type 2 diabetes. Cardiovasc Diabetol. 2016; 15: 49.

33. Watts JA, Lee YY, Gellar MA, Fulkerson MB, Hwang SI, Kline JA. Proteomics of microparticles after experimental pulmonary embolism. Thromb Res. 2012 Jul;130 (1):122-8. doi:10.1016/j.thromres.2011.09.016.

34. Michal Harel, Pazit Oren-Giladi, Orit Kaidar-Person,Yuval Shaked, Tamar Geiger. Proteomics of Microparticles with SILAC Quantification (PROMIS-Quan): A Novel Proteomic Method for Plasma Biomarker Quantification. Am J Transl Res. 2016; 8 (1): 209-220. doi:10.1074/mcp.M114.043364.

35. Kalra H, Simpson RJ, Ji H, et al. Vesiclepedia: A Compendium for Extracellular Vesicles with Continuous Community Annotation. PLoS Biol. 2012. doi:10.1371/journal.pbio.1001450

36. Orozco AF, Jorgez CJ, Horne C, et al. Membrane protected apoptotic trophoblast microparticles contain nucleic acids: Relevance to preeclampsia. Am J Pathol. 2008. doi:10.2353/ajpath.2008.080414

37. Reich CF, Pisetsky DS. The content of DNA and RNA in microparticles released by Jurkat and HL-60 cells undergoing in vitro apoptosis. Exp Cell Res. 2009. doi:10.1016/j.yexcr.2008.12.014

38. Diehl P, Fricke A, Sander L, et al. Microparticles: Major transport vehicles for distinct microRNAs in circulation. Cardiovasc Res. 2012. doi:10.1093/cvr/cvs007

39. Pisetsky DS. The origin and properties of extracellular DNA: From PAMP to DAMP. Clin Immunol. 2012. doi:10.1016/j.clim.2012.04.006

40. Boon RA, Vickers KC. Intercellular transport of MicroRNAs. Arterioscler Thromb Vasc Biol. 2013. doi:10.1161/ATVBAHA.112.300139

41. Alexandru N. Circulating microparticles and microRNAs as players in atherosclerosis. World J Hematol. 2013. doi:10.5315/wjh.v2.i2.16

42. Xia L, Zeng Z, Tang WH. The Role of Platelet Microparticle Associated microRNAs in Cellular Crosstalk. Front Cardiovasc Med. 2018. doi:10.3389/fcvm.2018.0002

43. Zhao L, Bi Y, Kou J, Shi J, Piao D. Phosphatidylserine exposing-platelets and microparticles promote procoagulant activity in colon cancer patients. J Exp Clin Cancer Res. 2016. doi:10.1186/s13046-016-0328-9

44. He Z, Zhang Y, Cao M, et al. Increased phosphatidylserine-exposing microparticles and their originating cells are associated with the coagulation process in patients with IgA nephropathy. Nephrol Dial Transplant. 2016. doi:10.1093/ndt/gfv403

45. van der Meijden PEJ, van Schilfgaarde M, van Oerle R, Renné T, ten Cate H, Spronk HMH. Platelet- and erythrocyte-derived microparticles trigger thrombin generation via factor XIIa. J Thromb Haemost. 2012. doi:10.1111/j.1538-7836.2012.04758.x

46. Aleman MM, Gardiner C, Harrison P, Wolberg AS. Differential contributions of monocyte- and platelet-derived microparticles towards thrombin generation and fibrin formation and stability. J Thromb Haemost. 2011. doi:10.1111/j.1538-7836.2011.04488.x

47. Mackman N. On the trail of microparticles. Circ Res. 2009 Apr 24;104 (8):925-7. doi:10.1161/CIRCRESAHA.109.196840.

48. Nielsen CT, Østergaard O, Rasmussen NS, Jacobsen S, Heegaard NHH. A review of studies of the proteomes of circulating microparticles: Key roles for galectin-3-binding protein-expressing microparticles in vascular diseases and systemic lupus erythematosus. Clin Proteomics. 2017. doi:10.1186/s12014-017-9146-0

49. Vykoukal J, Sun N, Aguilar-Bonavides C, et al. Plasma-derived extracellular vesicle proteins as a source of biomarkers for lung adenocarcinoma. Oncotarget. 2017. doi:10.18632/oncotarget.20748

50. Min-Dan Xu, Xian-Zheng Wu, Yun Zhou, Ying Xue, Ke-Qin Zhang. Proteomic characteristics of circulating microparticles in patients with newly-diagnosed type 2 diabetes. Cardiovasc Diabetol. 2016; 15: 49.

51. Watts JA, Lee YY, Gellar MA, Fulkerson MB, Hwang SI, Kline JA. Proteomics of microparticles after experimental pulmonary embolism. Thromb Res. 2012 Jul;130 (1):122-8. doi:10.1016/j.thromres.2011.09.016.

52. Felix Jansen, Han Wang, David Przybilla, et al. Vascular endothelial microparticles-incorporated microRNAs are altered in patients with diabetes mellitus. Cardiovasc Diabetol. 2016 Mar 22;15:49. doi:10.1186/s12933-016-0367-8.

53. Jansen F1, Yang X, Hoelscher M, et al. Endothelial microparticle-mediated transfer of MicroRNA-126 promotes vascular endothelial cell repair via SPRED1 and is abrogated in glucose-damaged endothelial microparticles. Circulation. 2013 Oct 29;128(18):2026-38. doi: 10.1161/CIRCULATIONAHA.113.001720.

54. Patz S1, Trattnig C, Grünbacher G, et al. More than cell dust: microparticles isolated from cerebrospinal fluid of brain injured patients are messengers carrying mRNAs, miRNAs, and proteins. J Neurotrauma. 2013 Jul 15;30 (14):1232-42. doi:10.1089/neu.2012.2596.

55. Charles F. Reich III. The content of DNA and RNA in microparticles released by Jurkat and HL-60 cells undergoing in vitro apoptosis. J Neurotrauma. 2013 Jul 15;30 (14):1232-42. doi:10.1016/j.yexcr.2008.12.014.

56. Théry C, Amigorena S, Raposo G, Clayton A. Isolation and characterization of exosomes from cell culture supernatants and biological fluids. Curr Protoc Cell Biol. 2006 Apr; Chapter 3:Unit 3.22. doi: 10.1002/0471143030.cb0322s30.

57. Gámez-Valero A, Monguió-Tortajada M, Carreras-Planella L, Franquesa M, Beyer K, Borràs FE. Size-Exclusion Chromatography-based isolation minimally alters Extracellular Vesicles' characteristics compared to precipitating agents. Sci Rep. 2016. doi:10.1038/srep33641

58. Szatanek R, Baran J, Siedlar M, Baj-Krzyworzeka M. Isolation of extracellular vesicles: Determining the correct approach (review). Int J Mol Med. 2015. doi:10.3892/ijmm.2015.2194

59. Konoshenko MY, Lekchnov EA, Vlassov AV, Laktionov PP. Isolation of Extracellular Vesicles: General Methodologies and Latest Trends. Biomed Res Int. 2018 Jan 30; 2018:8545347. Doi:10.1155/2018/8545347.

60. Mateescu B, Kowal EJK, van Balkom BWM, et al. Obstacles and opportunities in the functional analysis of extracellular vesicle RNA - An ISEV position paper. J Extracell Vesicles. 2017. doi:10.1080/20013078.2017.1286095

61. Dinkla S, Brock R, Joosten I, Bosman GJ. Gateway to understanding microparticles: standardized isolation and identification of plasma membrane-derived vesicles. Nanomedicine (Lond). 2013 Oct; 8(10):1657-68. doi:10.2217/nnm.13.149.

62. Yuana Y, Levels J, Grootemaat A, Sturk A, Nieuwland R. Co-isolation of extracellular vesicles and high density lipoproteins using density gradient ultracentrifugation. J Extracell Vesicles. 2014 Jul 8;3. doi:10.3402/jev.v3.23262.

63. Böing AN, van der Pol E, Grootemaat AE, Coumans FA, Sturk A, Nieuwland R. Single-step isolation of extracellular vesicles by size-exclusion chromatography. J Extracell Vesicles. 2014 Sep 8;3. doi:10.3402/jev.v3.23430.

64. Xavier Gallart-Palau, Aida Serra,Siu Kwan Sze. Enrichment of extracellular vesicles from tissues of the central nervous system by PROSPR. Mol Neurodegener. 2016 May 23;11(1):41. doi:10.1186/s13024-016-0108-1.

65. The Free Dictionary by Farlex. Cholesterol. https://encyclopedia2.thefreedictionary.com/cholesterol.

66. Harvard Health Publishing. How it's made: Cholesterol production in your body. https://www.health.harvard.edu/heart-health/how-its-made-cholesterol-production-in-your-body. Accessed February 2017.

67. Wikipedia. Cholesterol. https://en.wikipedia.org/wiki/Cholesterol. Accessed July 16, 2019.

68. Berg JM, Tymoczko JL, Stryer L. Biochemistry.5th edition. New York: WH Freeman. 2002

69. Martini C, Pallottini V. Cholesterol: From feeding to gene regulation. Genes Nutr. 2007;2(2):181-193. doi:10.1007/s12263-007-0049-y

70. Walker HK, Hall WD, Hurst JW. Clinical Methods: The History, Physical, and Laboratory Examinations. 3rd edition. Boston: Butterworths; 1990

71. Mayo Clinic. Cholesterol test. https://www.mayoclinic.org/tests-procedures/cholesterol-test/about/pac-20384601

72. Shapiro MD, Fazio S. Apolipoprotein B-containing lipoproteins and atherosclerotic cardiovascular disease. F1000Research. 2017;6(0):134. doi:10.12688/f1000research.9845.1

73. Pourmousa M, Song HD, He Y, Heinecke JW, Segrest JP, Pastor RW. Tertiary structure of apolipoprotein A-I in nascent high-density lipoproteins. Proc Natl Acad Sci. 2018. doi:10.1073/pnas.1721181115

74. Meeusen JW. Comparing Measures of HDL: On the Right Path with the Wrong Map. Clin Chem. 2018. doi:10.1373/clinchem.2017.284208

75. Frank PG, Marcel YL. Apolipoprotein A-I : structure – function relationships. J Lipid Res. 2000 Jun;41(6):853-72

76. Young SG. Recent progress in understanding apolipoprotein B. Circulation. 1990. doi:10.1161/01.CIR.82.5.1574

77. Tudorache IF, Trusca VG, Gafencu AV. Apolipoprotein E - A Multifunctional Protein with Implications in Various Pathologies as a Result of Its Structural Features. Comput Struct Biotechnol J. 2017. doi:10.1016/j.csbj.2017.05.003

78. Medical dictionary: Lipoprotein. https://medicine.academic.ru/4788/. Accessed 2011

79. Axel F. Sigurdsson. VLDL-The Role of Triglyceride-Rich Lipoproteins and Remnant Cholesterol. https://www.docsopinion.com/2017/01/30/vldl-triglyceride-remnant-cholesterol/. Accessed January 30, 2017

80. Goluszko P, Nowicki B. Membrane Cholesterol: a Crucial Molecule Affecting Interactions of Microbial Pathogens with Mammalian Cells. Infect Immun. 2005. doi:10.1128/iai.73.12.7791-7796.2005

81. Marquer C, Laine J, Dauphinot L, et al. Increasing membrane cholesterol of neurons in culture recapitulates Alzheimer's disease early phenotypes. Mol Neurodegener. 2014 Dec 18;9:60. doi:10.1186/1750-1326-9-60.

82. Maxfield FR, Tabas I Role of cholesterol and lipid organization in disease. Nature. 2005 Dec 1;438(7068):612-21

83. Arispe N, Doh M Plasma membrane cholesterol controls the cytotoxicity of Alzheimer's disease AbetaP (1-40) and (1-42) peptides. FASEB J. 2002 Oct;16 (12):1526-36.

84. Wikipedia: Cell membrane. https://en.wikipedia.org/wiki/Cell_membrane. Accessed July 19, 2019

85. Vikram Jairam, Koji Uchida, Vasanthy Narayanaswami. Lipoproteins - Role in Health and Diseases. Chapters published October 03, 2012 under CC BY 3.0 license.

86. Hafiane A, Genest J High density lipoproteins: Measurement techniques and potential biomarkers of cardiovascular risk. BBA Clin. 2015 Jan 31;3:175-88. doi:10.1016/j.bbacli.2015.01.005.

87. Boekholdt SM, Arsenault BJ, Mora S, et al. Association of LDL cholesterol, non-HDL cholesterol, and apolipoprotein B levels with risk ofcardiovascular events among patients treated with statins: a meta-analysis. JAMA. 2012 Mar 28;307(12):1302-9. doi:10.1001/jama.2012.366.

88. Varbo A, Freiberg JJ, Nordestgaard BG. Extreme non-fasting remanant cholesterol vs extreme LDL cholesterol as contributors to cardiovascular disease and all-cause mortality in 90000 individuals from the general population. Clin Chem. 2015 Mar;61(3):533-43. doi:10.1373/clinchem.2014.234146.

89. Podrez EA. Anti-oxidant properties of high-density lipoprotein and atherosclerosis. Clin Exp Pharmacol Physiol. 2010. doi:10.1111/j.1440-1681.2010.05380.x

90. Toft-Petersen AP, Tilsted HH, Aarøe J, et al. Small dense LDL particles--a predictor of coronary artery disease evaluated by invasive and CT-based techniques: a case-control study. Lipids Health Dis. 2011 Jan 25;10:21. doi:10.1186/1476-511X-10-21.

91. Moore KJ, Sheedy FJ, Fisher EA. Macrophages in atherosclerosis: a dynamic balance. Nat Rev Immunol. 2013 Oct;13(10):709-21. doi:10.1038/nri3520.

92. Zhang Y, Mu Q, Zhou Z, et al. Protective Effect of Irisin on Atherosclerosis via Suppressing Oxidized Low Density Lipoprotein Induced Vascular Inflammation and Endothelial Dysfunction. PLoS One. 2016 Jun 29;11(6) doi:10.1371/journal.pone.0158038

93. Besler C, Lüscher TF, Landmesser U. Molecular mechanisms of vascular effects of High-density lipoprotein: alterations in cardiovascular disease. EMBO Mol Med. 2012 Apr;4(4):251-68. doi:10.1002/emmm.201200224.

94. Yvan-Charvet L, Welch C, Pagler TA, et al. Increased inflammatory gene expression in ABC transporter-deficient macrophages: Free cholesterol accumulation, increased signaling via toll-like receptors, and neutrophil infiltration of atherosclerotic lesions. Circulation. 2008.

95. Nicholls SJ, Tuzcu EM, Sipahi I, et al. Statins, high-density lipoprotein cholesterol, and regression of coronary atherosclerosis. JAMA. 2007 Feb 7;297(5):499-508.

96. Tall AR, Rader DJ. Trials and Tribulations of CETP Inhibitors. Circ Res. 2018. doi:10.1161/CIRCRESAHA.117.311978

97. Xu S, Liu Z, Liu P. HDL cholesterol in cardiovascular diseases: the good, the bad, and the ugly? Int J Cardiol. 2013 Oct 9;168(4):3157-9. doi:10.1016/j.ijcard.2013.07.210.

98. Ahn N, Kim K. High-density lipoprotein cholesterol (HDL-C) in cardiovascular disease: effect of exercise training. Integr Med Res. 2016. doi:10.1016/j.imr.2016.07.001

99. Kon V, Yang H, Fazio S. Residual Cardiovascular Risk in Chronic Kidney Disease: Role of High-density Lipoprotein. Arch Med Res. 2015. doi:10.1016/j.arcmed.2015.05.009

100. Pan B, Yu B, Ren H, et al. High-density lipoprotein nitration and chlorination catalyzed by myeloperoxidase impair its effect of promoting endothelial repair. Free Radic Biol Med. 2013 Jul;60:272-81. doi:10.1016/j.freeradbiomed.2013.02.004.

101. Bae JM, Yang YJ, Li ZM, Ahn YO. Low cholesterol is associated with mortality from cardiovascular diseases: a dynamic cohort study in Korean adults. J Korean Med Sci. 2012 Jan; 27 (1):58-63. doi:10.3346/jkms.2012.27.1.58.

102. Yi SW, Yi JJ, Ohrr H. Total cholesterol and all-cause mortality by sex and age: a prospective cohort study among 12.8 million adults. Sci Rep. 2019. doi:10.1038/s41598-018-38461-y

103. Zhong Y, Tang H, Zeng Q, et al. Total cholesterol content of erythrocyte membranes is associated with the severity of coronary artery disease and the therapeutic effect of rosuvastatin. Ups J Med Sci. 2012 Nov;117(4):390-8. doi:10.3109/03009734.2012.672345.

104. de la Llera Moya M, McGillicuddy FC, Hinkle CC, et al. Inflammation modulates human

HDL composition and function in vivo. Atherosclerosis. 2012. doi:10.1016/j.atherosclerosis.2012.02.032

105. Escolà-Gil JC, Llaverias G, Julve J, Jauhiainen M, Méndez-González J, Blanco-Vaca F. The cholesterol content of western diets plays a major role in the paradoxical increase in high-density lipoprotein cholesterol and upregulates the macrophage reverse cholesterol transport pathway. Arterioscler Thromb Vasc Biol. 2011. doi:10.1161/ATVBAHA.111.236075
106. Maxfield FR, Wüstner D. Analysis of cholesterol trafficking with fluorescent probes. Methods Cell Biol. 2012. doi:10.1016/B978-0-12-386487-1.00017-1
107. Sezgin E, Can FB, Schneider F, et al. A comparative study on fluorescent cholesterol analogs as versatile cellular reporters. J Lipid Res. 2016 Feb;57(2):299-309. doi:10.1194/jlr.M065326.
108. Faletrov YV, Bialevich KI, Edimecheva IP, et al. 22-NBD-cholesterol as a novel fluorescent substrate for cholesterol-converting oxidoreductases. J Steroid Biochem Mol Biol. 2013 Mar;134:59-66. doi:10.1016/j.jsbmb.2012.09.035.
109. Ostašov P, Sýkora J, Brejchová J, Olżyńska A, Hof M, Svoboda P. FLIM studies of 22- and 25-NBD-cholesterol in living HEK293 cells: plasma membrane change induced by cholesterol depletion. Chem Phys Lipids. 2013 Feb-Mar;167-168:62-9. doi:10.1016/j.chemphyslip.2013.02.006
110. Solanko KA, Modzel M, Solanko LM, Wüstner D. Fluorescent sterols and cholesteryl esters as probes for intracellular cholesterol transport. Lipid Insights. 2015. doi:10.4137/Lpi.s31617
111. Ishii H, Shimanouchi T, Umakoshi H, Walde P, Kuboi R. Analysis of the 22-NBD-cholesterol transfer between liposome membranes and its relation to the intermembrane exchange of 25-hydroxycholesterol. Colloids Surf B Biointerfaces. 2010 May 1;77(1):117-21. doi:10.1016/j.colsurfb.2010.01.002.

112. Cayman Chemical. 3-hexanoyl-NBD Cholesterol. https://www.caymanchem.com/product/13221

113. Chaplin DD. Overview of the immune response. J Allergy Clin Immunol. 2010. doi:10.1016/j.jaci.2009.12.980

114. Shanker A, Thounaojam MC, Mishra MK, Dikov MM. Innate-adaptive immune crosstalk 2016. J Immunol Res. 2017;2017. doi:10.1155/2017/3503207

115. Cheroutre H, Huang Y. Crosstalk between adaptive and innate immune cells leads to high quality immune protection at the mucosal borders. In: Advances in Experimental Medicine and Biology. ; 2013. doi:10.1007/978-1-4614-6217-0_5

116. Ito T, Connett JM, Kunkel SL, Matsukawa A. The linkage of innate and adaptive immune response during granulomatous development. Front Immunol. 2013. doi:10.3389/fimmu.2013.00010

117. Janeway CA. How the Immune System Recognizes Invaders. Sci Am. 2009. doi:10.1038/scientificamerican0993-72

118. Mogensen TH. Pathogen recognition and inflammatory signaling in innate immune defenses. Clin Microbiol Rev. 2009. doi:10.1128/CMR.00046-08

119. Kumar H, Kawai T, Akira S. Pathogen recognition by the innate immune system. Int Rev Immunol. 2011. doi:10.3109/08830185.2010.529976

120. Carrillo JLM, Rodríguez FPC, Coronado OG, García MAM, Cordero JFC. Physiology and Pathology of Innate Immune Response Against Pathogens. In: Physiology and Pathology of Immunology. ; 2017. doi:10.5772/intechopen.70556

121. Liaskou E, Wilson D V., Oo YH. Innate immune cells in liver inflammation. Mediators Inflamm. 2012. doi:10.1155/2012/949157

122. Boltjes A, van Wijk F. Human dendritic cell functional specialization in steady-state and inflammation. *Front Immunol*. 2014. doi:10.3389/fimmu.2014.00131

123. Hirayama D, Iida T, Nakase H. The phagocytic function of macrophage-enforcing innate

immunity and tissue homeostasis. Int J Mol Sci. 2018. doi:10.3390/ijms19010092

124. Olière S, Hernandez E, Lézin A, et al. HTLV-1 evades type I interferon antiviral signaling by inducing the suppressor of cytokine signaling 1 (SOCS1). PLoS Pathog. 2010. doi:10.1371/journal.ppat.1001177

125. Shepardson KM, Schwarz B, Larson K, et al. Induction of antiviral immune response through recognition of the repeating subunit pattern of viral capsids is toll-like receptor 2 dependent. MBio. 2017. doi:10.1128/mBio.01356-17

126. Brandstadter JD, Yang Y. Natural killer cell responses to viral infection. J Innate Immun. 2011. doi:10.1159/000324176

127. Getts DR, Chastain EML, Terry RL, Miller SD. Virus infection, antiviral immunity, and autoimmunity. Immunol Rev. 2013. doi:10.1111/imr.12091

128. Pasare C, Medzhitov R. Toll-like receptors: Linking innate and adaptive immunity. In: Advances in Experimental Medicine and Biology. ; 2005z

129. Wikipedia. Toll-like receptor. https://en.wikipedia.org/wiki/Toll-like_receptor. Accessed September 26, 2019

130. Toll-like Receptors in inflammation: Host Defense Webinar Series Part 2. frohttps://www.slideshare.net/QIAGENscience/the-crosstalk-between-cancer-inflammation-and-immunity-host-defense-webinar-series-part-4 . Accessed 2016, Apr 28.

131. Chen L, Deng H, Cui H, et al. Inflammatory responses and inflammation-associated diseases in organs. Oncotarget. 2018. doi:10.18632/oncotarget.23208

132. Duffy L, O'Reilly SC. Toll-like receptors in the pathogenesis of autoimmune diseases: recent and emerging translational developments. Immunotargets Ther. 2016 Aug 22;5:69-80. doi:10.2147/ITT.S89795.

133. Chester Brown. The Human Toll-like Receptor Family. https://www.pinterest.ie/pin/509188301592362903/?lp=true

134. Jang JH, Shin HW, Lee JM, Lee HW, Kim EC, Park SH. An Overview of Pathogen Recognition Receptors for Innate Immunity in Dental Pulp. Mediators Inflamm. 2015. doi:10.1155/2015/794143

135. Tang D, Kang R, Coyne CB, Zeh HJ, Lotze MT. PAMPs and DAMPs: Signal 0s that spur autophagy and immunity. Immunol Rev. 2012. doi:10.1111/j.1600-065X.2012.01146.x

136. Barton GM, Medzhitov R. Toll-like receptor signaling pathways. Science (80-). 2003. doi:10.1126/science.1085536

137. Takeda K, Akira S. Toll-like receptors in innate immunity. Int Immunol. 2005 Jan;17(1):1-14.

138. Wang L, Wang FS, Gershwin ME. Human autoimmune diseases: A comprehensive update. J Intern Med. 2015. doi:10.1111/joim.12395

139. Bierc J, Borzym K, Waszkiel D, Daniszewska I, Zalewska A. [Pathogenesis of Sjögren's syndrome]. Wiad Lek. 2014;67(4):520-7

140. Kyttaris VC. Systemic lupus erythematosus: From genes to organ damage. Methods Mol Biol. 2010. doi:10.1007/978-1-60761-800-3_13

141. Moulton VR, Suarez-Fueyo A, Meidan E, Li H, Mizui M, Tsokos GC. Pathogenesis of Human Systemic Lupus Erythematosus: A Cellular Perspective. Trends Mol Med. 2017 Jul;23(7):615-635. doi:10.1016/j.molmed.2017.05.006.

142. Pathak S, Mohan C Cellular and molecular pathogenesis of systemic lupus erythematosus: lessons from animal models. Arthritis Res Ther. 2011;13(5):241. doi:10.1186/ar3465.

143. Wei Y. The pathogenesis of systemic lupus erythematosus - An update. In: Dermatology Research Advances. ; 2014.

144. Petri M, Orbai AM, Alarcón GS et al. Derivation and validation of the Systemic Lupus International Collaborating Clinics classification criteria for systemic lupus erythematosus. Arthritis Rheum. 2012 Aug;64(8):2677-86.doi: 10.1002/art.34473.

145. Perhimpunan Peneliti Hati Indonesia, Penyakit P, Kronik G, et al. Curr Cardiol Rep. 2014;42(1):1-38. doi:10.1097/00008483-200207000-00004

146. Aletaha D, Smolen JS. Diagnosis and Management of Rheumatoid Arthritis: A Review. JAMA - J Am Med Assoc. 2018. doi:10.1001/jama.2018.13103

147. Bullock J, Rizvi SAA, Saleh AM, et al. Rheumatoid arthritis: A brief overview of the treatment. Med Princ Pract. 2019. doi:10.1159/000493390

148. Guo Q, Wang Y, Xu D, Nossent J, Pavlos NJ, Xu J. Rheumatoid arthritis: Pathological mechanisms and modern pharmacologic therapies. Bone Res. 2018. doi:10.1038/s41413-018-0016-9

149. Gibofsky A. Epidemiology, pathophysiology, and diagnosis of rheumatoid arthritis: A synopsis. Am J Manag Care. 2014

150. Mateen S, Zafar A, Moin S, Khan AQ, Zubair S. Understanding the role of cytokines in the pathogenesis of rheumatoid arthritis. Clin Chim Acta. 2016 Apr 1;455:161-71. doi:10.1016/j.cca.2016.02.010

151. Wasserman M, Amy M. Diagnosis and Management of Rheumatoid Arthritis. Am Fam Physician. 2011;84(11):1245-1252. doi:10.1109/EMEIT.2011.6023444

152. Moudgil KD, Choubey D. Cytokines in autoimmunity: Role in induction, regulation, and treatment. J Interf Cytokine Res. 2011. doi:10.1089/jir.2011.0065

153. Chatzantoni K, Mouzaki A. Anti-TNF-alpha antibody therapies in autoimmune diseases. Curr Top Med Chem. 2006;6 (16):1707-14

154. Glass CK, Olefsky JM. Inflammation and lipid signaling in the etiology of insulin resistance. Cell Metab. 2012. doi:10.1016/j.cmet.2012.04.001

155. Parameswaran N, Patial S. Tumor necrosis factor-a signaling in macrophages. Crit Rev Eukaryot Gene Expr. 2010. doi:10.1615/CritRevEukarGeneExpr.v20.i2.10

156. Martelli L, Olivera P, Roblin X, Attar A, Peyrin-Biroulet L. Cost-effectiveness of drug monitoring of anti-TNF therapy in inflammatory bowel disease and rheumatoid arthritis: a systematic review. J Gastroenterol. 2017. doi:10.1007/s00535-016-1266-1

157. Taylor PC, Peters AM, Paleolog E, et al. Reduction of chemokine levels and leukocyte traffic to joints by tumor necrosis factor alpha blockade in patients with rheumatoid arthritis. Arthritis Rheum. 2000 Jan;43(1):38-47.

158. Zhu LJ, Yang X, Yu XQ. Anti-TNF-alpha therapies in systemic lupus erythematosus. J Biomed Biotechnol. 2010;2010:465898. doi:10.1155/2010/465898.

159. Alexy T, Rooney K, Weber M, Gray WD, Searles CD. TNF-α alters the release and transfer of microparticle-encapsulated miRNAs from endothelial cells. Physiol Genomics. 2014 Nov 15;46(22):833-40. doi: 10.1152/physiolgenomics.00079.2014.

160. Boudreau LH, Duchez AC, Cloutier N, et al. Platelets release mitochondria serving as substrate for bactericidal group IIA-secreted phospholipase A2 to promote inflammation. Blood. 2014 Oct 2;124(14):2173-83. doi:10.1182/blood-2014-05-573543.

161. Suades R, Padró T, Badimon L. The Role of Blood-Borne Microparticles in Inflammation and Hemostasis. Semin Thromb Hemost. 2015 Sep;41(6):590-606. doi:10.1055/s-0035-1556591.

162. McGregor L, Martin J, McGregor JL. Platelet-leukocyte aggregates and derived microparticles in inflammation, vascular remodelling and thrombosis. Front Biosci. 2006 Jan 1;11:830-7.

163. Angelillo-Scherrer A. Leukocyte-derived microparticles in vascular homeostasis. Circ Res. 2012 Jan 20;110(2):356-69. doi:10.1161/CIRCRESAHA.110.233403

164. Ciurtin C, Ostas A, Cojocaru VM, Walsh SB, Isenberg DA. Advances in the treatment of ocular dryness associated with Sjögren′s syndrome Semin Arthritis Rheum. 2015 Jun 18. doi:10.1016/j.semarthrit.2015.06.007.

165. Zhou J, Jin JO, Patel ES, Yu Q. Interleukin 6 inhibits apoptosis of exocrine gland tissues under inflammatory conditions. Cytokine. 2015 Dec;76(2):244-52. doi:10.1016/j.cyto.2015.07.027.

166. Sellam J, Proulle V, Jüngel A, et al. Increase levels of circulating microparticles in primary Sjögren's syndrome, systemic lupus erythematosus and rheumatoid arthritis and relation with disease activity. Arthritis Res Ther. 2009;11(5):R156. doi: 10.1186/ar2833.

167. Bartoloni E, Alunno A, Bistoni O, Caterbi S, Luccioli F et al. Characterization of circulating endothelial microparticles and endothelial progenitor cells in primary Sjögren's syndrome: new markers of chronic endothelial damage? Rheumatology (Oxford). 2015 Mar;54(3):536-44. doi: 10.1093/rheumatology/keu320.

168. Shahwan KT, Kimball AB. Psoriasis and Cardiovascular Disease. Med Clin North Am. 2015. doi:10.1016/j.mcna.2015.08.001

169. Tamagawa-Mineoka R, Katoh N, Kishimoto S. Platelet activation in patients with psoriasis: increased plasma levels of platelet-derived microparticles and soluble P-selectin. J Am Acad Dermatol. 2010 Apr;62(4):621-6. doi: 10.1016/j.jaad.2009.06.053.

170. Martínez-Sales V, Vila V, Ricart JM, et al. Increased circulating endothelial cells and microparticles in patients with psoriasis. Clin Hemorheol Microcirc. 2015. doi:10.3233/CH-131766.

171. Takeshita J, Mohler ER, Krishnamoorthy P, Moore J, Rogers WT. E. Endothelial cell-, platelet-, and monocyte/macrophage derived microparticles are elevated in psoriasis beyond cardiometabolic risk factors. J Am Heart Assoc. 2014 Feb 28; 3 (1): e000507. doi: 10.1161/JAHA.113.000507.

172. Pirro M, Stingeni L, Vaudo G, et al. Systemic inflammation and imbalance between endothelial injury and repair in patients with psoriasis are associated with preclinical atherosclerosis. Eur J Prev Cardiol. 2015. doi:10.1177/2047487314538858

173. Pelletier F, Garnache-Ottou F, Biichlé S, et al. Effects of anti-TNF-α agents on circulating endothelial-derived and platelet-derived microparticles in psoriasis. Exp Dermatol. 2014. doi:10.1111/exd.12551.

174. Podolska MJ, Biermann MHC, Maueröder C, Hahn J, Herrmann M. Inflammatory etiopathogenesis of systemic lupus erythematosus: An update. J Inflamm Res. 2015. doi:10.2147/JIR.S70325.

175. Rasmussen NS, Jacobsen S. Microparticles - culprits in the pathogenesis of systemic lupus erythematosus? Expert Rev Clin Immunol. 2018. doi:10.1080/1744666X.2018.1474100

176. Pereira J, Alfaro G, Goycoolea M, et al. Circulating platelet-derived microparticles in systemic lupus erythematosus. Association with increased thrombin generation and procoagulant state. Thromb Haemost. 2006. doi:10.1160/TH05-05-0310.

177. Parker B, Al-Husain A, Pemberton P, et al. Suppression of inflammation reduces endothelial microparticles in active systemic lupus erythematosus. Ann Rheum Dis. 2014;73(6):1144-1150. doi:10.1136/annrheumdis-2012-203028.

178. Duval A, Helley D, Capron L, et al. Endothelial dysfunction in systemic lupus patients with low disease activity: Evaluation by quantification and characterization of circulating endothelial microparticles, role of anti-endothelial cell antibodies. Rheumatology. 2010. doi:10.1093/rheumatology/keq041.

179. Viñuela-Berni V, Doníz-Padilla L, Figueroa-Vega N, et al. Proportions of several types of plasma and urine microparticles are increased in patients with rheumatoid arthritis with active disease. Clin Exp Immunol. 2015. doi:10.1111/cei.12598.

180. Niessen A, Heyder P, Krienke S, et al. Apoptotic-cell-derived membrane microparticles and IFN-α induce an inflammatory immune response. J Cell Sci. 2015. doi:10.1242/jcs.162735.

181. Dieker J, Tel J, Pieterse E, et al. Circulating Apoptotic Microparticles in Systemic Lupus Erythematosus Patients Drive the Activation of Dendritic Cell Subsets and Prime Neutrophils for NETosis. Arthritis Rheumatol. 2016. doi:10.1002/art.39417.

182. Mayo Clinic. Rheumatoid arthritis. https://www.mayoclinic.org/diseases-conditions/rheumatoid-arthritis/symptoms-causes/syc-20353648

183. Knijff-Dutmer EAJ, Koerts J, Nieuwland R, Kalsbeek-Batenburg EM, Van De Laar MAFJ. Elevated levels of platelet microparticles are associated with disease activity in rheumatoid arthritis. Arthritis Rheum. 2002. doi:10.1002/art.10312.

184. Berckmans RJ, Nieuwland R, Kraan MC, et al. Synovial microparticles from arthritic patients modulate chemokine and cytokine release by synoviocytes. Arthritis Res Ther. 2005.

185. Umekita K, Hidaka T, Ueno S, et al. Leukocytapheresis (LCAP) decreases the level of platelet-derived microparticles (MPs) and increases the level of granulocytes-derived MPs: A possible connection with the effect of LCAP on rheumatoid arthritis. Mod Rheumatol. 2009. doi:10.1007/s10165-009-0164-2.

186. Wei X, Song H, Yin L, et al. Fatty acid synthesis configures the plasma membrane for inflammation in diabetes. Nature. 2016. doi:10.1038/nature20117

187. Reboldi A, Dang E. Cholesterol metabolism in innate and adaptive response. F1000Research. 2018. doi:10.12688/f1000research.15500.1.

188. Goluszko P, Nowicki B. Membrane Cholesterol: a Crucial Molecule Affecting Interactions of Microbial Pathogens with Mammalian Cells. Infect Immun. 2005. doi:10.1128/iai.73.12.7791-7796.2005.

189. Tall AR, Yvan-Charvet L. Cholesterol, inflammation and innate immunity. Nat Rev Immunol. 2015. doi:10.1038/nri3793

190. Madsen CM, Varbo A, Nordestgaard BG. Low HDL Cholesterol and High Risk of Autoimmune Disease: Two Population-Based Cohort Studies Including 117341 Individuals. Clin Chem. 2019. doi:10.1373/clinchem.2018.299636.

191. Erum U, Ahsan T, Khowaja D. Lipid abnormalities in patients with Rheumatoid Arthritis. Pak J Med Sci. 2017;33(1):227–230. doi:10.12669/pjms.331.11699

192. Ali Abdalla M, Mostafa El Desouky S, Sayed Ahmed A. Clinical significance of lipid profile in systemic lupus erythematosus patients: Relation to disease activity and therapeutic potential of drugs. Egypt Rheumatol. 2017. doi:10.1016/j.ejr.2016.08.004.

193. Eren E. High Density Lipoprotein and it's Dysfunction. Open Biochem J. 2012. doi:10.2174/1874091x01206010078

194. Tselios K, Koumaras C, Gladman DD, Urowitz MB. Dyslipidemia in systemic lupus erythematosus: Just another comorbidity? Semin Arthritis Rheum. 2016. doi:10.1016/j.semarthrit.2015.10.010.

195. Blum A, Adawi M. Rheumatoid arthritis (RA) and cardiovascular disease. Autoimmun Rev. 2019 May 3. pii: S1568-9972(19) 30108-9. doi: 10.1016/j.autrev.2019.05.005.

196. England BR, Thiele GM, Anderson DR, Mikuls TR. Increased cardiovascular risk in rheumatoid arthritis: Mechanisms and implications. BMJ. 2018;361:1-17. doi:10.1136/bmj.k1036

197. Myasoedova E, Crowson CS, Kremers HM, et al. Lipid paradox in rheumatoid arthritis: The impact of serum lipid measures and systemic inflammation on the risk of cardiovascular disease. Ann Rheum Dis. 2011. doi:10.1136/ard.2010.135871

198. Huang LH, Zinselmeyer BH, Chang CH, et al. Interleukin-17 Drives Interstitial Entrapment of Tissue Lipoproteins in Experimental Psoriasis. Cell Metab. 2019. doi:10.1016/j.cmet.2018.10.006.

199. Malvern Panalytical Ltd. Dynamic light scattering: An introduction in 30 minutes. Tecnical note (MRK656-01). 2018:1-8.

200. The principles of dynamic light scattering. https://wiki.anton-paar.com/en/the-principles-of-dynamic-light-scattering/.

201. Carr B, Wright M. Nanoparticle Tracking Analysis: a review of applications and usage 2012-2012. NanoSight Ltd. 2012;1(0):188.

202. Resources. Flow Cytoemtry Guide. https://www.creative-diagnostics.com/flow-cytometry-

guide.htm

203. G-Biosciences. Dot Blot Analysis. https://www.gbiosciences.com/image/pdfs/protocol/BE-502_protocol.pdf

204. Repnik U, Knezevic M, Jeras M. Simple and cost-effective isolation of monocytes from buffy coats. J Immunol Methods. 2003. doi:10.1016/S0022-1759(03)00231-X

205. Laresche C, Pelletier F, Garnache-Ottou F, et al. Increased levels of circulating microparticles are associated with increased procoagulant activity in patients with cutaneous malignant melanoma. J Invest Dermatol. 2014. doi:10.1038/jid.2013.288

206. Angelillo-Scherrer A. Leukocyte-derived microparticles in vascular homeostasis. Circ Res. 2012. doi:10.1161/CIRCRESAHA.110.233403

207. Lovren F, Verma S. Evolving role of microparticles in the pathophysiology of endothelial dysfunction. Clin Chem. 2013. doi:10.1373/clinchem.2012.199711

208. György B, Módos K, Pállinger É, et al. Detection and isolation of cell-derived microparticles are compromised by protein complexes resulting from shared biophysical parameters. Blood. 2011. doi:10.1182/blood-2010-09-307595

209. Yuana Y, Levels J, Grootemaat A, Sturk A, Nieuwland R. Co-isolation of extracellular vesicles and high-density lipoproteins using density gradient ultracentrifugation. J Extracell Vesicles. 2014. doi:10.3402/jev.v3.23262

210. Szatanek R, Baran J, Siedlar M, Baj-Krzyworzeka M. Isolation of extracellular vesicles: Determining the correct approach (review). Int J Mol Med. 2015. doi:10.3892/ijmm.2015.2194

211. Gámez-Valero A, Monguió-Tortajada M, Carreras-Planella L, Franquesa M, Beyer K, Borràs FE. Size-Exclusion Chromatography-based isolation minimally alters Extracellular Vesicles' characteristics compared to precipitating agents. Sci Rep. 2016. doi:10.1038/srep33641

212. Davis CN, Phillips H, Tomes JJ, et al. The importance of extracellular vesicle purification

for downstream analysis: A comparison of differential centrifugation and size exclusion chromatography for helminth pathogens. *PLoS Negl Trop Dis*. 2019. doi:10.1371/journal.pntd.0007191

213. Lacroix R, Robert S, Poncelet P, Kasthuri RS, Key NS, Dignat-George F. Standardization of platelet-derived microparticle enumeration by flow cytometry with calibrated beads: results of the International Society on Thrombosis and Haemostasis SSC Collaborative workshop. J Thromb Haemost. 2010. doi:10.1111/j.1538-7836.2010.04047.x
214. Sódar BW, Kittel Á, Pálóczi K, et al. Low-density lipoprotein mimics blood plasma-derived exosomes and microvesicles during isolation and detection. Sci Rep. 2016. doi:10.1038/srep24316
215. van der Vlist EJ, Nolte-'t Hoen ENM, Stoorvogel W, Arkesteijn GJA, Wauben MHM. Fluorescent labeling of nano-sized vesicles released by cells and subsequent quantitative and qualitative analysis by high-resolution flow cytometry. Nat Protoc. 2012. doi:10.1038/nprot.2012.065
216. Chaichompoo P, Kumya P, Khowawisetsut L, et al. Characterizations and proteome analysis of platelet-free plasma-derived microparticles in β-thalassemia/hemoglobin E patients. J Proteomics. 2012 Dec 5;76 Spec No.:239-50. doi: 10.1016/j.jprot.2012.06.004
217. Pfrieger FW, Vitale N. Cholesterol and the journey of extracellular vesicles. J Lipid Res. 2018;59(12):2255-2261. doi:10.1194/jlr.r08421
218. Pisetsky DS. Microparticles as biomarkers in autoimmunity: From dust bin to center stage. Arthritis Res Ther. 2009. doi:10.1186/ar2856
219. Cunningham M, Marks N, Barnado A, Wirth JR, Gilkeson G, Markiewicz M. Are Microparticles the Missing Link between Thrombosis and Autoimmune Diseases? Involvement in Selected Rheumatologic Diseases. Semin Thromb Hemost. 2014. doi:10.1055/s-0034-1387924
220. Burbano C, Rojas M, Vásquez G, Castaño D. Microparticles That Form Immune Complexes

as Modulatory Structures in Autoimmune Responses. Mediators Inflamm. 2015. doi:10.1155/2015/267590

221. Crow MK, Olferiev M, Kirou KA. Targeting of type i interferon in systemic autoimmune diseases. Transl Res. 2015. doi:10.1016/j.trsl.2014.10.005

222. Atehortúa L, Rojas M, Vásquez G, et al. Endothelial activation and injury by microparticles in patients with systemic lupus erythematosus and rheumatoid arthritis. Arthritis Res Ther. 2019;21(1):1-15. doi:10.1186/s13075-018-1796-4

223. Turpin D, Truchetet ME, Faustin B, et al. Role of extracellular vesicles in autoimmune diseases. Autoimmun Rev. 2016. doi:10.1016/j.autrev.2015.11.004

224. Ito A, Hong C, Oka K, et al. Cholesterol Accumulation in CD11c+ Immune Cells Is a Causal and Targetable Factor in Autoimmune Disease. Immunity. 2016. doi:10.1016/j.immuni.2016.11.008

225. Ronda N, Favari E, Borghi MO, et al. Impaired serum cholesterol efflux capacity in rheumatoid arthritis and systemic lupus erythematosus. Ann Rheum Dis. 2014. doi:10.1136/annrheumdis-2012-202914

226. Marina I. Arleevskaya, Aleksey Zabotin, Aida Gabdoulkhakova, Julia Filina, Anatoly Tsibulkin. A Possible Interconnection of Cholesterol Overloading and Phagocytic Activityof the Monocytes in the Prone to Rheumatoid Arthritis Individuals. Lupus Open Acess 2016, 1:1.

227. Fang W, Bi D, Zheng R, et al. Identification and activation of TLR4-mediated signalling pathways by alginate-derived guluronate oligosaccharide in RAW264.7 macrophages. Sci Rep. 2017. doi:10.1038/s41598-017-01868-0

228. Fairweather DL, Rose NR. Women and autoimmune diseases. In: Emerging Infectious Diseases. ; 2004. doi:10.3201/eid1011.040367

229. Michael BR, Misra D, Chengappa K, Negi V. Relevance of elevated microparticles in peripheral blood and synovial fluid of patients with rheumatoid arthritis. Indian J Rheumatol.

2018;13(4):222. doi:10.4103/injr.injr_101_18

230. Parker B, Zaki A, Alexander MY, Bruce IN. Endothelial Microparticles As a Biomarker for Endothelial Dysfunction in Active Systemic Lupus Erythematosus. Arthritis Rheum. 2012;64(10, S):S270

231. McCarthy EM, Moreno-Martinez D, Wilkinson FL, et al. Microparticle subpopulations are potential markers of disease progression and vascular dysfunction across a spectrum of connective tissue disease. BBA Clin. 2017. doi:10.1016/j.bbacli.2016.11.003

232. Erum U, Ahsan T, Khowaja D. Lipid abnormalities in patients with rheumatoid arthritis. Pakistan J Med Sci. 2017;33(1):227-230. doi:10.12669/pjms.331.11699

233. Shao WH. The Role of Microparticles in Rheumatic Diseases and their Potentials as Therapeutic Tools. J Mol Immunol. 2016;1(1). pii: 101.

234. Ardoin SP, Pisetsky DS. The role of cell death in the pathogenesis of autoimmune disease: HMGB1 and microparticles as intercellular mediators of inflammation. Mod Rheumatol. 2008. doi:10.1007/s10165-008-0054-z

235. Harifi G, Sibilia J. Pathogenic role of platelets in rheumatoid arthritis and systemic autoimmune diseases: Perspectives and therapeutic aspects. Saudi Med J. 2016;37(4):354-360. doi:10.15537/smj.2016.4.14768

236. Ceroi A, Delettre FA, Marotel C, et al. The anti-inflammatory effects of platelet-derived microparticles in human plasmacytoid dendritic cells involve liver X receptor activation. Haematologica. 2016. doi:10.3324/haematol.2015.135459

237. Njock MS, Cheng HS, Dang LT, et al. Endothelial cells suppress monocyte activation through secretion of extracellular vesicles containing antiinflammatory microRNAs. Blood. 2015. doi:10.1182/blood-2014-11-611046

238. Čebatariūnienė A, Kriaučiūnaitė K, Prunskaitė J, Tunaitis V, Pivoriūnas A. Extracellular vesicles suppress basal and Lipopolysaccharide-induced NFκB activity in human periodontal ligament stem cells. Stem Cells Dev. 2019. doi:10.1089/scd.2019.0021

239. Yvan-Charvet L, Wang N, Tall AR. Role of HDL, ABCA1, and ABCG1 transporters in cholesterol efflux and immune responses. Arterioscler Thromb Vasc Biol. 2010. doi:10.1161/ATVBAHA.108.17928

240. Wüstner D, Solanko K. How cholesterol interacts with proteins and lipids during its intracellular transport. Biochim Biophys Acta - Biomembr. 2015. doi:10.1016/j.bbamem.2015.05.010

241. Chaudhuri A, Anand D. Cholesterol: Revisiting its fluorescent journey on 200th anniversary of Chevruel's "cholesterine." Biomed Spectrosc Imaging. 2017. doi:10.3233/bsi-170166

242. Sodhi HS, Kudchodkar BJ.Labeling plasma lipoproteins with radioactive cholesterol. J Lab Clin Med. 1973 Jul;82(1):111-24.

243. Malhotra S, Kritchevsky D. Cholesterol exchange between the red blood cells and plasma of young and old rats. Mech Ageing Dev. 1975. doi:10.1016/0047-6374(75)90015-9

244. Steck TL, Ye J, Lange Y. Probing red cell membrane cholesterol movement with cyclodextrin. Biophys J. 2002. doi:10.1016/S0006-3495(02)73972-6

245. Gold JC, Phillips MC. Effects of membrane lipid composition on the kinetics of cholesterol exchange between lipoproteins and different species of red blood cells. BBA - Biomembr. 1990. doi:10.1016/0005-2736(90)90052-P

246. Quarfordt SH, Hilderman HL. Quantitation of the in vitro free cholesterol exchange of human red cells and lipoproteins. J Lipid Res. 1970.

247. Lange Y, Molinaro AL, Chauncey TR, Steck TL. On the mechanism of transfer of cholesterol between human erythrocytes and plasma. J Biol Chem. 1983.

248. Song W, Wang W, Wang Y, Dou L, Chen L, Yan X. Characterization of fluorescent NBD-cholesterol efflux in THP-1-derived macrophages. Mol Med Rep. 2015. doi:10.3892/mmr.2015.4154

249. Frolov A, Petrescu A, Atshaves BP, et al. High density lipoprotein-mediated cholesterol uptake and targeting to lipid droplets in intact L-cell fibroblasts. A single- and multiphoton fluorescence approach. J Biol Chem. 2000. doi:10.1074/jbc.275.17.12769

250. Storey SM, Atshaves BP, McIntosh AL, et al. Effect of sterol carrier protein-2 gene ablation on HDL-mediated cholesterol efflux from cultured primary mouse hepatocytes. Am J Physiol - Gastrointest Liver Physiol. 2010. doi:10.1152/ajpgi.00446.2009

251. Chuo STY, Chien JCY, Lai CPK. Imaging extracellular vesicles: Current and emerging methods. J Biomed Sci. 2018. doi:10.1186/s12929-018-0494-5

252. Costa Verdera H, Gitz-Francois JJ, Schiffelers RM, Vader P. Cellular uptake of extracellular vesicles is mediated by clathrin-independent endocytosis and macropinocytosis. J Control Release. 2017. doi:10.1016/j.jconrel.2017.09.019

253. Mulcahy LA, Pink RC, Carter DRF. Routes and mechanisms of extracellular vesicle uptake. J Extracell Vesicles. 2014. doi:10.3402/jev.v3.24641

254. Liu ML, Reilly MP, Casasanto P, McKenzie SE, Williams KJ. Cholesterol enrichment of human monocyte/macrophages induces surface exposure of phosphatidylserine and the release of biologically-active tissue factor-positive microvesicles. Arterioscler Thromb Vasc Biol. 2007;27(2):430–435. doi:10.1161/01.ATV.0000254674.47693.e8

255. Batool S, Abbasian N, Burton JO, Stover C. Microparticles and their Roles in Inflammation: A Review. Open Immunol J. 2013;6(1):1-14. doi:10.2174/1874226201306010001

8.0 Appendix

Appendix I: List of awards, presentations, publication and modules

Awards

- Early Career Investigator Travel Stipend Awards for Kern Lipid Conference 2018, USA
- 68th Lindau Nobel Laureate meeting award, 2018 (selected from over 20,000 students)
- Student Travel Award for attendance at CYTO, 2018, Prague

Presentations

- International Conference on Euro Oncology, Breast Cancer & Biomarkers 2018" Studies on extracellular vesicle cholesterol in systemic lupus erythematosus Poster presentation (October, 2018, Netherlands)
- Irish Society for Immunology Annual Meeting 2018," Cholesterol containing microparticles accentuates MYD88 dependent pathways in autoimmune diseases." Poster presentation (August, 2018, Dublin)
- Kern Lipid Conference 2018," Studies on Extracellular Vesicles Cholesterol in Systemic Lupus Erythematosus." Poster presentation (August, 2018, US)
- 64th Annual Scientific and Standardization Committee Meeting of the International Society on Thrombosis and Homeostasis", Circulating cholesterol containing platelet-derived microparticles contribute to the procoagulant state observed in Systemic Lupus Erythematosus." Poster presentation (July, 2018, Dublin)
- 68th Lindau Nobel Laureate Meeting Germany, selected from over 20,000 applicants globally to attend this meeting which will include 43 Nobel Laureate presentations and a trip to the Max Planck Institute. Poster presentation and Master Class attendance, (June, 2018, Germany)
- 33rd Congress of the International Society for Advancement of Cytometry," Novel Application of 3-Hexanoyl-NBD Cholesterol (3NBDC) as a Biomedical Tool to Detect

Membrane Cholesterol by Flow Cytometry ", Poster presentation (April, 2018, Czech Republic)

- ISEV Workshop "Membranes and EVs" Development of 3-Hexanoyl- NBD Cholesterol (3NBDC) as a biochemical tool to detect cholesterol in microparticle membranes", Oral presentation (March, 2018, USA)
- DIT 7th Annual Graduate Research Symposium," Circulating microparticles are a novel carrier of cholesterol in the blood stream", Poster presentation, (Feb, 2017, DIT, Ireland)
- Annual Meeting of the Cytometry Society of Ireland. "Application of novel 3-NBD-cholesterol in cell biology", Poster presentation (Nov, 2016, Ireland)
- 4th Helmholtz-Nature Medicine Diabetes conference, "Decreasing $CD51^{+}$EMP in diabetes patients with hypertension", Oral presentation at the Scientific Round Table Session (Sept, 2016, Germany)

Publications

- ***Shuaishuai Hu***, Claire Wynne, Steve Meaney. (2018) Studies on extracellular vesicle cholesterol in systemic lupus erythematosus (Abstract accepted in Conference proceeding) Journal of Cancer Science and Therapy (10) DOI: 10.4172/1948-5956-C12-157
- Ashley E. Russell , Alexandra Sneider, Paolo Bergese, Suvendra Bhattacharyya, Alexander Cocks, Emanuele Cocucci, Uta Erdbruegger, Juan M. Falcon-Perez, David Freeman, Thomas M. Gallagher, ***Shuaishuai Hu***, Yiyao Huang, Steven M. Jay et al. Biological membranes in EV biogenesis, stability, uptake, and cargo transfer: An ISEV Position Paper arising from the ISEV Membranes and EVs Workshop. Journal of Extracellular Vesicles (Accepted).

Modules

Discipline skills training: 20 Credits

- Animal cell culture and proteomic technology (5 credits)
- Diagnostic Immunology and Transplantation (5 credits)
- Metabolic and Endocrine Disorder (5 credits)
- Cell Biology and Immunology (5 credits)

Employability skills training: 20 Credits

- Introduction to Pedagogy (5 credits)
- Writing in Science and Engineering (6 credits)
- Research Methods and Biostatistics (10 credits)